5-2003

Effect of Surface Treatment on the Conductivity of Polyurethane-Carbon Composites

Leina Barros Tocchetto
University of Tennessee - Knoxville

To the Graduate Council:

I am submitting herewith a thesis written by Leina Barros Tocchetto entitled "Effect of Surface Treatment on the Conductivity of Polyurethane-Carbon Composites." I have examined the final electronic copy of this thesis for form and content and recommend that it be accepted in partial fulfillment of the requirements for the degree of Master of Science, with a major in Polymer Engineering.

Roberto S. Benson, Major Professor

We have read this thesis and recommend its acceptance:

Kevin Kit, Felix Paulauskas

Accepted for the Council:
Dixie L. Thompson

Vice Provost and Dean of the Graduate School

(Original signatures are on file with official student records.)

To the Graduate Council:

I am submitting herewith a thesis written by Leina Barros Tocchetto entitle "Effect of Surface Treatment on the Conductivity of Polyurethane-Carbon Composites." I have examined the final electronic copy of this thesis for form and content and recommend that it be accepted in partial fulfillment of the requirements for the degree of Master of Science, with a major in Polymer Engineering.

Roberto S. Benson

Major Professor

We have read this thesis

And recommend its acceptance:

Kevin Kit

Felix Paulauskas

Accepted for the Council:

Dr. *Anne Mayhew*

Vice Provost

Dean of Graduate Students

(Original signatures are on file with official student records.)

EFFECT OF SURFACE TREATMENT ON THE CONDUCTIVITY OF POLYURETHANE-CARBON COMPOSITES

A Thesis

Presented for the

Masters of Science Degree

The University of Tennessee Knoxville

Leina Barros Tocchetto

May 2003

ACKNOWLEDGEMENTS

I wish to express my sincere appreciation for my advisor, Professor Dr. Roberto S. Benson for his help and guidance throughout this study. I would also like to express my gratitude to the other committee members, Dr. Kevin Kit and Dr. Felix Paulauskas for their contributions for this research.

I would like to thank the Material Science and Engineering Department for the investment in my education, and all staff and faculty who in many different ways have helped through my degree.

I greatly appreciate the ORNL for providing material and Solid State Division for allowed some tests in their division, especially Jian He for his help.

My appreciation is extended to Xiaoyu Luo, Chris Stephen, George Jacob, Sudhakar and Chris Lewis for their help, support and specially for the good memories.

I give all my respect and appreciation to the most important people in my life, my parents and husband, for their unconditional love and support.

ABSTRACT

The effect of plasma surface treatment on the mechanical and electrical properties was investigated by comparing untreated particulate carbon filler and treated carbon filler in a polyurethane matrix. For achieving this goal, samples of the composites were prepared with different percentages of carbon fillers (0 – 50 wt %) and conductivity measurements, dynamic mechanical analysis, mechanical properties, infrared spectroscopy and scanning electron microscopy were used to determine the effect of surface modification and concentration.

The conductivity measurements showed that the percolation threshold was shifted to lower concentrations of carbon as compared to the predicted value especially for the untreated carbon filled samples. The untreated filled carbon composite samples exhibited this behavior due to precipitation of filler particles during the solvent casting of the film.

In terms of mechanical properties (dynamic and transient), the effect of filler content and filler surface treatment was noted. FT-IR results indicates some degree of interaction between the treated filler surface and polyurethane. Scanning electron microscopy showed that composites based on a modified filler had better dispersion.

TABLE OF CONTENTS

LIST OF FIGURES

LIST OF TABLES

1. INTRODUCTION

Composite systems, comprised of conductive filler in a polymer matrix, create a material that in general is tough, flexible, and electrically conductive. Conductive polymer composites have found use in a variety of applications. These materials are ideally suited for antistatic layers, electromagnetic interference shielding, chemical vapor sensors, and thermal resistors [1]. The composites are able to combine high electric conductivity with the favorable properties of polymer materials such as elasticity, flexibility, resistance to chemicals and the environment [2]. The addition of suitable types and concentration of filler particles generally leads to compounds with a wide range of conductivity values [3].

A proper balance among the electrical conductivity, mechanical properties, and processing characteristics is an important requirement for the design of the electroconductive thermoplastic composites [4]. The presence of fillers in a thermoplastic matrix usually leads to higher stiffness of the material and a decrease in deformability and toughness. The extent of these changes depends on the concentration and shape of the filler (surface area) [4]. Carbon black tends to aggregate in polymeric systems, and at high concentrations they are expected to form a continuous filler network by physical contact between particles [5]. Carbon black-polymer composites have been the subject of extensive research due to their high conductive value, relatively low price and ultimately their processing properties [3].

Surface treatment enable the modification of fillers by placement chemical groups capable of enhancing interactions and hence improving filler-matrix bonding [6]. Carbon

black is well known for ease and stability of modification. Surface treated carbon black has good electrical conductivity, thermal stability, heat transfer properties, flexural and tensile modulus, ductility, heat distortion temperature, abrasion and chemical resistance, and good surface quality [7].

Plasma treatment is an effective surface modification technique used for polymeric materials [8]. A plasma consists of a mixture of electrons, ions, and radicals (gas phase) that are able to interact with surfaces of polymeric materials to initiate chemical reactions such as hydrogen abstraction, bond scission, and radical formation [8] [9].

The main goal of this work is to understand the effect of plasma surface treatment by comparing untreated particulate carbon filler in a polyurethane matrix, and a plasma treated particulate carbon filler in the same matrix. Samples of varying weight percent of filler were prepared and conductivity measurements, dynamic mechanical analysis, mechanical properties, infrared spectroscopy and scanning electron microscopy were used to determine the effect of modification and concentration.

2. LITERATURE REVIEW

2.1. Polymer Composites

A composite is formed by combining two or more materials on a macroscopic scale to form a useful material. Composites usually exhibit the best qualities of their constituents and often some qualities that neither constituent possesses [10].

Polymer composites are composed of a rigid component embedded in a polymeric matrix [11]. The composites include a variety of components which display behavior ranging from toughened elastomers through impact-resistant plastics to fiber-reinforced thermosets and polymer-impregnated concrete [12]. The improvements in properties obtained with different fillers are summarized in Table 2.1.1 [13]. The design of a composite material depends on the need and required mechanical properties.

Composite materials can be divided in three general classes: particulate-filled materials consisting of a continuous matrix phase and a discontinuous filler phase made up of discrete particles; fiber filled composites; and skeletal or interpenetrating network composites consisting of two continuous phase, e.g. filled open-cell foams and sintered mats or meshes filled with some material [14]. Due to the interest in the properties of a polyurethane filled carbon composites, more details on particulate filled polymers will be presented later.

The fiber filled composite is a system made of a macro scale high strength continuous or chopped fibers into a matrix of lower mechanical strength. Such composite materials usually have high strength and stiffness, and many of them are anisotropic with

Table 2.1.1. Effects of fillers on properties of polymers

Filler or Reinforcement	*Chemical resistance*	*Heat resistance*	*Electrical insulation*	*Impact strength*	*Tensile strength*	*Dimensional stability*	*Stiffness*	*Hardness*	*Lubricity*	*Electrical Conductivity*	*Thermal Conductivity*	*Moisture resistance*	*Processability*
Alumina tabular	*	*				*							
Calcium carbonate		*				*	*	*					*
Carbon black		*				*	*			*	*		*
Fibrous glass	*	*	*	*	*	*	*	*					*
Graphite	*				*	*	*	*	*	*	*		
Kaolin	*	*				*	*	*	*			*	*
Mica	*	*	*		*	*	*	*	*			*	
Nylon	*	*	*	*	*	*	*	*	*				*
TFE-Flourcarbon						*	*	*	*				
Talc	*	*	*			*	*	*	*			*	*

high strength in one or two directions. A nano structure composite is a system made of high strength nanosized rigid entities dispersed in a continuous polymeric matrix. The enhancement in properties of nano-composites due to a molecular level reinforcement. By the successful dispersion of rigid entities, a nano structure composite may have mechanical properties that are comparable to chopped fiber reinforcement composite. The down side of nano-composites is the tendency to aggregate and phase separate from the host matrix as the concentration exceeds a certain critical value [15].

2.1.1. Particulate-filled Polymers

Particulate fillers can provide improved materials, as compared with the unfilled matrix and also can be synergistic with a filler reinforcement to further the system performance [16]. The final behavior of the composite will depend not only on the individual properties of the two components, but the volume fraction of the filler, size, shape, state of agglomeration and degree of adhesion between filler and matrix [12].

There are many types of particulate fillers, that can be classified as mineral (calcium carbonate, clay, feldspar, talk), natural or synthetic (glass beads, metal powders and synthetic silicas), inorganic or organic (wood flour, carbon black, reclaimed rubber). Specific particulate filler gives a composite special characteristics.

The particulate fillers can be characterized by shape, function and surface properties. The shape of a particulate filler is an important consideration in the selection of the optimum filler for a specific end use. The fillers can be microsphere, flakes or irregular shaped particulates. When characterizing by function, they can be fire

retardants, lightweight fillers, high density fillers, high hardness fillers, high thermal conductivity fillers, electrically conductive particulate fillers, magnetic particulate fillers and low friction particulate fillers. The surface characteristics of a particulate filler are important in determining the final properties of the composite. Some chemicals used to treat the surface of the fillers and reinforcements are silanes, titanates and zirconates and miscellaneous coupling agents [16].

2.1.1.1. Modulus of Particulate Composites

From a simple model of an aggregate dispersed in a matrix, Einstein proposed an expression for shear modulus of a filled polymer composite in which the interface between the matrix and the filler particles have perfect adhesion (Equation 3). A second equation (Equation 4) took into consideration slippage at the interface between the matrix and the filler.

$$G = G_1(1 + 2.5\phi_2) \qquad \text{Equation 3}$$

$$G = G_1(1 + \phi_2) \qquad \text{Equation 4}$$

where,

G → shear modulus of the composite

G_1 → shear modulus of the matrix

ϕ_2 → filler weight fraction

Einstein's equations were based on the volume fraction of filler and its interfacial adhesion with the matrix. However, the equation only predicted the modulus at low concentrations. One of the modifications to Einstein's original theory was proposed by Eilers-Van Dijek [17] that accounts for the effective volume of the filler (Equation 5), but this relation has limitations since the modulus predictions is greater than experimental values [18].

$$\frac{G}{G_1} = \left\{1 + \left[\frac{1.25\phi_2}{\left(1 - V\phi_2\right)}\right]\right\}^2 \qquad \text{Equation 5}$$

where,

V → constant equivalent to the ratio of sedimentation volume of the filler relative to the true volume of the filler

Kerner developed an expression to evaluate the filler material's contribution over the entire range of the two phase system (Equation 6).

$$G = G_1\left[\frac{\frac{\phi_2 G_2}{\left(7-5\nu_1\right)G_1 + \left(8-10\nu_1\right)G_2} + \frac{\phi_1}{15(1-\nu_1)}}{\frac{\phi_2 G_1}{\left(7-5\nu_1\right)G_1 + \left(8-10\nu_1\right)G_2} + \frac{\phi_1}{15(1-\nu_1)}}\right] \qquad \text{Equation 6}$$

where,

G_2 → shear modulus of the filler

ϕ_1 → matrix weight fraction

ν_1 → Poisson's ratio

For relatively rigid particles in a polymer matrix, this equation will be reduced to a simpler form, with the value of ϕ and ν being included (Equation 7). Shear and elastic modulus are related through Poisson's ratio according to Equation 8.

$$\frac{G}{G_1} = 1 + \frac{15(1-\nu)}{(8-10\nu)}\frac{\phi_2}{\phi_1} \qquad \text{Equation 7}$$

$$E = 2G(1+\nu) \qquad \text{Equation 8}$$

where,

E → elastic modulus

2.1.1.2. <u>Tensile Properties of Particulate Composites</u>

Adding particulate fillers to a polymer matrix makes the modulus of the system increase with volume fraction of filler, but this is not always the case with the tensile strength. It has been observed that an increase in the actual density of the material is a contributing factor to increase tensile properties. The tensile strength of a filled polymer can be predicted by Equation 9. At relatively high porosity, the tensile tensile strength is reduced due to the loss of adhesion between the matrix and filler [17].

$$\sigma_B = \sigma_{BO} e^{(-AP)} \qquad \text{Equation 9}$$

where,

σ_B → tensile strength of the composite

σ_{BO} → tensile strength of the material without porosity

P → volume fraction of voids

In particulate filled polymer composites it is assumed that elongation comes from the matrix. So, a reduction in the volume fractions of the matrix should lead to a reduction in elongation. Based on this principle, Nielsen developed Equation 10.

$$\frac{\varepsilon_{B(filled)}}{\varepsilon_{B(unfilled)}} = 1 - \phi_2^{1/3} \qquad \text{Equation 10}$$

where,

ε → elongation of the filled and unfilled polymer.

Rigid particulate fillers increase the modulus as measured from the slope of the stress-strain curve, at least in the case of good adhesion. Generally, fillers cause a dramatic decrease in elongation to break, and tensile strength of a material. Typical stress strain curves for polyurethane filled with powdered rock salt are shown in Figure 2.1.1.2.1 [14]. The elongation at break effect is due to the fact that the actual elongation experienced by the polymer matrix is much greater than the measured elongation of the specimen.

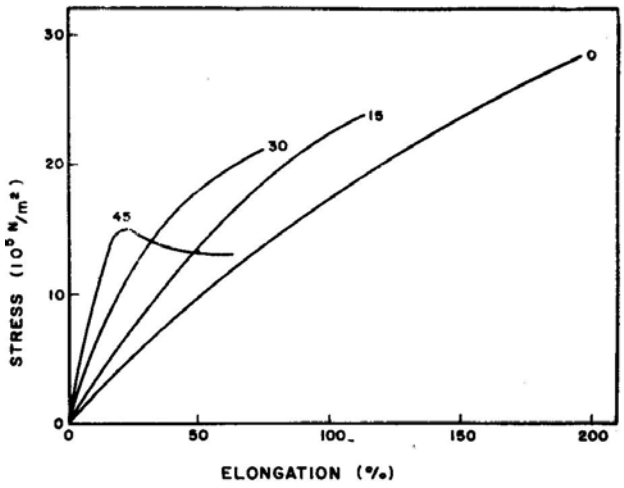

Figure 2.1.1.2.1. Stress strain curve for a PU/rock salt composite

2.2. Conductive Filled Polymers

Conductivity in polymeric material can be achieved by conductive polymers or adding conductive additives in the matrix [4]. The latter is a binary conductive system comprised of a conductive filler (e.g., carbon black, metal powder, etc.) in a polymer matrix, creating a material that is tough, flexible, and electrically conductive [1].

The conductivity is a result of the development of a network of touching filler particles [19]. Electrical conductivity in filled polymers becomes a function of volumetric relationships between the conductive filler and insulating matrix. Under these conditions, the size and shape of the filler and their surface chemistry become significant [20].

The critical concentration of a given filler depends strongly on its aspect ratio, defined as the ratio of the long and short dimension of the filler particles. The effect of

aspect ratio on network formation can be seen in three computer simulations of two-dimensional composites given in Figure 2.2.1 [21]. In each frame, the filler particles occupy 20 percent of total area with the same randomly assigned positions and orientations, but their aspect ratio varies from frame to frame. The effect of the aspect ratio on the composite properties will be discussed later.

Percolation can be defined as a phase-transition at which a dramatic change occurs at one sharply defined parameter value, as this parameter is continuously changed [1]. In the case of conductive filled composites, the amount of conductive filler required to achieved the insulator-conductive transition is often referred as the percolation threshold (critical concentration of filler), as show in Figure 2.2.2. In low filler concentration, there is not enough filler to form a conductive network. Up to a critical filler concentration, the resistivity of the composite is hardly reduced by the filler (or conductivity is hardly increased), until it reaches a point in which further increase in filler

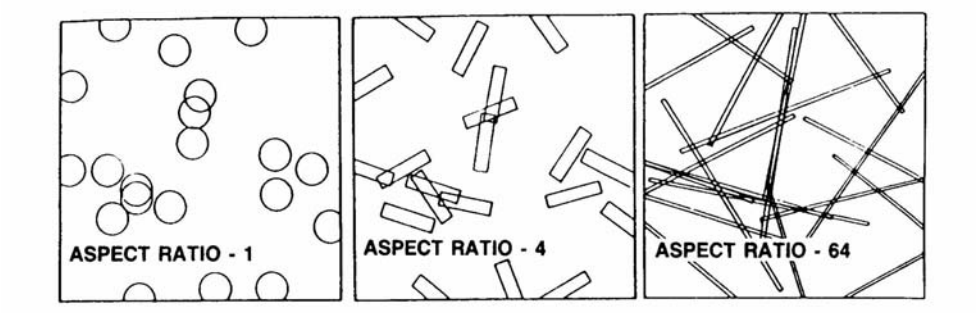

Figure 2.2.1. Effect of filler particle aspect ratio on the network

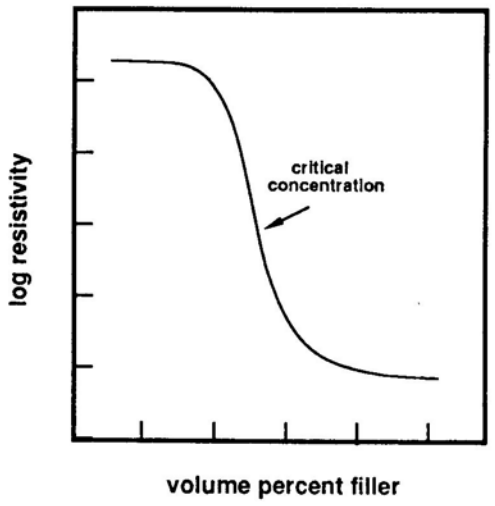

Figure 2.2.2. Critical filler concentration (percolation threshold)

content decrease the resistivity but at a much lower rate. Considering aspect ratio, the network formation begins at lower filler concentrations as the aspect ratios increases. The filler distribution plays an important role in the electrical properties of composites, and the tendency of particles to form aggregates can also affect the critical filler concentration.

Another factor that alter the percolation threshold is the optimum condition of the filler, in which may shift the S-shape dependency of the electrical conductivity of the composites to different values. According to Yu et al. [22], the percolation threshold for a carbon black-LDPE composite was found to be 15 wt% of filler. After a titanate treatment of the carbon, the percolation was 1.24 wt% lower than the untreated version. Li et al.[2], in a carbon/polyurethane composite, found a percolation threshold of 20 wt% of filler. According to Pinto et al. [23], the critical concentration of zinc in a nylon 6 compote was 18 % (v/v).

In general, there are three main regions that control conductivity of filled polymer composites. At low filler loadings (Region A of Figure 2.2.3) the conductivity of the composite is still very close to the polymer matrix. There is a region that produces a significant increase in conductivity with very little increase in filler amount (Region B). At high filler loadings, the conductivity levels off, and approaches that of the filler material (Region C) [24].

Theoretically, many percolation models have been developed to define the conditions at which a network is formed in conductive polymer compounds. Among particles dispersed in polymers two competitive forces have to be considered. The first one is the force responsible to get the particles to stick together, and this force is the London-van der Waals force of attraction. The second force is the Coulomb repulsive force, in which surfaces of particles dispersed become charged. Depending on the amount of charging, the coulombic force can cause a potential energy barrier, not allowing the particles to come close enough to each other to form the network and

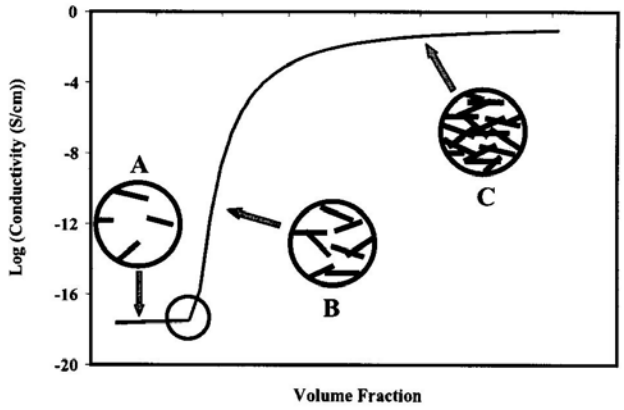

Figure 2.2.3. Dependence of electrical conductivity on filler volume fraction

achieve the minimum contact necessary to be electrically conductive [19]. Figure 2.2.4 illustrates the total potential energy as a function of particle distance.

According to Clingerman et al. [25] in their evaluation of electrical conductive models for conductive polymer composites, the model that provided the best fit of the experimental data is the Mamunya's model, since it incorporated the aspect ratio and surface energy into the conductive calculation.

The model proposed by Mamunya, fits into the thermodynamic model category, and shows that percolation behavior is dependent on the polymer-filler interaction, in addition to size and amount of filler material. At all points above the percolation threshold, the conductivity of the composite is given by the expression (Equations 11-15):

$$\log\sigma = \log\sigma_P + (\log\sigma_F - \log\sigma_p)\left(\frac{\phi - \phi_c}{F - \phi_c}\right)^k \qquad \text{Equation 11}$$

$$k = \frac{K\phi_c}{(\phi - \phi_c)^{0.75}} \qquad \text{Equation 12}$$

$$K = A - B\gamma_{pf} \qquad \text{Equation 13}$$

$$\gamma_{pf} = \gamma_p + \gamma_f - 2(\gamma_p\gamma_f)^{0.5} \qquad \text{Equation 14}$$

$$F = \frac{5}{\frac{75}{10 + AR} + AR} \qquad \text{Equation 15}$$

where,

$\sigma \rightarrow$ composite conductivity

$\sigma_p \rightarrow$ conductivity of the polymer

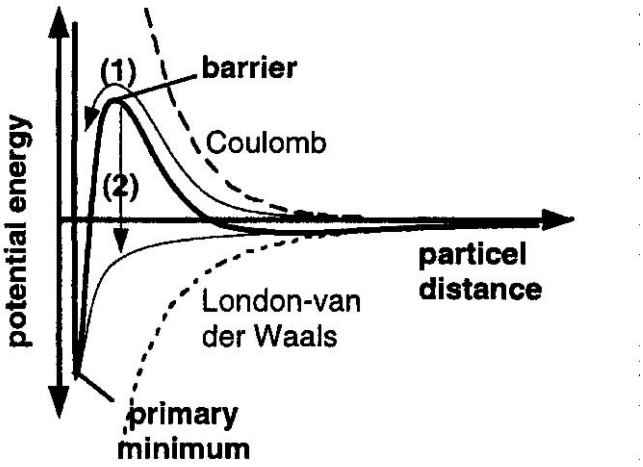

Figure 2.2.4. Potential energy curve of two colloidal particles

σ_F → conductivity at F fraction

F → maximum packing fraction

ϕ → volume fraction

ϕ_c → percolation threshold of volume fraction

γ_{pf} → interfacial tension

A and B → constants

γ_p → surface energy of the polymer

γ_f → surface energy of the filler

AR → aspect ratio

2.3. Segmented Polyurethane

It was during 1930s that Prof. Otto Bayer synthesized polymer fibers (fiber-forming Polyurethane) to compete with the existent nylon [26], becoming commercial

after the Second World War [27]. Polyurethanes are probably the most versatile class of polymers due to the great variety o raw materials that can be used in their formation [28].

The typical morphology of block copolymers is a phase separated structure which usually consists of a dispersed phase of one block in a continuous matrix mainly composed of another block. Polyurethanes elastomers are segmented block copolymers formed by the combination of hard and soft segments. The hard an soft segments are usually made of soft and flexible chains having glass transition temperature (Tg) at far below room temperature and rigid and polar chains having relatively high glass transition temperature.

For the polymerization of segmented polyurethanes, a two stage step polymerization is employed, allowing the formation of polymers having more narrowly distributed molecular weights and larger blocks than one stage reaction. The initial reaction is the endcapping reaction of a of a polyether glycol with a diisocianate to form a prepolymer. The second reaction is the coupling of the prepolymer with a diol or diamine to form a poly(ether-urethane) or a poly(ether-urethane-urea), respectivally [29]. Figure 2.3.1 illustrates a typical two stage reaction to prepare segmented polyurethane [30].

It is possible to prepare a number of polyurethanes by simple combinations of a hard segment, soft segment and chain extender. The hard segment is formed by extending a diisocyanate with a low molecular weight diol such as 1,4-butanodiol. In segmented polyurethanes, phase separation of the urethane hard segments into microdomains has been observed even when the segmented length is relatively short [31]. Polyurethanes behave as cross-linked polymers, and are termed as virtually cross-linked,

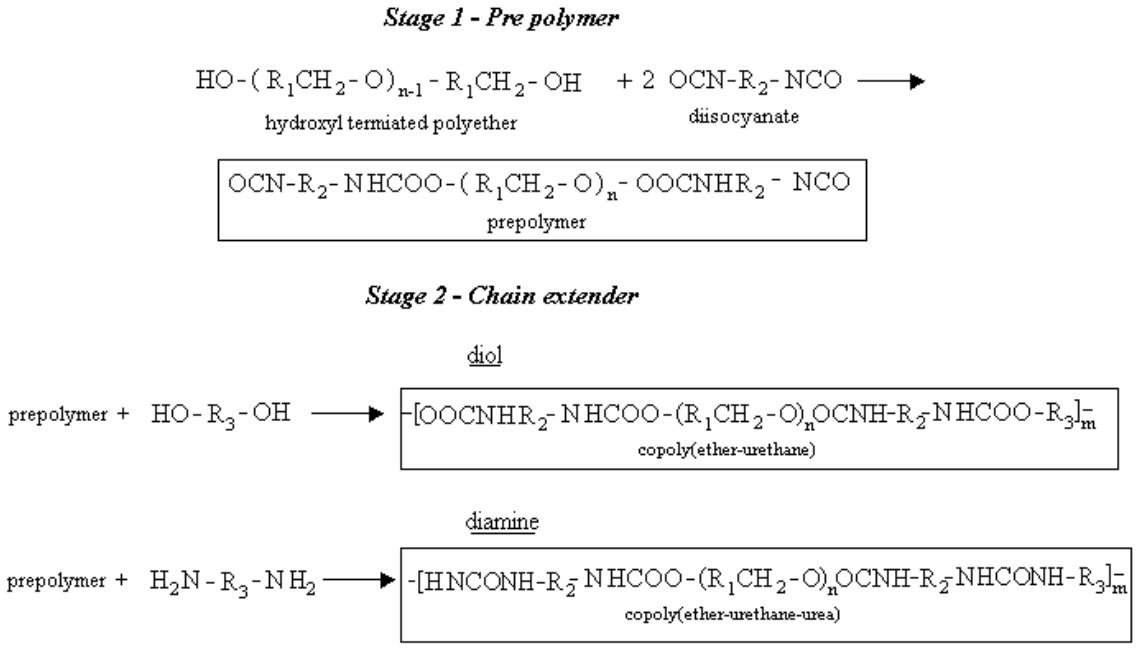

Figure 2.3.1. Two stage step polymerization of segmented polyurethane

as shown in Figure 2.3.2 [26] . Factors that control the degree of microphase separation include copolymer composition, block length, crystallizability of either segment, and the method of sample fabrication [31].

Segmented polyurethanes are two-phase systems, and phase separation strongly affects the properties. The soft segment contributes to the high extension and elastic recovery, while the hard segment contributes high modulus and strength to the composite. Phase separation will depend of the phases crystallinity, temperature, and previous thermal history [26].

Another important factor that affect material properties is the existence of hydrogen bond. A hydrogen bond is formed between two groups, one being the proton

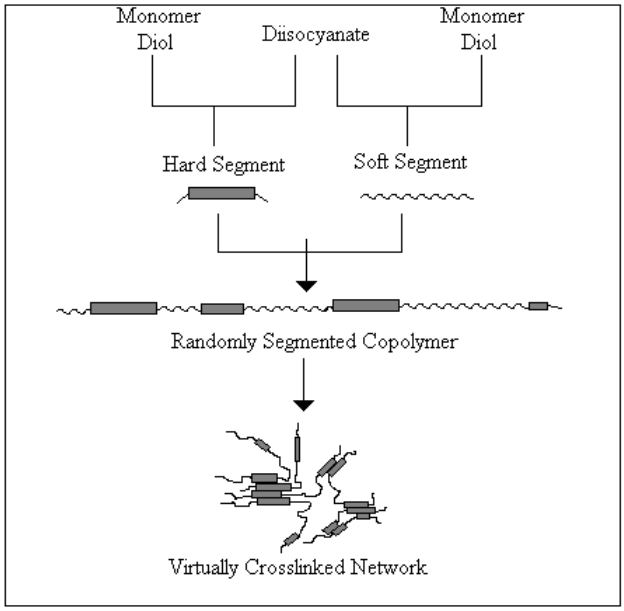

Figure 2.3.2. Virtually cross-linked network of PU

donor (normally hydroxyl or amino groups) and the other the proton acceptor. In polyurethane, the urethane band contains a strong proton donor (N-H group) and a proton acceptor as well (C=O group). Another possible proton acceptor is the oxygen (-O-) from the urethane group with its free electron pairs [26].

Molecular weight and crystallization can affect the structure-property relationship in polyurethane polymers. As molecular weight and ability of the soft segment to crystallize increases, properties such as tensile strength, elongation and Tg will increase. Crystallization is a response of linearity and close fit of polymer chains. Figure 2.3.3 shows the transient morphologies of segmented polyurethanes, while Figure 2.3.4 presents an idealized view of crystallization in polymers, including polyurethanes (bundle crystallization).

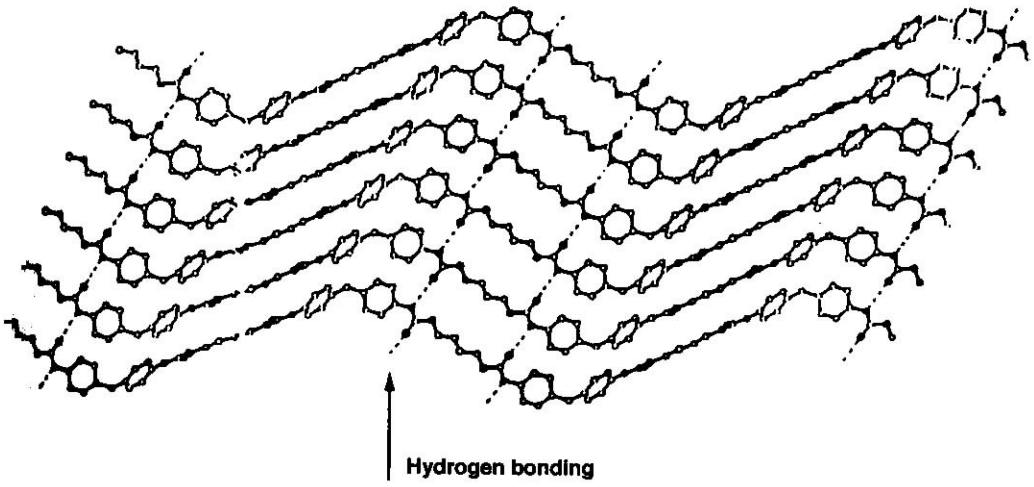

Figure 2.3.3. Polyurethane elastomer structure, crystallization and hydrogen bonding

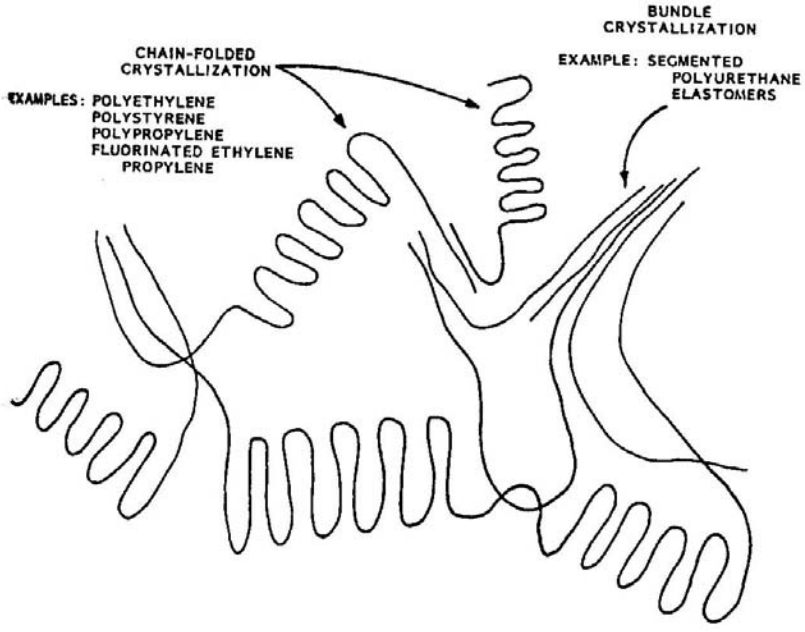

Figure 2.3.4. Mechanisms of crystallization in polymers

2.4. Carbon

Particulate carbon is available commercially from many suppliers in various forms. The filler known as carbon black is obtained from the pyrolysis of hydrocarbon gases or oils [16]. Most carbon blacks are formed by conducting the pyrolysis in a flame or by subjecting it to a flame after beginning of pyrolysis [13]. Particle size, surface area, hydrogen content, oxygen content and structure are the five primary properties of carbon black that determine its effect on the properties of an elastomer [32].

The uses of carbon black include filling and reinforcement, coloring agent, electric and thermal conductive components in polymer composite [16]. For many years, finely divided carbon black has been a valuable addition to polymers used to enhance their conductivity. Many patent references refer to carbon black and its ability to improve and stabilize conductivity, and enhance UV light and thermal degradation stability [20].

2.5. Polyurethane/Carbon System

Polyurethane composites with conducting carbon may serve as polymer conductors or semi-conductors and can be applicable in the fields of electrical and electronic industry. The final product will combine the high electric conductivity of the carbon with the favorable properties of the polyurethane [2].

The relationship between the conductivity of the polyurethane/carbon composite and carbon black concentration illustrated in Figure 2.5.1, shows that conductivity increases slowly for low concentration of carbon until a dramatic increase occur at the percolation threshold.

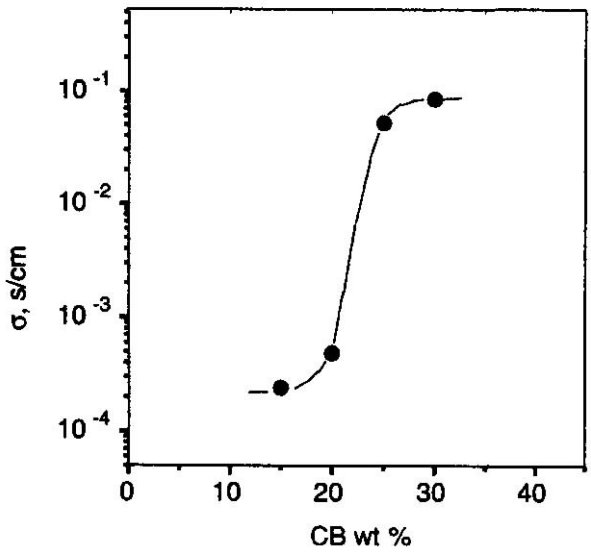

Figure 2.5.1. Relationship between electric conductivity and carbon concentrations in the composites

The conductivity of polyurethane/carbon composites before and after a certain stretching ratio was studied by Li et al [2] (Table 2.5.1), showing that a unilateral stretching destroys the networks of conductive pathways throughout the polymer along the deformation direction of the high carbon loaded composites.

2.6. Surface Modification

In recent years, many advances have been made in developing surface treatments to alter the chemical and physical properties of polymer surfaces without affecting bulk properties. The desired results are to place special functional groups at the surface to enable specific interactions with other groups, increase surface energy, hydrophobicity or hydrophilicity, improve chemical inertness, introduce surface cross-linking, remove weak

Table 2.5.1. Conductivity of polyurethane-conducting carbon composites

Sample	Carbon wt%	σ (s.cm^{-1})	
		λ=0	λ=1.5
PU-CB00	0	___	___
PU-CB05	5	___	___
PU-CB10	10	___	___
PU-CB15	15	2.4 x 10^{-4}	___
PU-CB20	20	4.9 x 10^{-4}	___
PU-CB25	25	5.2 x 10^{-2}	2.0 x 10^{-2}
PU-CB30	30	8.4 x 10^{-2}	3.2 x 10^{-2}

boundary layers or contaminants, modify surface morphology, increase surface electrical conductivity and/or surface lubricity [33].

There are two technical approaches to physically modify polymers surfaces, one is chemically altering the surface layer and second is depositing an extraneous layer on the existing material. The former can be achieved by flame treatments, corona and plasma treatment, and requires generating high energy species (radicals, ions, molecules in excited electronic states). The latter involves the generation of atoms or atoms clusters (high energy methods) to be deposit on polymer surfaces. Examples of these techniques are plasma polymerization, thermally or electron beam-induced evaporation [34].

2.6.1. Plasma Treatment

Plasma treatment has become an important industrial process for modifying polymer surfaces. It has been used to improve printability, wettability, bondability, biocompatibility, surface hardness, and surface heat resistance [33], playing an important role in microelectronic fabrication technologies [34]. It is the result of the interaction of a

conventional polymer (or other substrate) with a nonfilm-forming plasma [35], leading to a modified surface with better properties.

A plasma can be defined as a gas containing charged and neutral species such as electrons, ions, radicals, atoms and molecules. The different types of gas or mixtures of gases used for plasma treatment of polymers include argon, helium, hydrogen, nitrogen, ammonia, nitrous oxide, oxygen (most used due to effectiveness to increase surface energy of polymers), carbon dioxide, sulfur dioxide, water, tetrafluoromethane and fluorine (used to decrease the surface energy). Table 2.6.1.1 shows the improvement in bondability of a polymer was treated with an specific plasma gas [33]. Under normal evaluation conditions, the lap shear strength is a very good indicative of the improvement of the surface treatment.

Plasma treatment can be done to achieve crosslinking of the surfaces of polymeric substrates, introduction of functional groups on polymeric substrates and surface grafting of polymers onto plasma treated substrates [35]. For low temperature plasma treatment, the surface activation is achieved by the introduction of oxygen-containing functional groups, etching by formation of gaseous species, or coating deposition by plasma polymerization [34].

An oxygen plasma can react with a wide range of polymers to produce functional groups as C-O, C=O, O-C=O, C-O-O, and CO_3 at the surface. Two processes occur simultaneously at the surface: etching through the reactions of atomic oxygen with the surface carbon atoms; and the formation of oxygen functional groups through the reaction between the active species from the plasma and the surface atoms [33].

Table 2.6.1.1- Comparison between untreated and treated plasma surfaces

Material	Manufacturer	Type of Material	Preferred Plasma Gas	Lap Shear Strength (MPa)		Improvement
				Control	Plasma	
Valox 310	GE	Polyester thermoplastic	O_2	3.6	11.3	3.1X
Noryl 731	GE	Poly(phenylene ether)	NH_3	4.3	12.4	2.9X
Durel	Hoechst Celanese	Polyarylate	NH_3	1.7	14.9	8.6X
Vectra A625	Hoechst Celanese	Liquid crystal polymer	O_2	6.5	8.6	1.3X
Delrin 503	Du Pont	Acetal homopolymer	O_2	1.1	4.5	3.9X
Ulmen 1000	GE	Poly(ether imide)	NH_3	1.3	14.4	11.3X
Lexan 121	GE	Polycarbonate	O_2	11.8	15.5	1.3X

3. EXPERIMENTAL

The effect of surface treatment on the carbon filler in the Polyurethane-carbon composites was assessed in terms of conductivity, mechanical properties, possible chemical interactions and physical contact between particles.

3.1. Materials

The polymer used in this study was Pellethane 2363 (Dow Chemical Co). The polyurethane was formed by 4,4' diphenyl methane diisocyanate (MDI), polytetramethylene glycol (PTMG) and 1,4 butanediol (BTD). As a result the final structure is a poly(ether urethane). The final chemical structure of Pellethane is illustrated in Figure 3.1.1.

The carbon flakes were provided by Oak Ridge National Laboratory, where plasma treatment was performed on the carbon surface used in the treated samples. Treated carbon fillers had a oxygen content of approximately 3 to 5 wt% (No characterization was undertaken to evaluate the carbon filler prior to be added to the resin). Composites solutions containing different percentages - varying from 10 to 50 wt.% - of carbon filler were prepared (Table 3.1.1). The Polyurethane composite solutions were prepared with dimethylformamide as solvent (10 wt%) mixing at approximately 240 rpm (1-2 min), then deposited onto a Teflon® plate and placed in an oven (80°C) during 24 hours. The thin films were finally dried in a vacuum oven at 50°C for another 24 hours to ensure elimination of all residual solvent and moisture. The samples were then stored in a desiccator. Figure 3.1.2 shows the surface of two samples, one is the control Pellethane sample (Pel) and the Pellethane with 50 wt % of untreated C (50uC).

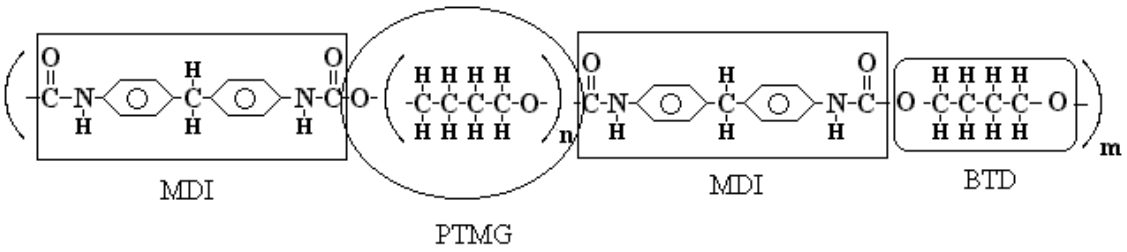

Figure 3.1.1. Chemical structure of Pellethane. 'm' and 'n' are estimated to be approximately 100 and 24, respectively.

Table 3.1.1. Sample description

Sample	Filler	Wt.% of filler
Pel	None	0
10C	Treated Carbon	10
20C	Treated Carbon	20
30C	Treated Carbon	30
40C	Treated Carbon	40
50C	Treated Carbon	50
10uC	Untreated Carbon	10
20uC	Untreated Carbon	20
30uC	Untreated Carbon	30
40uC	Untreated Carbon	40
50uC	Untreated Carbon	50

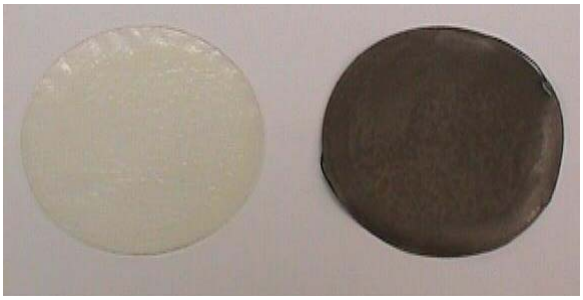

Figure 3.1.2. Comparison between two samples ; unfilled and 50 wt% of untreated C

3.2. Theoretical Techniques Background

3.2.1. Four Point Probe Conductivity

In a four point probe apparatus, four contacts are necessary in the sample. A known current is applied and according with the voltage obtained, a resistance value can be calculate. Figure 3.2.1. illustrates a typical sample with the 4 contacts (two for current and two for measuring the voltage) and the dimensions necessary to obtain the conductivity using Equations 15-17.

$$R = \frac{V}{I} \qquad \text{Equation 15}$$

$$\rho = R * \frac{w * t}{l} \qquad \text{Equation 16}$$

$$\sigma = \frac{1}{\rho} \qquad \text{Equation 17}$$

where,

R → resistance

V → voltage between the contacts

I → applied current

ρ → resistivity

σ → conductivity ($\Omega^{-1}cm^{-1}$ = S/cm)

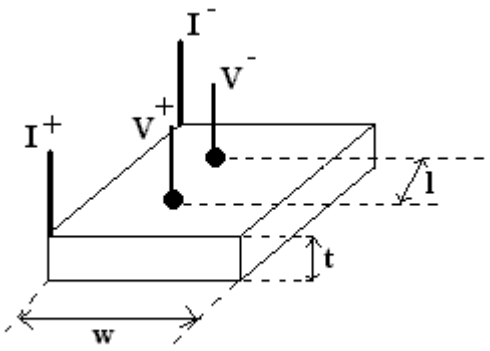

Figure 3.2.1. Conductivity sample

3.2.2. Dynamic Mechanical Analysis

The most popular mode of dynamic mechanical analysis is a forced strain modulation method in which a sinusoidal strain is applied to a solid sample and mathematically treats the a sinusoidal stress response. First, the sinusoidal strain ε of angular frequency ω (2π times the frequency in Hz) can be expressed as in Equation 18 if the material obeys Hooke's law, that is for an elastic material (ε_0 is the strain amplitude).

$$\varepsilon = \varepsilon_0 \sin\omega t \qquad \text{Equation 18}$$

The stress generated by the specimen is also sinusoidal but contains the out of phase angle (or phase lag) δ if the material is viscoelastic, as shown in Equations 19. The stress can be considered as being divided into two components; one in same phase, sinωt, and one in π/2 out of phase, cosωt, with the strains; i.e., $\sigma_0\cos\delta$ and $\sigma_0\sin\delta$ respectively (Equation 20).

$$\sigma = \sigma_0 sin(\omega t + \delta)$$ Equation 19

$$\sigma = \sigma_0 sin\omega t \cos\delta + \sigma_0 \cos\omega t sin\delta$$ Equation 20

From the stress-strain relationship, two dynamic moduli are defined, E' in phase and E" out of phase. The stress σ can be defined as Equation 21, and the phase angle δ defined by Equation 22 [30] .

$$\sigma = \varepsilon_0 E' sin\omega t + \varepsilon_0 E'' \cos\omega t$$ Equation 21

$$\tan\delta = \frac{sin\delta}{\cos\delta} = \frac{E'}{E''}$$ Equation 22

3.2.3. Tensile Strength Measurements

From the stress-strain curve the mechanical properties were obtained using the following equations for modulus, ultimate tensile strength and toughness (Equations 23-25).

$E = \frac{\Delta\sigma}{\Delta\varepsilon}$ in the elastic zone. Equation 23

$$UTS = \frac{\sigma_{UTS}}{\varepsilon}$$ Equation 24

$$U_T = \int_0^{\varepsilon} \sigma d\varepsilon$$ Equation 25

where,

E → modulus of elasticity

σ → stress

ε → strain

UTS → ultimate tensile strength

σ_{UTS} → maximum stress

U_T → Toughness

3.2.4. Infrared Spectroscopy

Infrared (IR) spectroscopy is a measure of the absorption of infrared light energy as a function of wavelength or frequency. The absorption of IR radiation takes place when the vibrational energy of the chemical moiety or groups in the molecules is matched with the energy of incident IR radiation and there is dipole moment change during the excitation generated by the interaction of the molecules with the electric field component of the electromagnetic radiation. The general rule is the stronger the dipole moment generated, the greater the absorption of IR radiation at the same vibrational energy. Figure 3.2.4.1 illustrates the vibrational frequency of interatomic bonds and change in the dipole moment.

Infrared spectrometers measure the absorption of infrared radiation as a funcion of the light frequency. The frequency at which radiation is absorbed is determined by the

vibrational modes of intermolecular bonds (bending, stretching, out of plane vibrations, wagging, rocking, and harmonics of these motions). Table 3.2.4.1 lists some major infrared band assignments for polyurethane.

3.2.5. Scanning Electron Microscopy

The impingement of a electron beam on the surface of materials leads to variety of electron emission such as secondary electrons (SE), backscattered electrons (BE), elastic scattered, auger electrons. The image is obtained by the reflected electron signal and captured by a detector. Secondary electrons have low energy, and they do not travel far

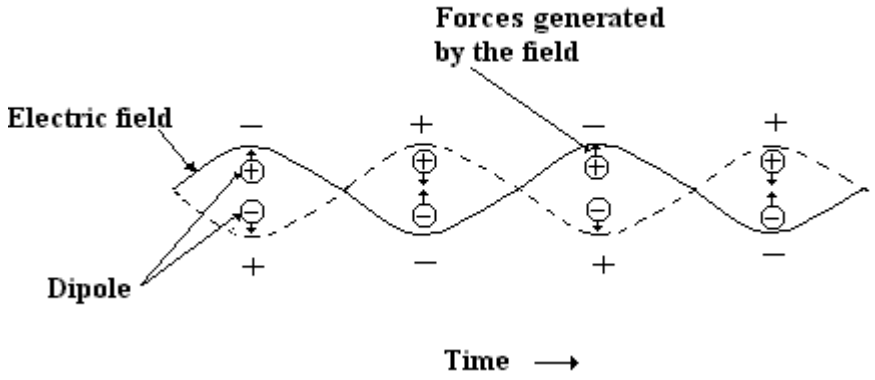

Figure 3.2.4.1. Diagram of the interaction of an oscillating electric field (light) with a vibrating dipole.

Table 3.2.4.1. Infrared band assignments for PU

Wavenumber (cm^{-1})	Assignment	Mode
3307-3287	(N-H) urea urethane, H-bonded	Stretching
2871-1856	(C-H) in CH_2	Assymetric Stretching
1732-1727	(C=O) free urethane	Stretching
1718-1709	(C=O) H-bonded urethane	Stretching
1649-1634	(C=O) H-bonded urea	Stretching
1599-1591	(C=C) aromatic ring	Stretching
1547-1532	(C-N)+(N-H) urethane	Stretching+Bending/Scissoring
1491-1459	(C-H) in CH_2	Assymetric Scissoring
1473-1446	(C-H) in CH_2	Symetric Scissoring
1412	(C=C) in aromatic ring	Stretching
1370	(C-H) in CH_2	Bending and Wagging
1310	(C-H) in aromatic ring	Scissoring
	(C-N)	Stretching
1270-1230	(=C-O-) ethers	
1221	(C-N)+(N-H)	Stretching+Bending/Scissoring
1225	(C-F)	
1200-1180	(O=CH-O-R) Formates	Stretching
1113-1105	(O=C-O-C) of urethane	Symetric stretching
	(C-O-C) of ether	Stretching
965-820	(O=C-O) of urethane	Bending or Wagging

in the sample. In the case of our experiment, a secondary electron detector as illustrated in Figure 3.2.5.1 was used to obtain the image.

3.3. Procedures

3.3.1. Four Point Probe Conductivity

A resistivity probe, integrated by a Keithley 220 current source, a Keithley 2182 nanovoltmeters and a Lakeshore 82C temperature controller was used to measure the conductivity of the samples. The geometry of the measuring device is a four-probe type and two samples can be measured simultaneously at a temperature ranging from 12 to 310 K. All the measurement parameters were controlled by a PC interface powered by Labview 6.0, with a real-time data display The current used for all tests was of 1mA, and sample dimensions were approximately 3 x 3 x 0.15mm ('w' x 'l' x 't').

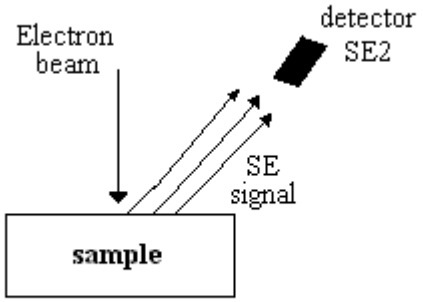

Figure 3.2.5.1. Sketch of a SEM with a secondary electron detector

3.3.2. Dynamic Mechanic Analysis

The Dynamic mechanic analysis (DMA) was performed by using a DTMA V from Rheometric Scientific. Two types of test were performed using this technique. The first, referred as dynamic temperature ramp, submitted the samples to a frequency of 10Hz and a temperature ranging from -140° C to 150° C, at a heating rate of 2^{o}C/minute. The second type of dynamic test used is referred as dynamic time sweep, submitting the samples to a frequency of 20Hz for 80 minutes (96,000 cycles) and 720 minutes (864,000 cycles) at room temperature for the determination of the effect of cyclic loads in the physical properties of the samples.

3.3.3. Tensile Strength Measurement

Mechanical tensile testing was carried out according to ASTM D 1708 tensile test procedure, using an Instron tensile tester (Table Model 1112) as illustrate in Figure 3.3.3.1. The gauge length of the samples was 22 mm and the crosshead speed was 10 mm/min. Mechanical properties such as elastic modulus, ultimate tensile strength and toughness (maximum at 300%) were determined from the mechanical test data.

3.3.4. Infrared Spectroscopy

A BioRad FTS-6000e Infrared Spectrometer equipped with a UMA-300 infrared microscope was used to obtain the IR spectra. The software used to analyze the scans was the IR Winpro®. A total of 1024 scans at a resolution of 4 were the parameters for all tests.

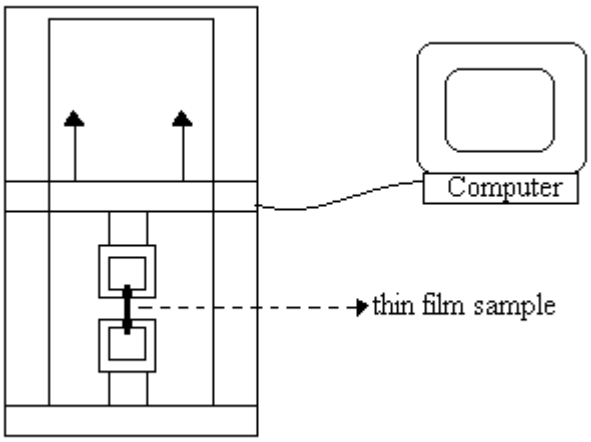

Figure 3.3.3.1. Sketch of the tensile machine

3.3.5. *Scanning Electron Microscopy (SEM)*

A Leo 1525 Gemini field emission scanning electron microscopy (FESEM) was used to analyze the fractured surfaces of the samples. A minimum emission voltage of 1 KV was used due to charging of the samples. The samples were dipped in liquid nitrogen, fractured and mounted on an aluminum sample holder. The upright placement allowed the fractured surface to be view at small working distances. No coating was necessary.

4. RESULTS

4.1. Conductivity

Figures 4.1.1 and 4.1.2 show the relationship between electric conductivity and carbon concentration in the composites at 23°C and -185°C, for treated and untreated carbon. The conductivity for both composites (treated and untreated) have similar behavior, where in low concentrations the conductivity is lower, an abrupt increase in conductivity is observed when the concentration increases and at higher concentration the conductivity achieves a plateau at 30% of carbon content. The composites based on the untreated carbon showed a higher conductivity for lower concentrations of carbon in both temperatures.

The variation of the conductivity with temperature for all composites are given in Figures 4.1.3 to 4.1.7. Both groups of composites exhibit similar temperature dependence and can be observed in figures 4.1.8 and 4.1.9, where the change in conductivity is expressed in percentage (%). For low concentrations and low temperatures, no change was observed in conductivity, while at higher temperature a dip in conductivity is observed around 240 K (~33°C) in all composites. For all compositions, the untreated composites presented higher conductivity.

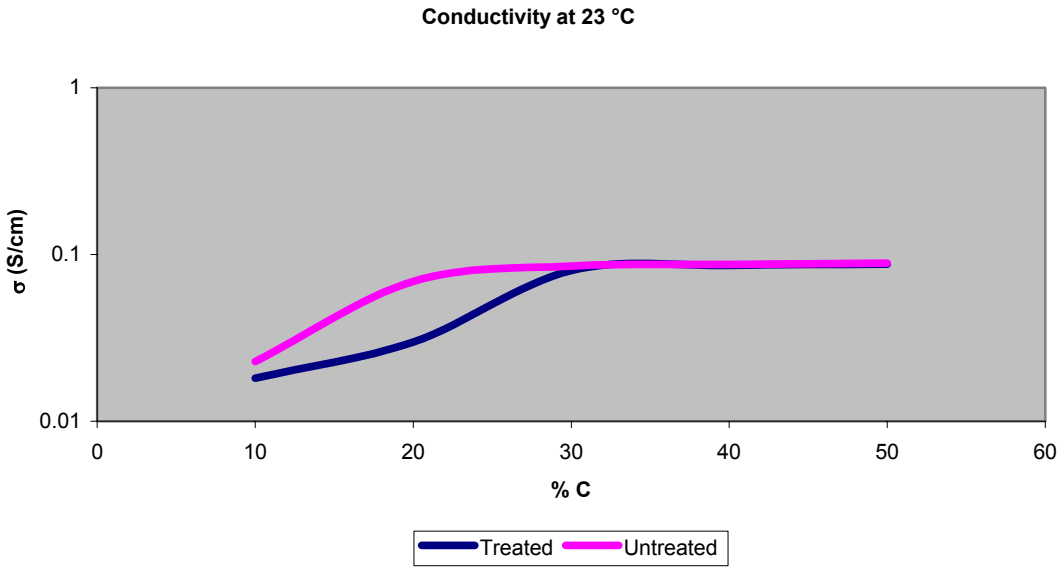

Figure 4.1.1. Conductivity at 23 °C according to the concentration of carbon

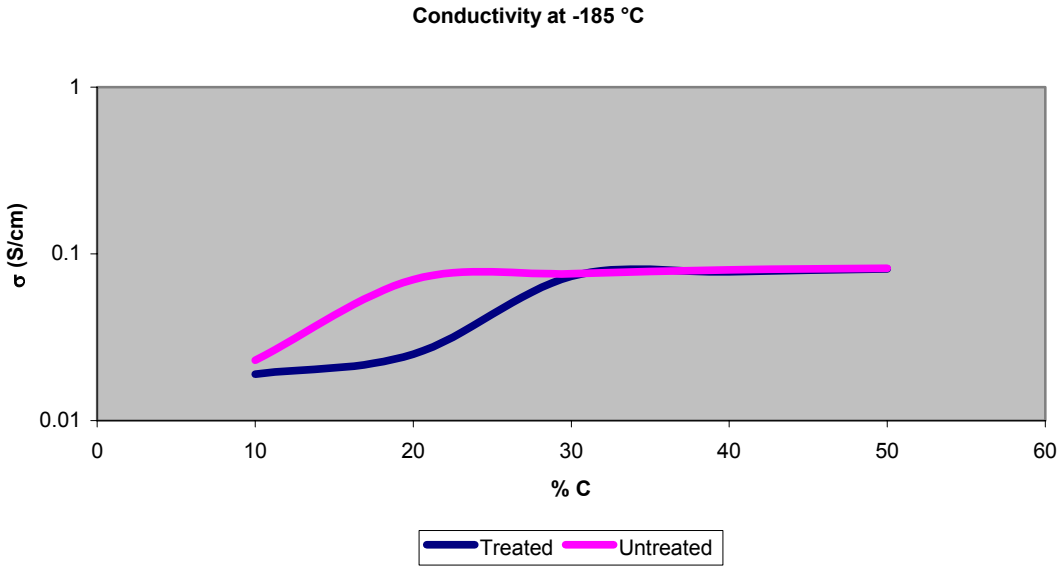

Figure 4.1.2. Conductivity at -185 °C according to the concentration of carbon

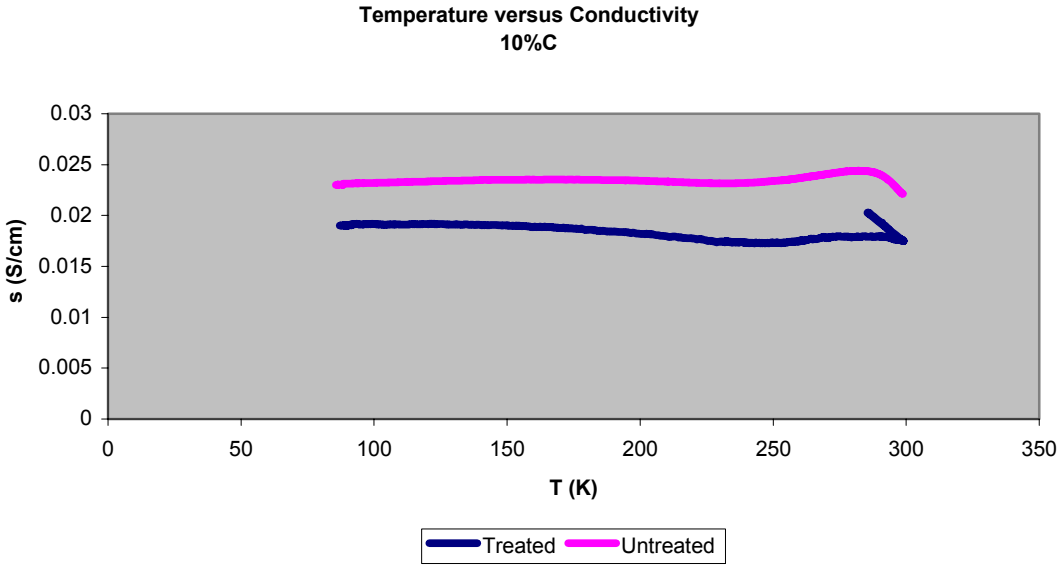

Figure 4.1.3. Conductivity according to temperature for 10% C composites

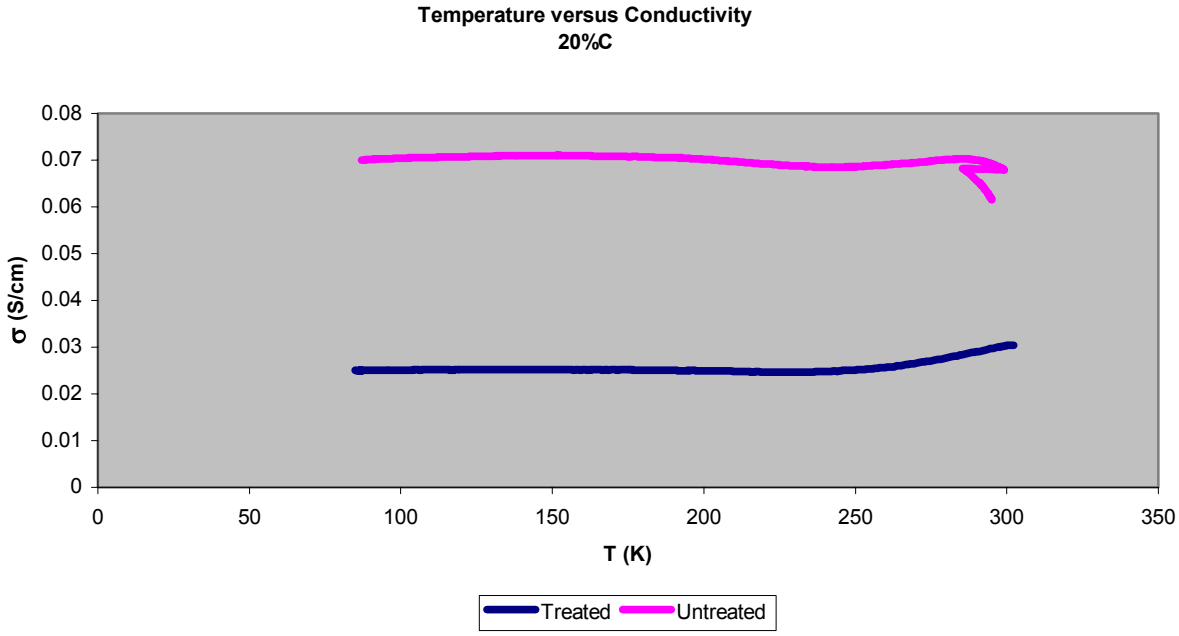

Figure 4.1.4. Conductivity according to temperature for 20% C composites

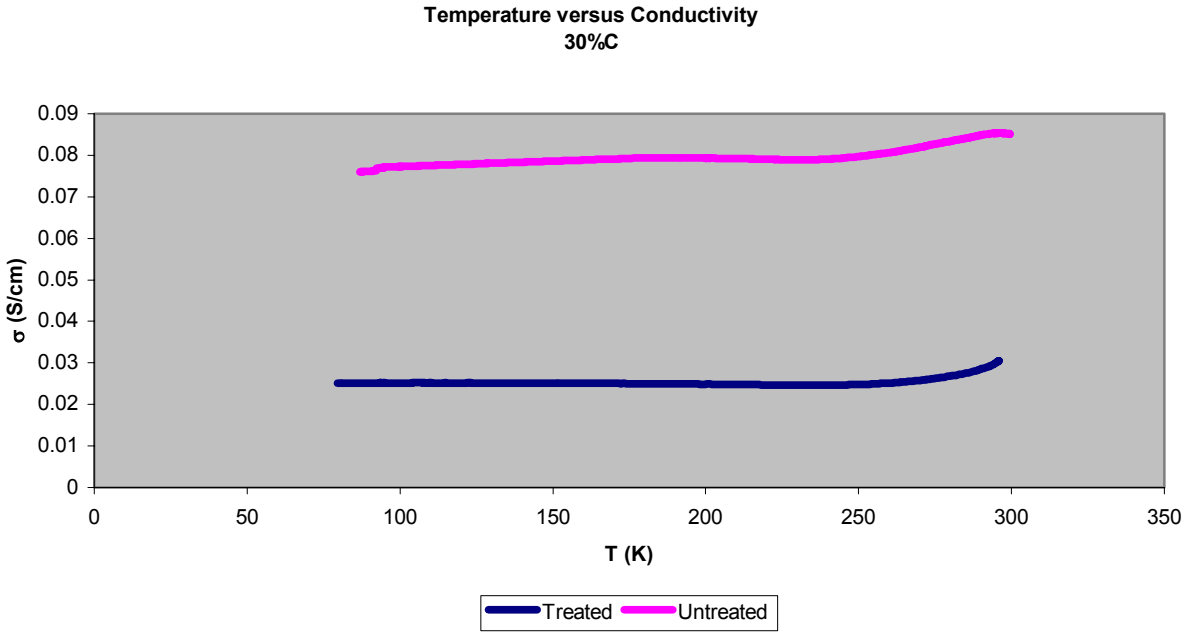

Figure 4.1.5. Conductivity according to temperature for 30% C composites

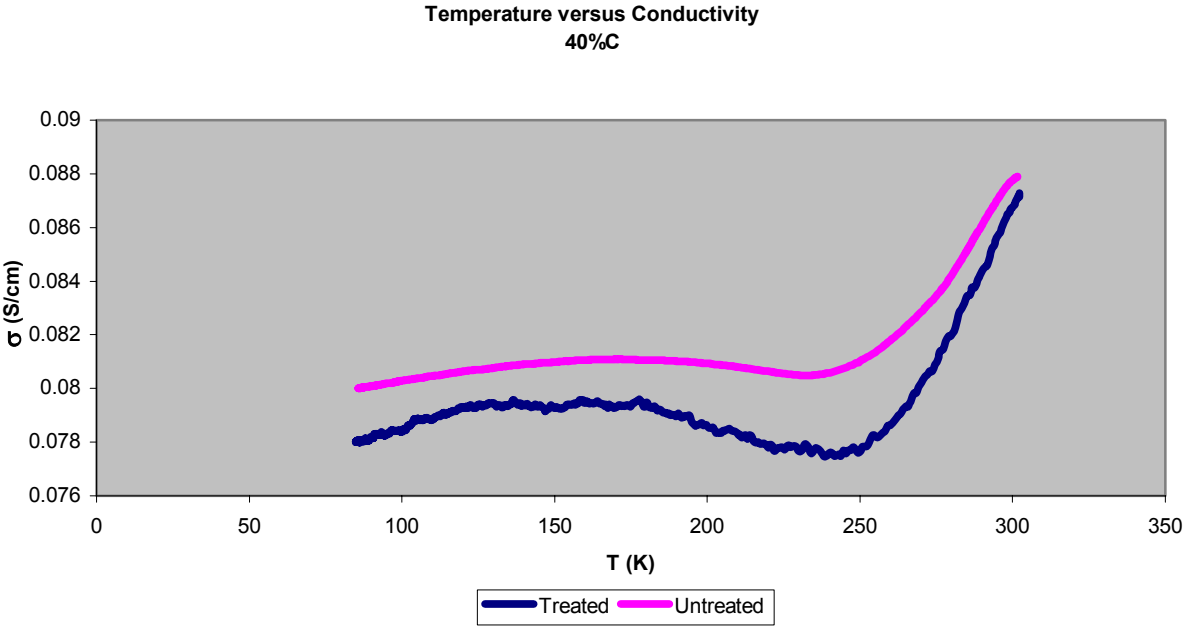

Figure 4.1.6. Conductivity according to temperature for 40% C composites

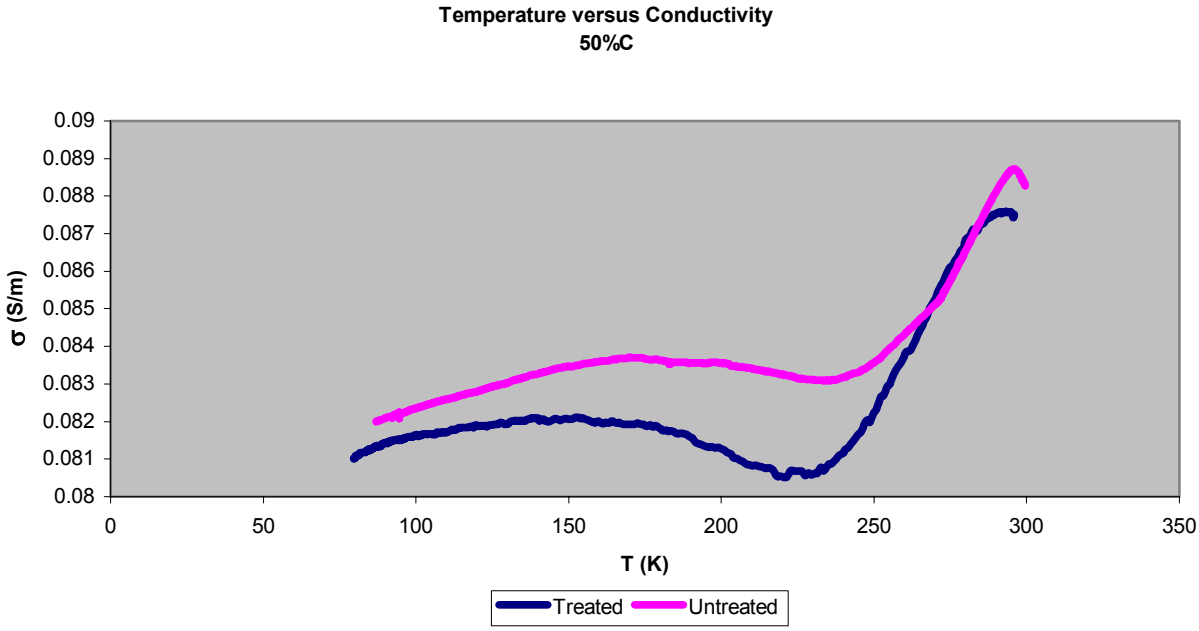

Figure 4.1.7. Conductivity according to temperature for 50% C composites

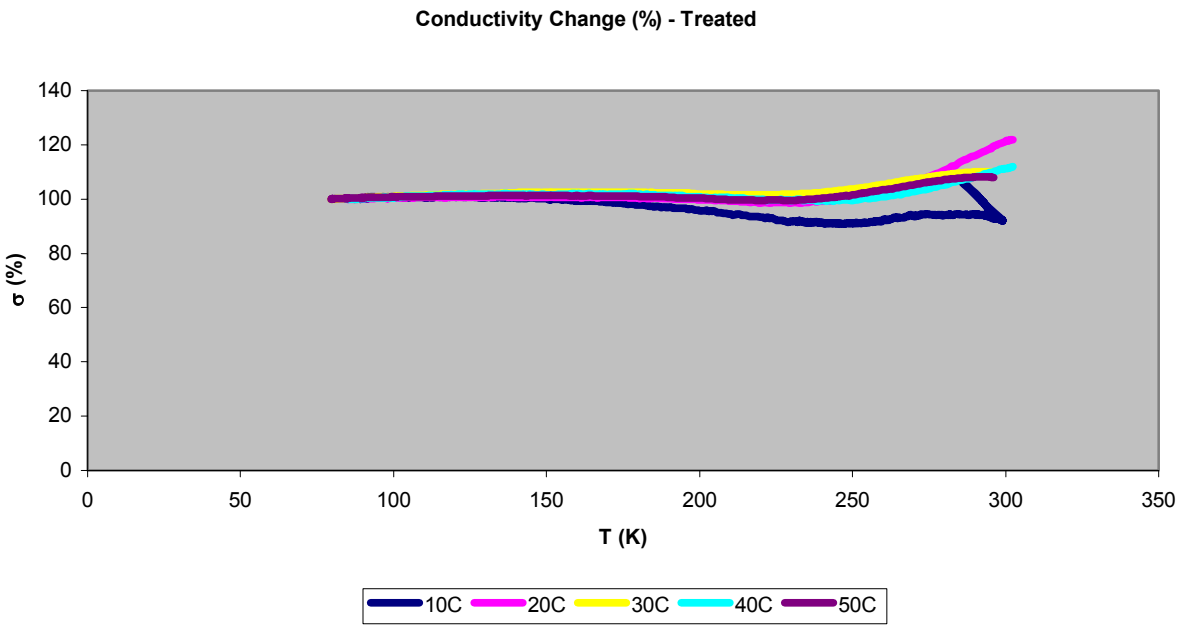

Figure 4.1.8. Conductivity change for treated carbon composites

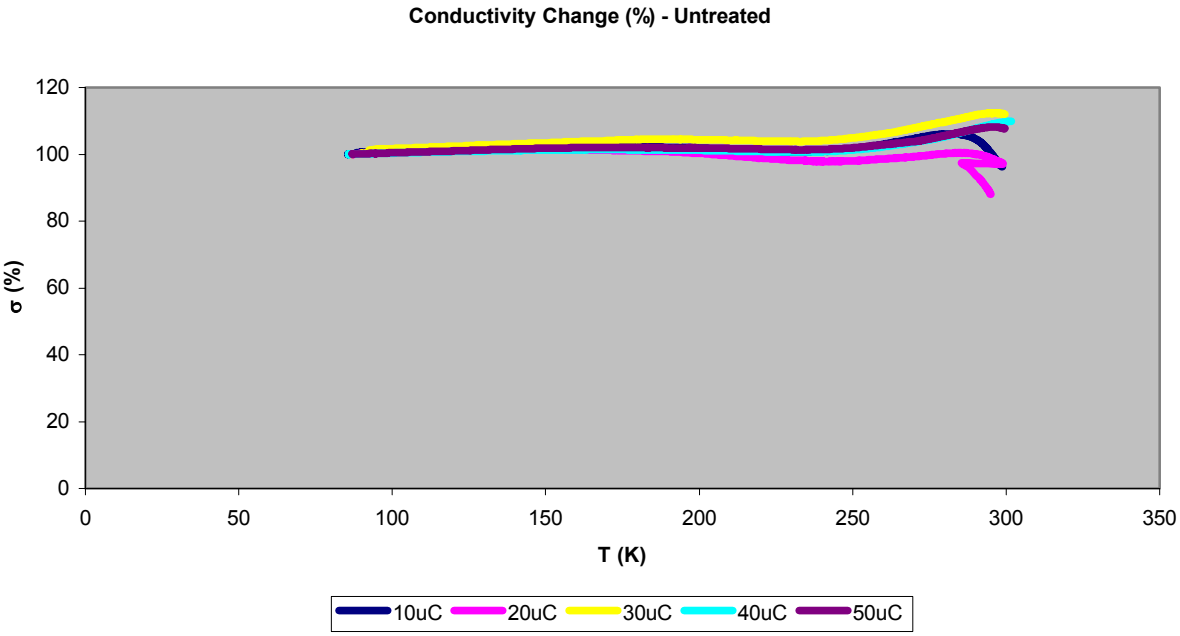

Figure 4.1.9. Conductivity change for untreated carbon composites

4.2. Dynamic Mechanic Analysis

Dynamic Mechanic Analysis provides information regarding the temperature dependence of E' , E'' and Tan δ. Figures 4.2.1 - 4.2.3 show the storage modulus, loss modulus and loss tangent for the composites with treated carbon fillers, and Figures 4.2.4 - 4.2.6 for the composites with untreated carbon fillers. The dynamic mechanical properties exhibit a dependence on the concentration of carbon present, especially for the treated composites. Note that 'Pel' means the unfilled sample (pure polymer).

Figure 4.2.7 shows change in Tg with concentration of carbon in the composite (according to Tan δ analysis). For the carbon treated composites, Tg shifts to higher temperatures with increase in carbon content until reaches 50%C when shifted to lower temperature. For the untreated composites, only the sample with 20%C shifted to higher temperatures .

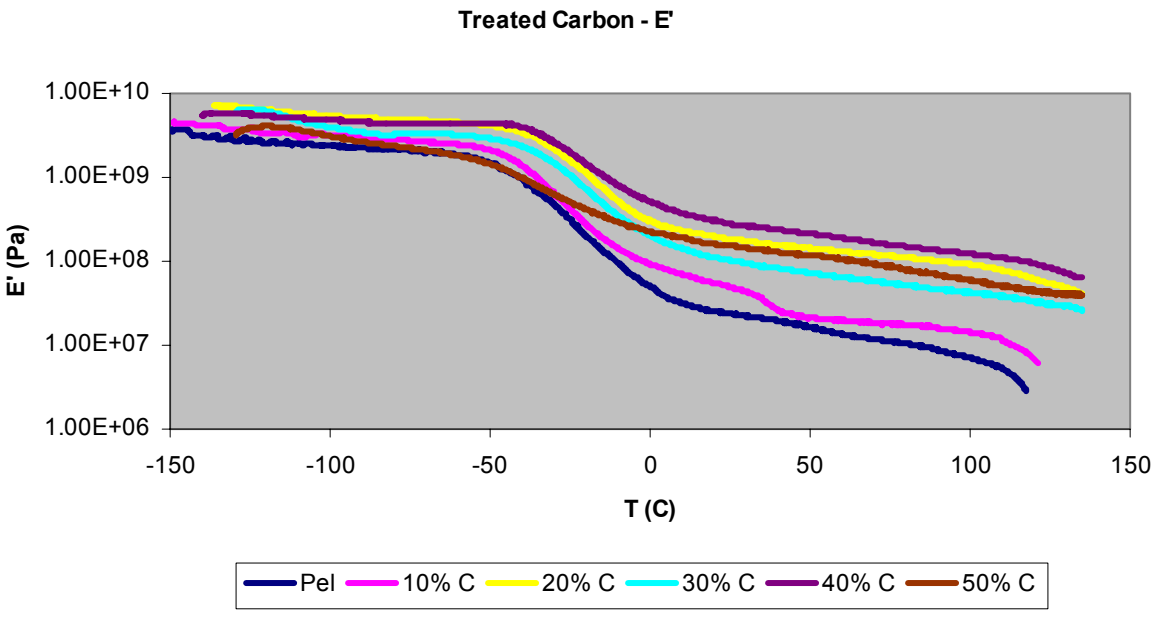

Figure 4.2.1. Elastic Modulus for treated composites

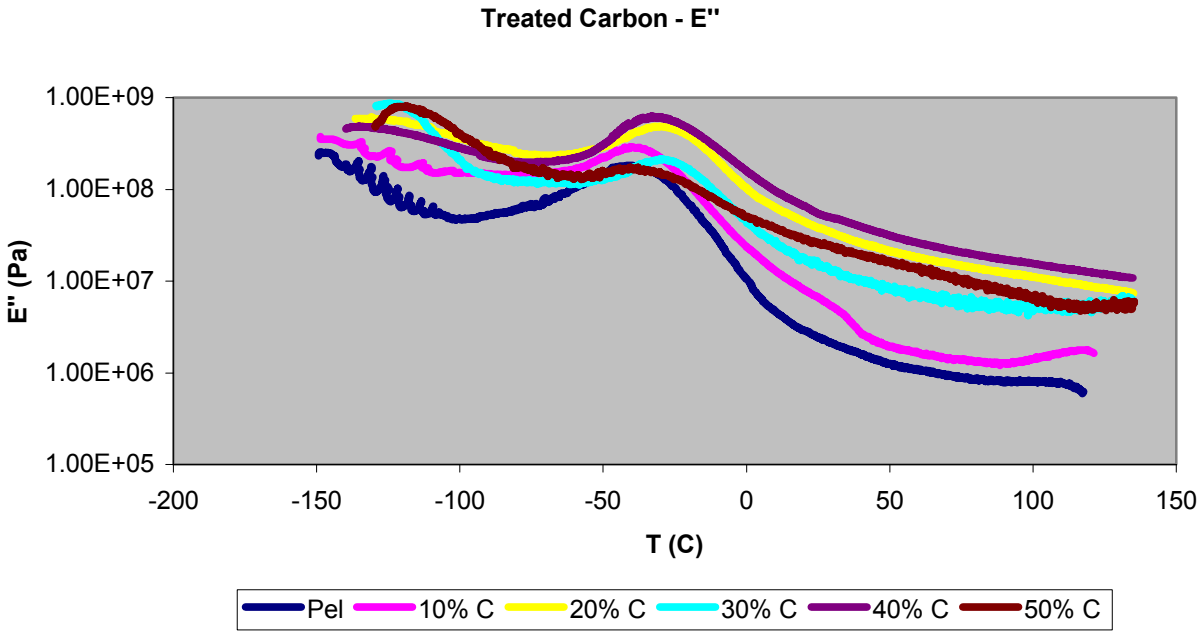

Figure 4.2.2. Loss Modulus for treated composites

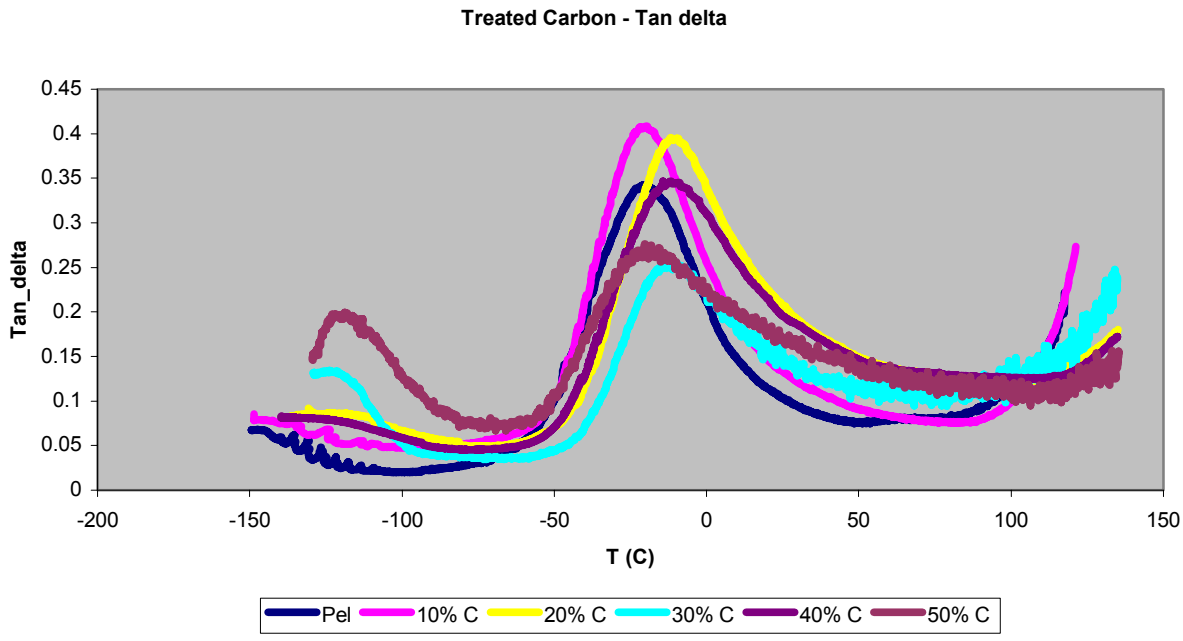

Figure 4.2.3. Tan δ for treated composites

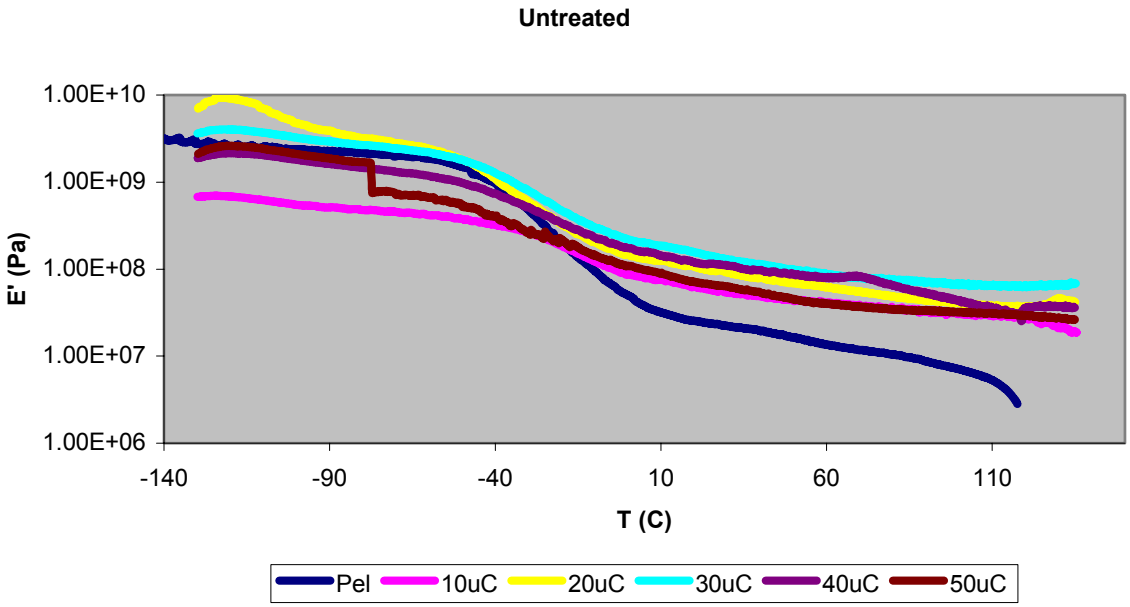

Figure 4.2.4. Elastic Modulus for untreated composites

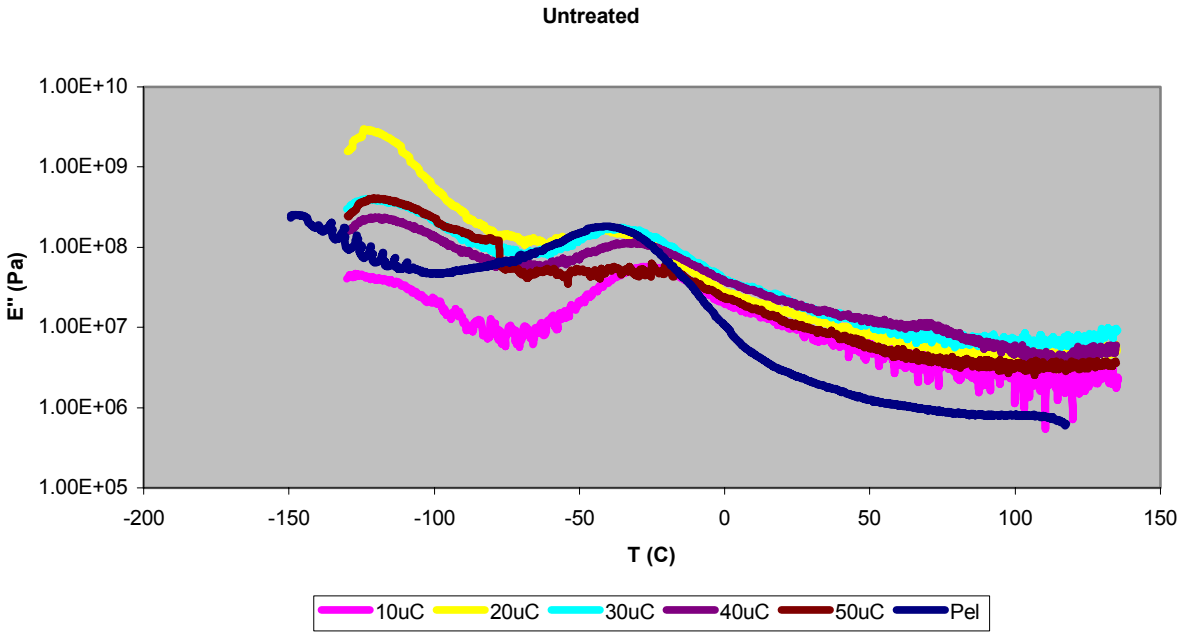

Figure 4.2.5. Loss Modulus for untreated composites

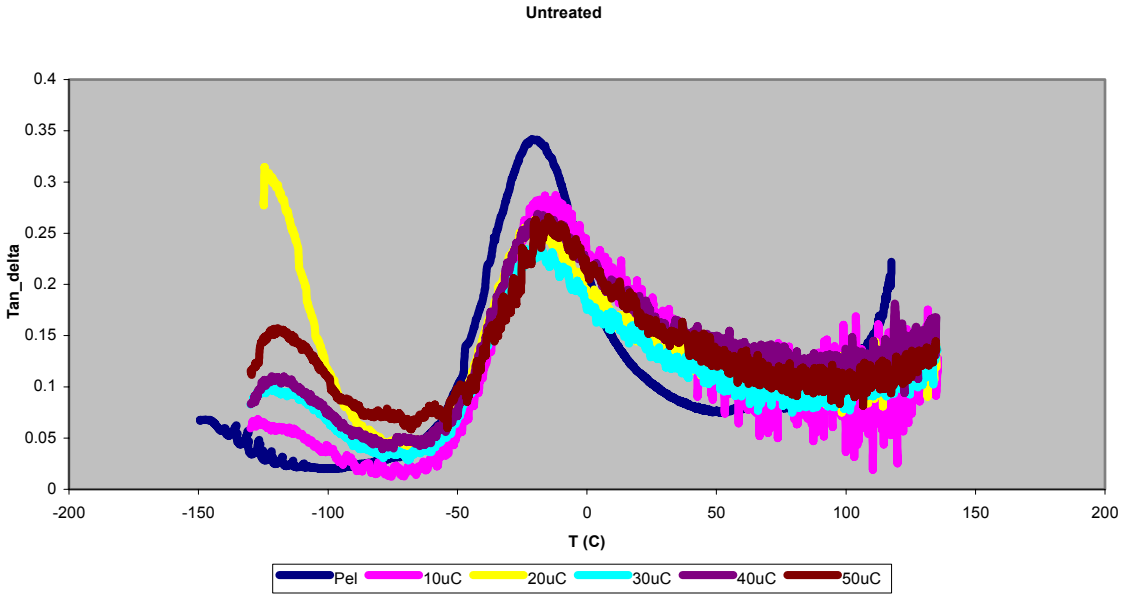

Figure 4.2.6. Tan δ for untreated composites

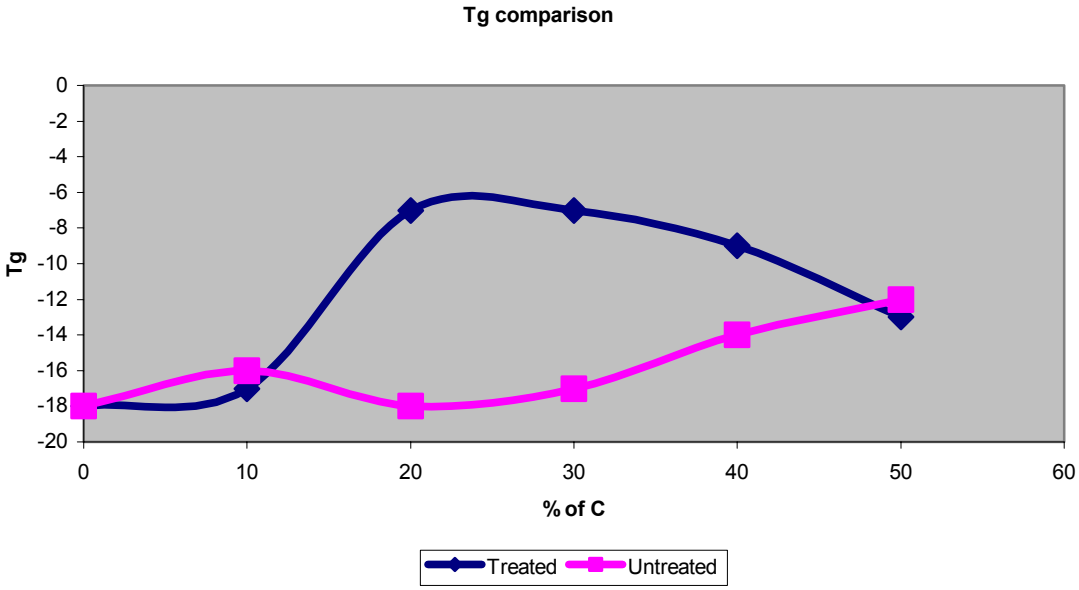

Figure 4.2.7. Variation of glass transition temperature with carbon concentration

4.3. Mechanical Properties

Stress versus strain curves were obtained for all composite materials studied. Figures 4.3.1 and 4.3.2 show the behavior of each composite, based on treated and untreated carbon, respectively. Figures 4.3.3 to 4.3.7 are composite plots for comparing the samples within each group. No difference was noticed between the treated and untreated filler containing samples with 10% carbon content. At 20% carbon content the untreated samples showed a shift to higher stress and higher elongation at fracture , while for 30% the treated showed the shift to higher stress for a strain between 0 – 0.3. For 40% and 50% the carbon treated composites presented higher elongation while the carbon untreated composites presented higher modulus.

The mechanical properties in terms of Young's modulus (E) (or elastic modulus), ultimate tensile strength (UTS) and toughness were analyzed using Figures 4.3.8 to 4.3.13. The results are shown as average of 3 measurements and the error bars represent the range. The E for carbon treated composites increases with the carbon content up to 30% when starts to decrease. The UTS remains constant, but a slightly drop is observed after 20 wt % of carbon. Samples for pure polymer (Pel) and 10%C did not fracture before the machine reached its extension limit, so their calculated toughness was based on the energy absorbed not at fracture, but at around 300% strain. For treated samples the toughness tended to decrease with increase of carbon content. The mechanical properties calculated for untreated and treated composites presented the same trend, but the E increased all the way with the increase in carbon content instead of only 30% as presented the carbon treated composites. Figures 4.3.14 to 4.3.16 compares the E, UTS and toughness between treated and untreated samples.

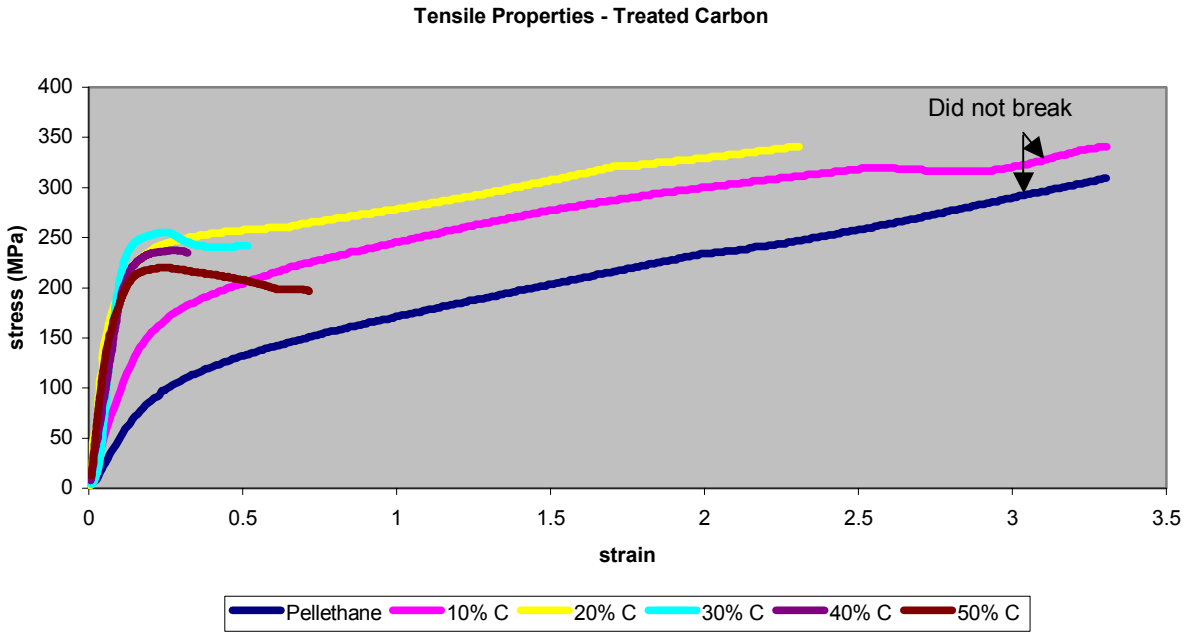

Figure 4.3.1. Stress-strain curve for treated carbon composites

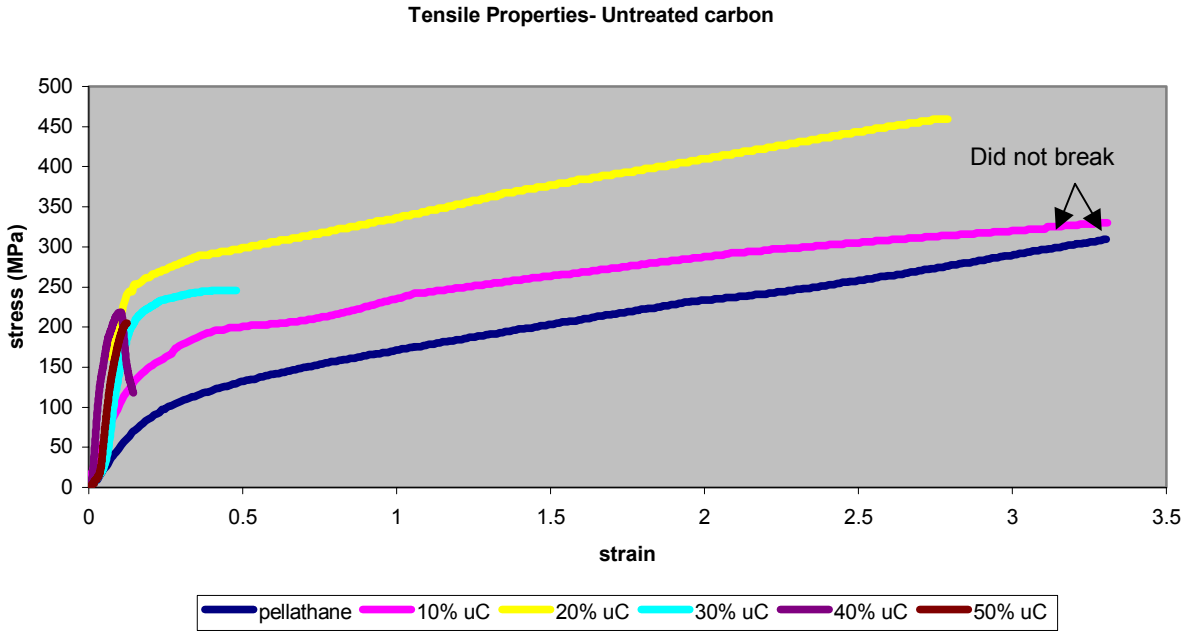

Figure 4.3.2. Stress-strain curve for untreated carbon composites

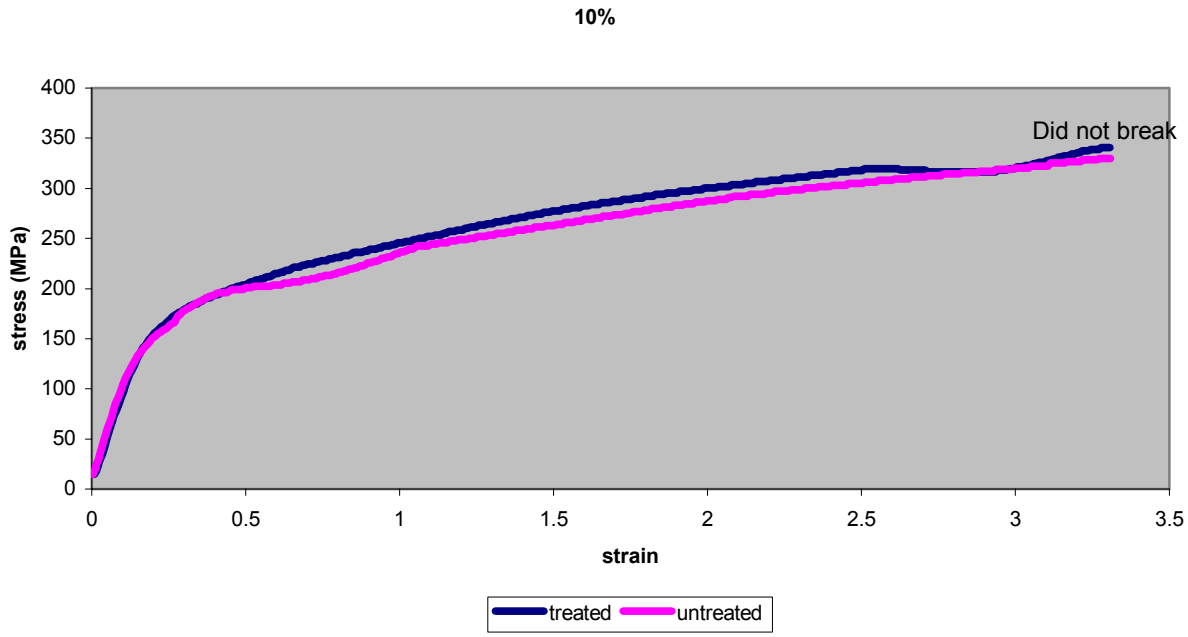

Figure 4.3.3. Stress-strain curve for 10% carbon composites

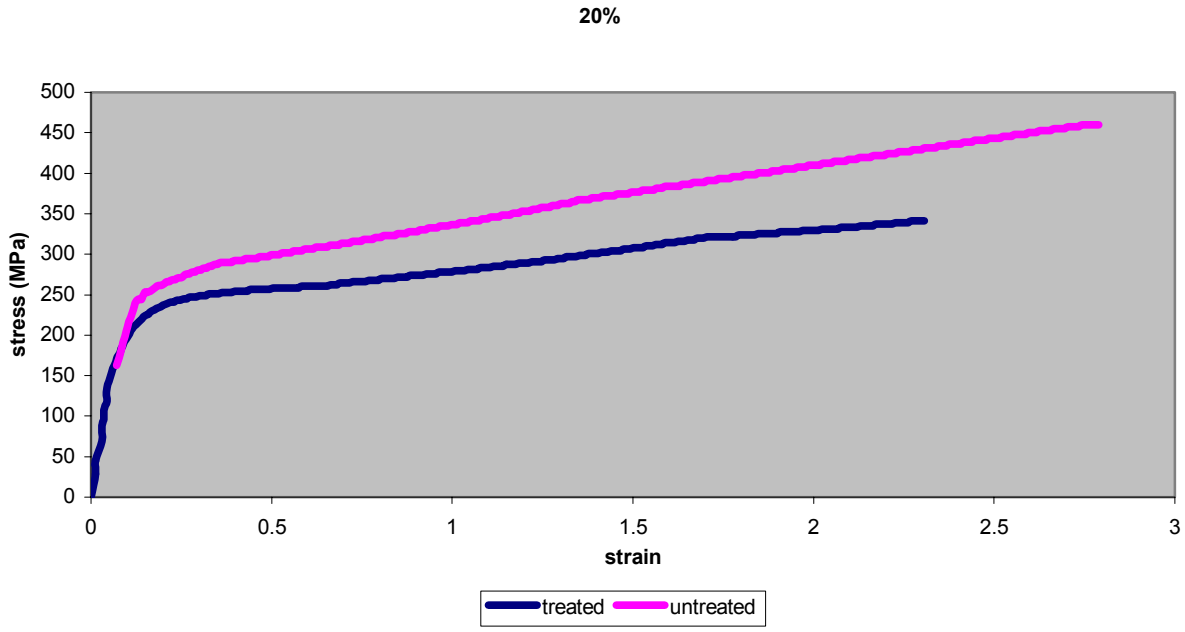

Figure 4.3.4. Stress-strain curve for 20% carbon composites

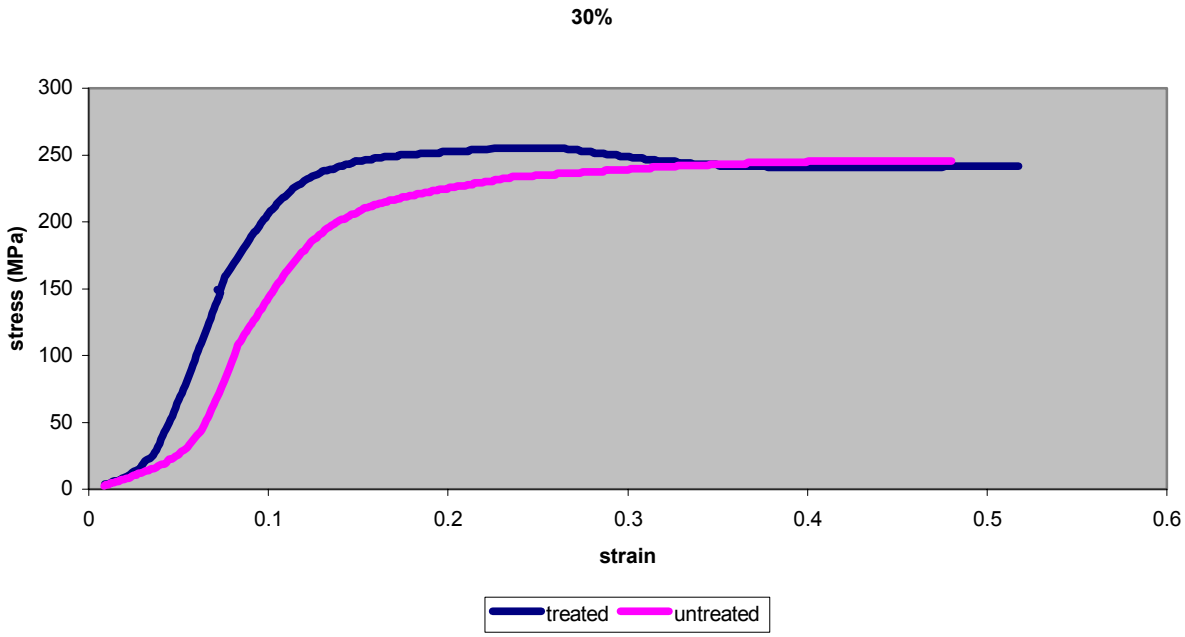

Figure 4.3.5. Stress-strain curve for 30% carbon composites

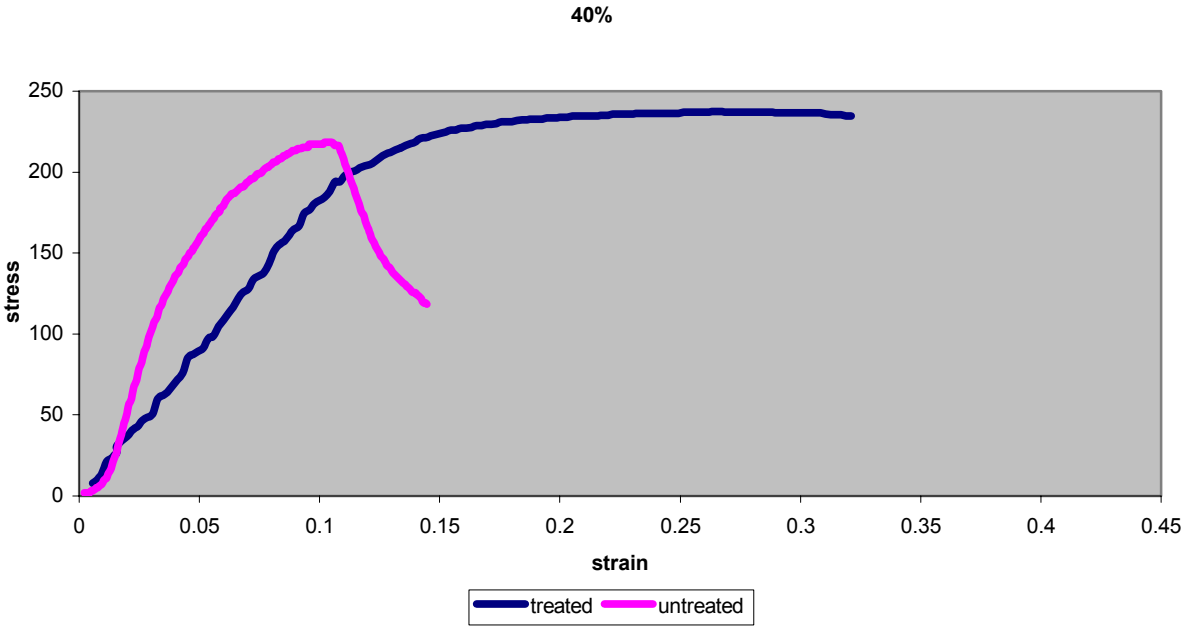

Figure 4.3.6. Stress-strain curve for 40% carbon composites

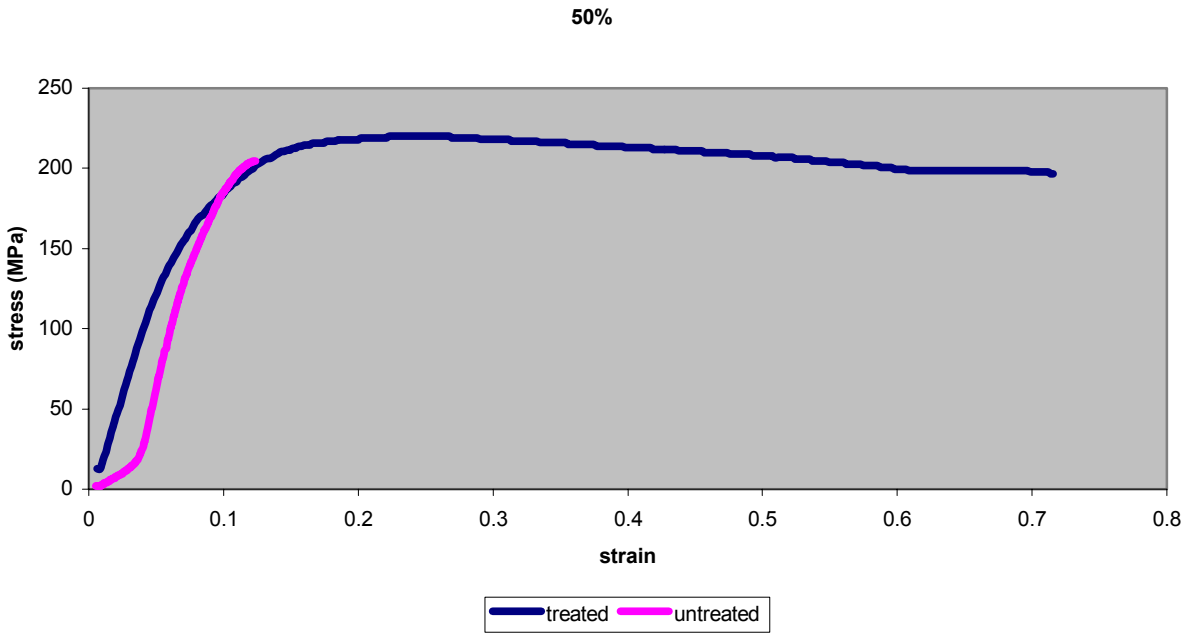

Figure 4.3.7. Stress-strain curve for 50% carbon composites

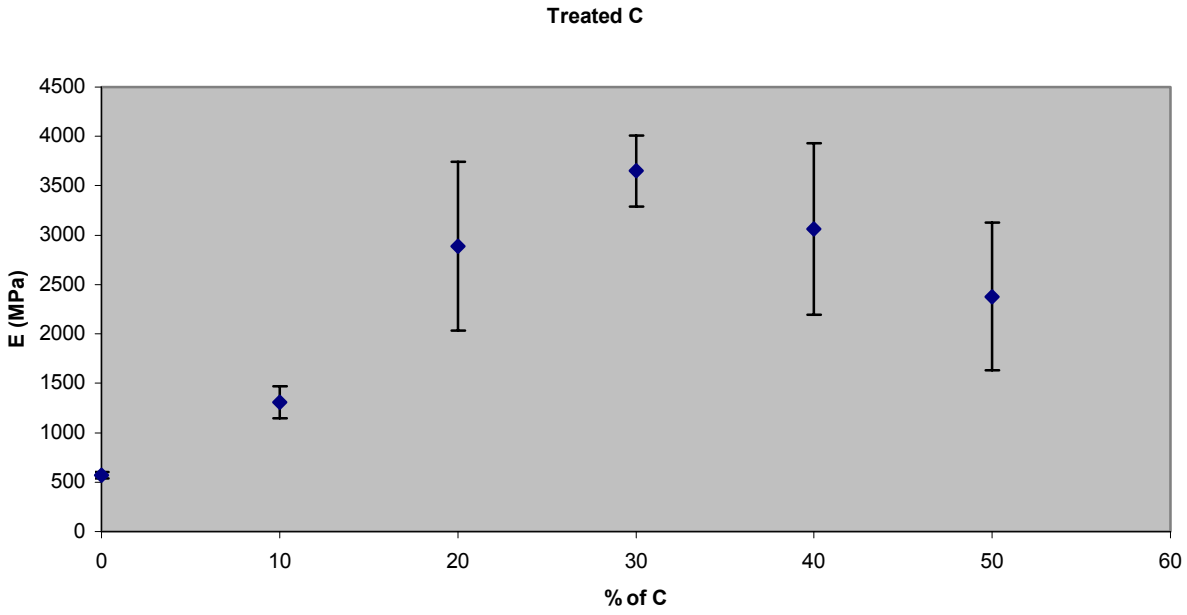

Figure 4.3.8. Elastic Modulus versus carbon content for treated composites

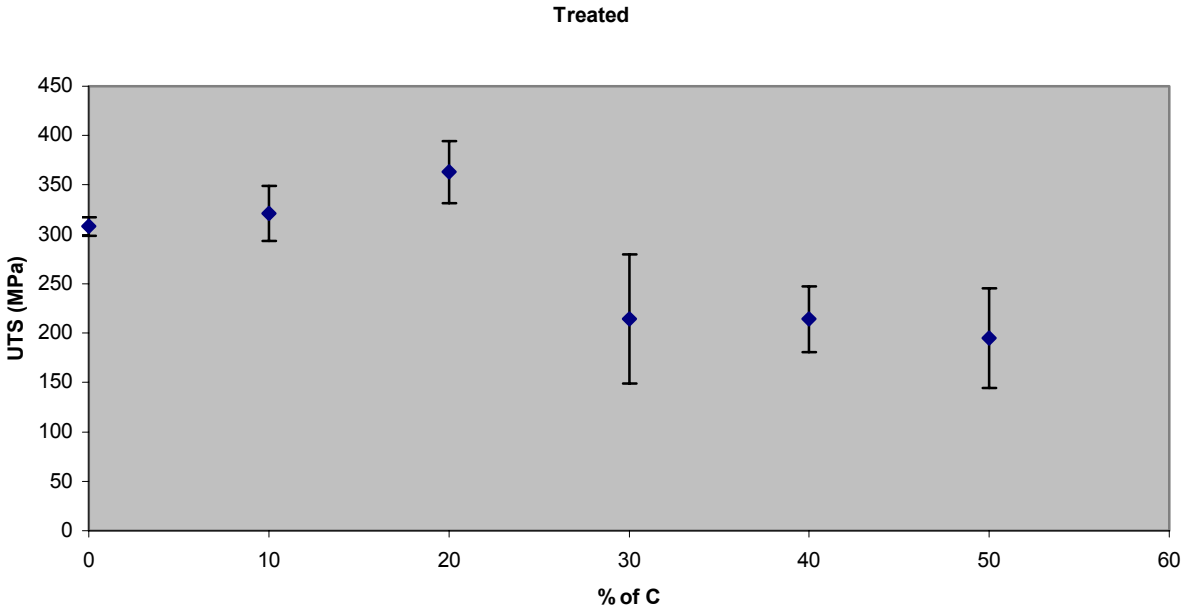

Figure 4.3.9. Ultimate Tensile Strength versus carbon content for treated composites

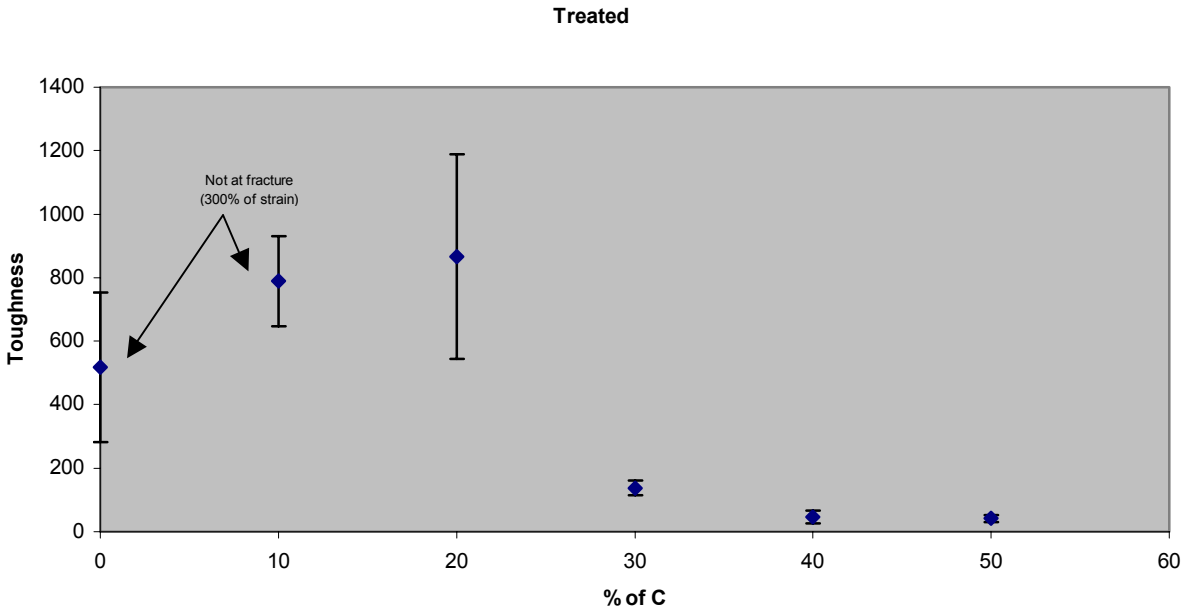

Figure 4.3.10. Toughness versus carbon content for treated composites

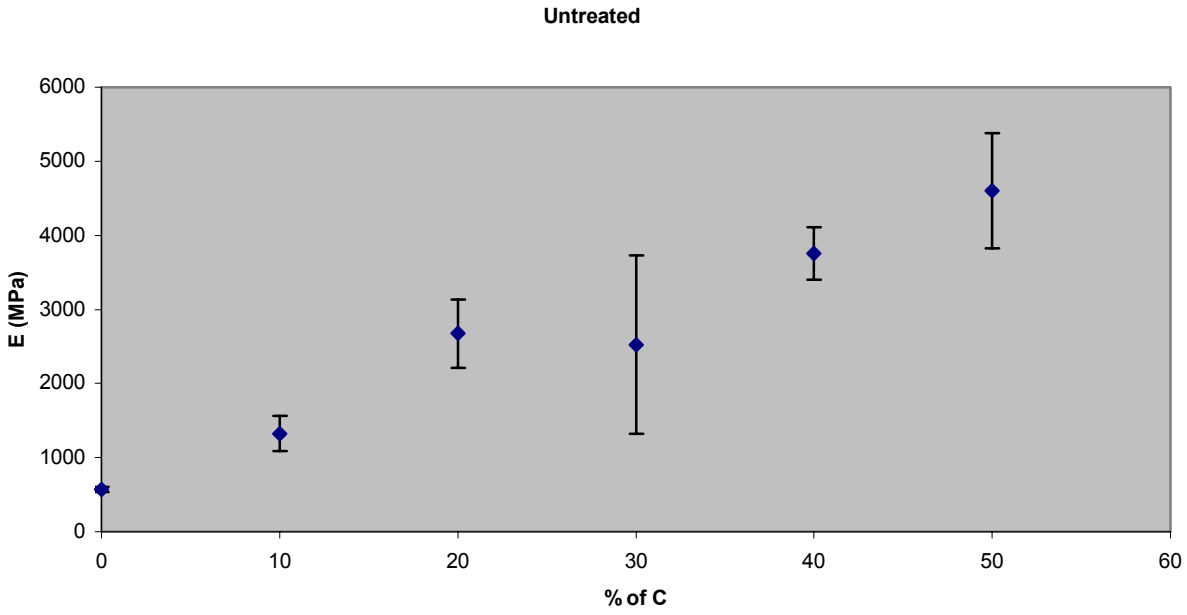

Figure 4.3.11. Elastic Modulus versus carbon content for untreated composites

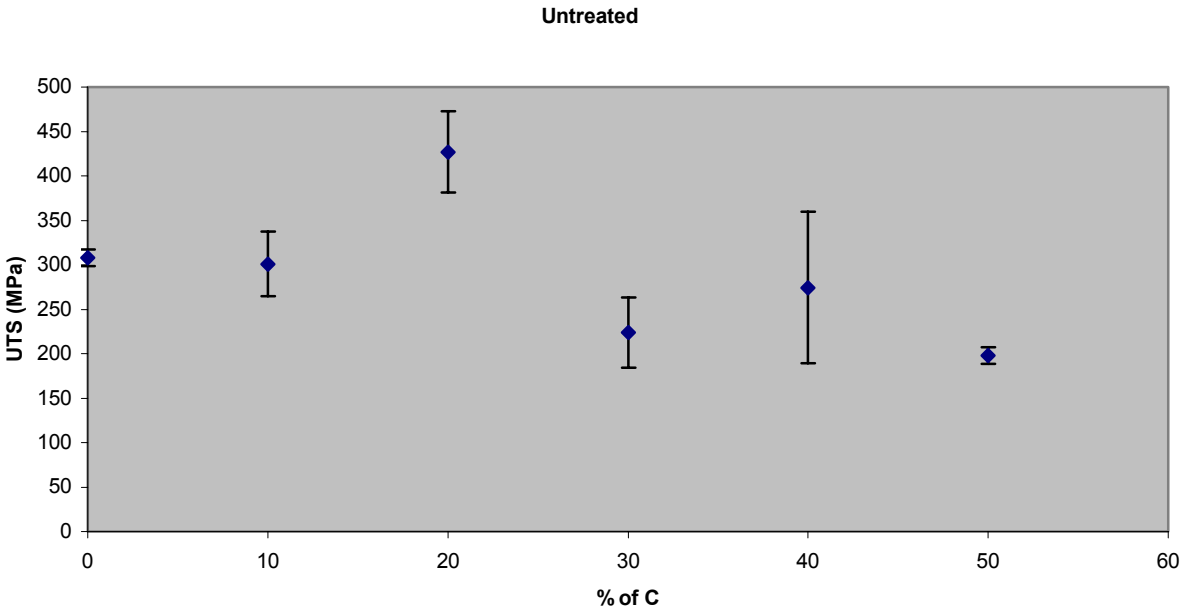

Figure 4.3.12. Ultimate Tensile Strength versus carbon content for untreated composites

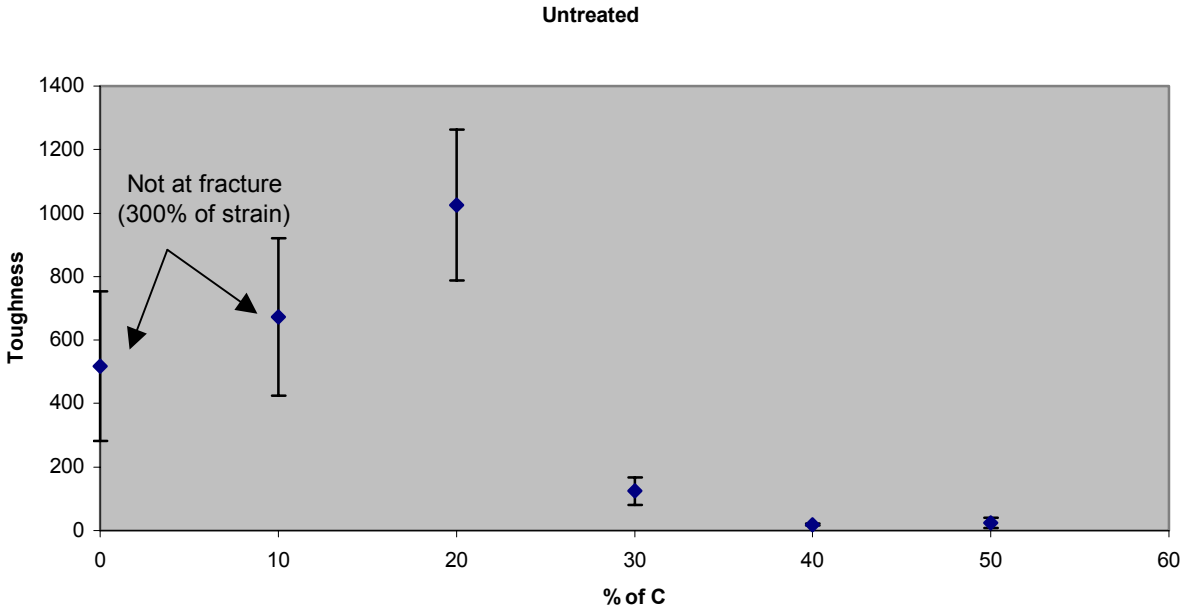

Figure 4.3.13. Toughness versus carbon content for untreated composites

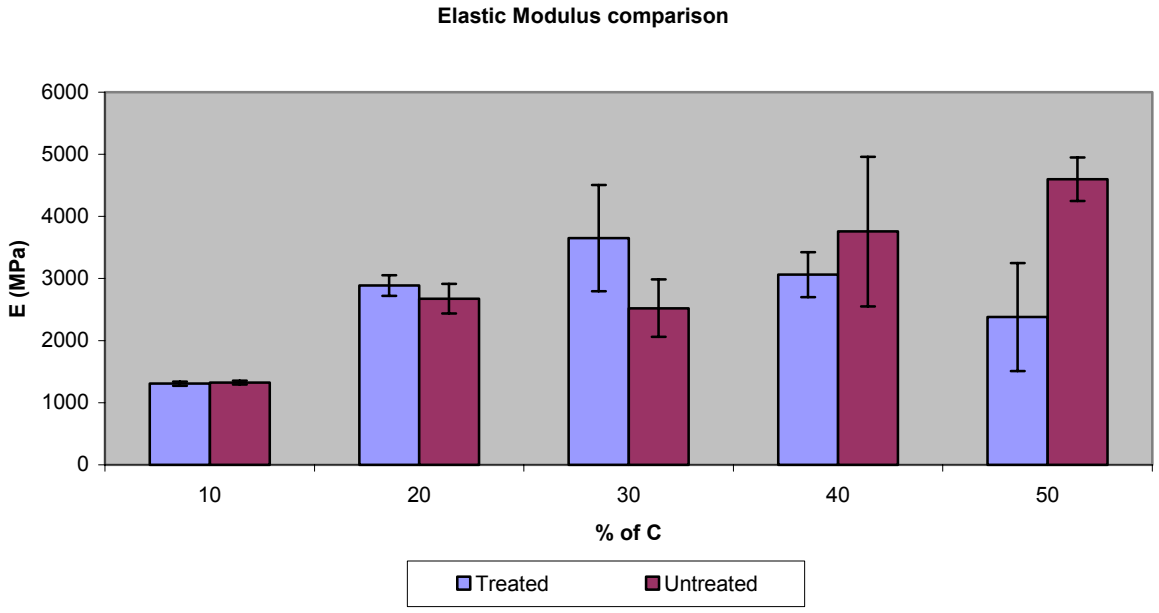

Figure 4.3.14. Elastic Modulus versus carbon content

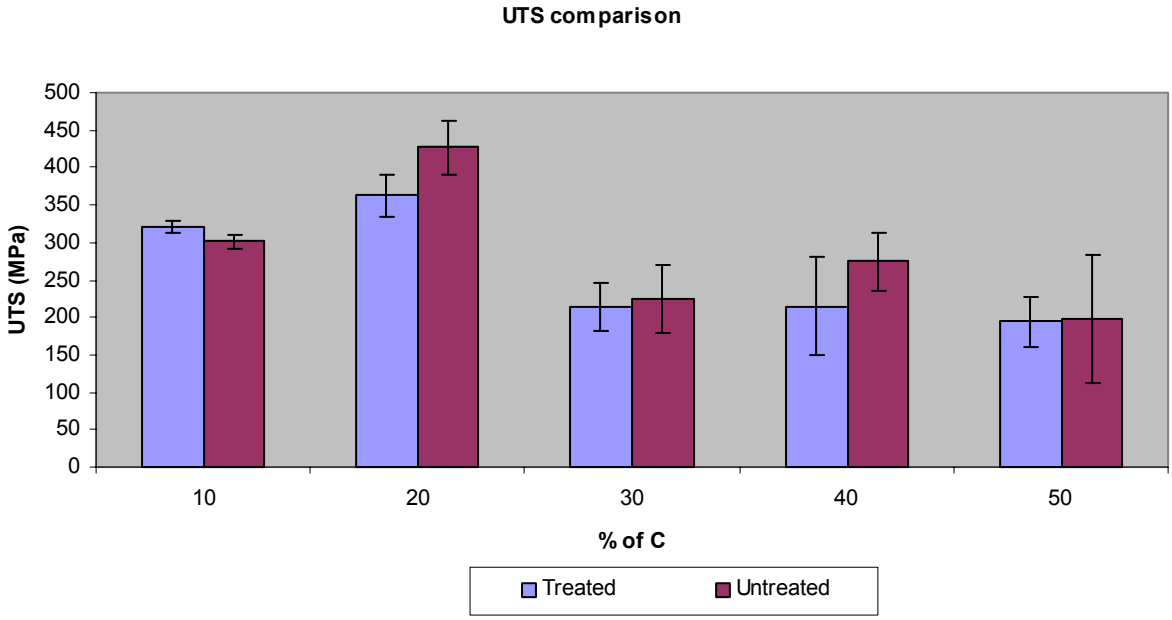

Figure 4.3.15. Ultimate Tensile Strength versus carbon content

Figure 4.3.16. Toughness versus carbon content

4.4. Infrared Spectroscopy

In the infrared analysis of the composites with treated and untreated carbon content is based on spectral changes. The composite spectra shown in Figures 4.4.1 to 4.4.6 illustrate the effect of carbon fillers addition to the polyurethane matrix.

Figure 4.4.1 and 4.4.4 shows the whole scanned region 4000 cm^{-1} to 800 cm^{-1} used for treated carbon and untreated carbon. Figures 4.4.2 and 4.4.5 show 3700 cm^{-1} to 3000 cm^{-1} spectral region in which the N-H stretching occurs (around 3300 cm^{-1}). The spectra for both treated and untreated composites exhibit a broad band due to free and hydrogen bonded -NH groups. These bands are more evident in composites based on treated carbon fillers.

Figures 4.4.3 and 4.4.6 present the spectral region (1900 cm^{-1} to 1400 cm^{-1}) in which the free and hydrogen bonded carbonyl (C=O) stretching occurs. They all present similar shape with differences in intensity, exhibiting more hydrogen bonded carbonyl than free, except for the 20% composite with untreated carbon filler, that shown presence of more free carbonyl than hydrogen bonded.

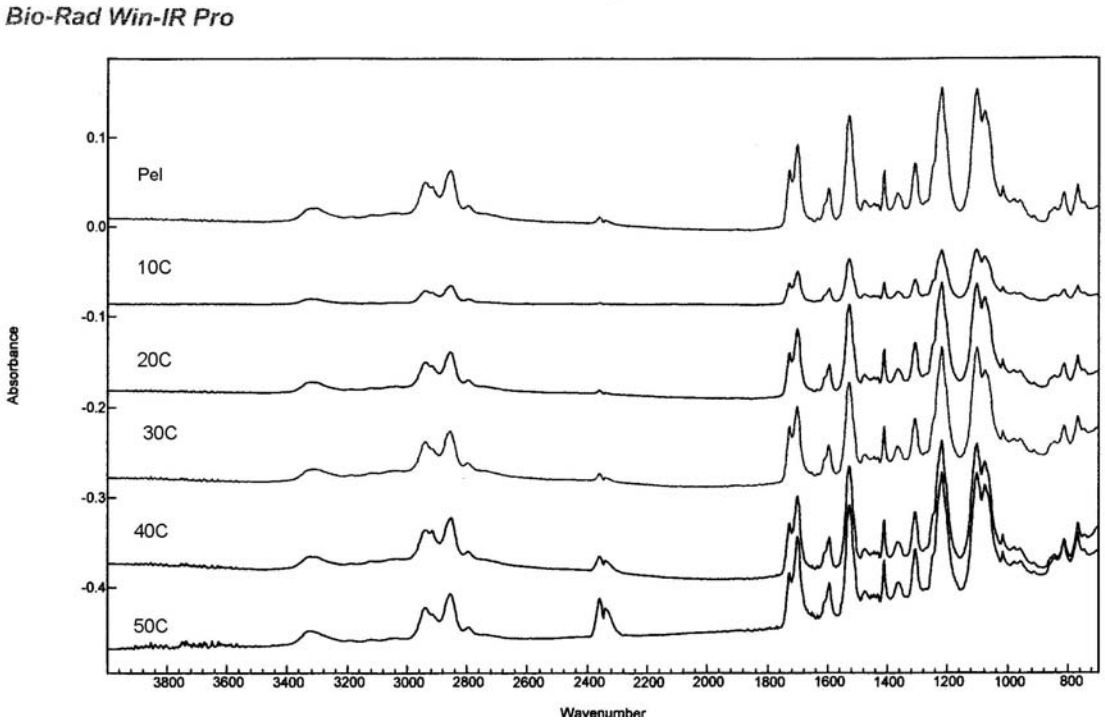

Figure 4.4.1. Composite spectra for treated samples

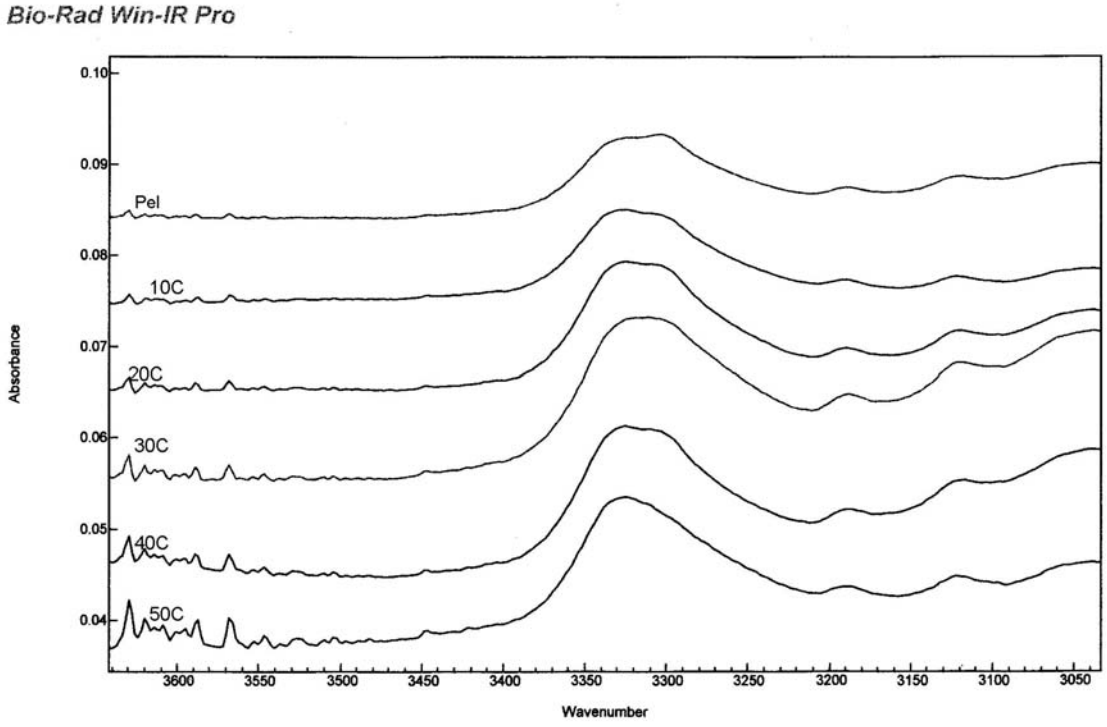

Figure 4.4.2. Composite spectra for treated samples – (N-H s)

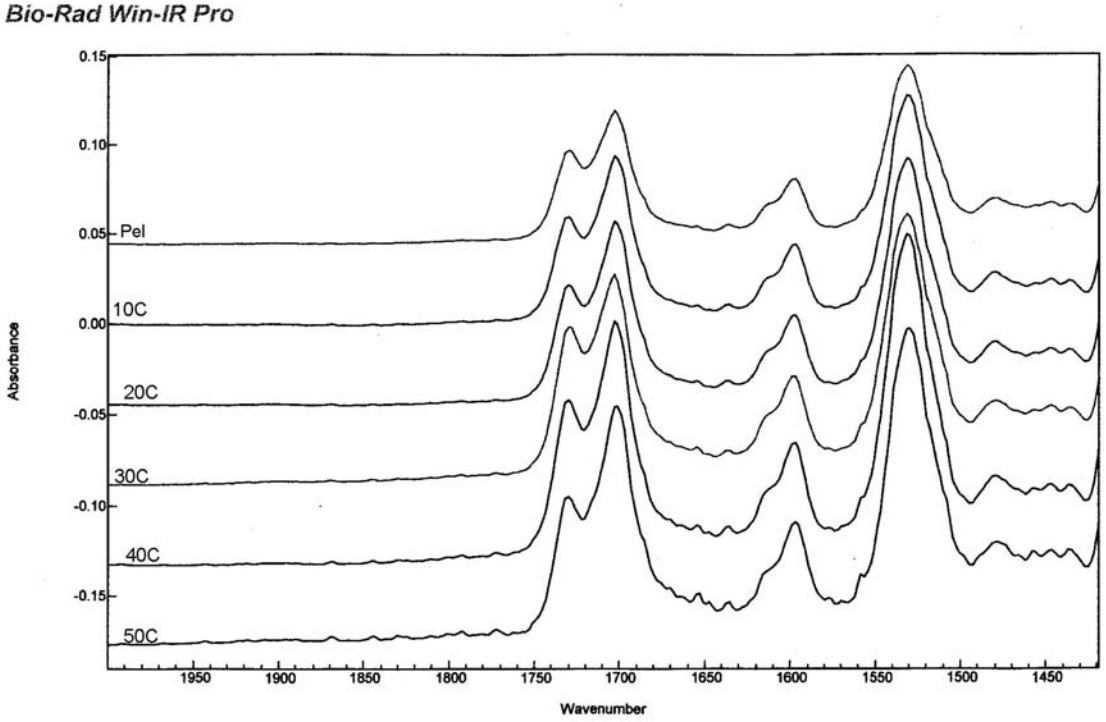

Figure 4.4.3. Composite spectra for treated samples – (C=O)

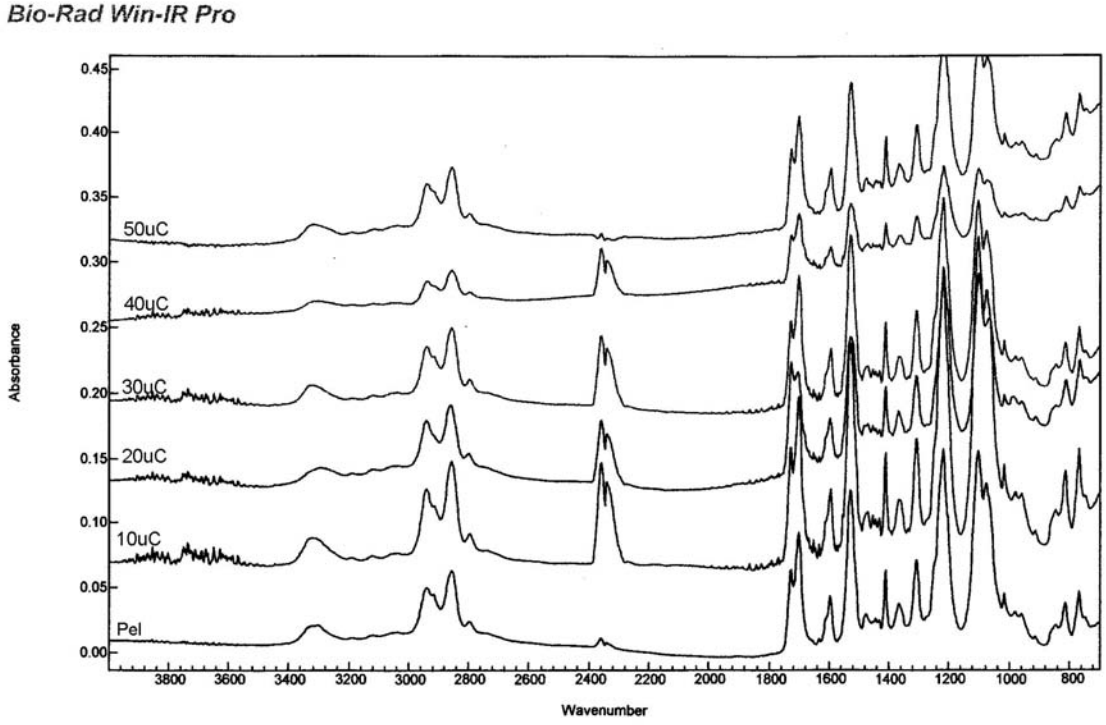

Figure 4.4.4. Composite spectra for untreated samples

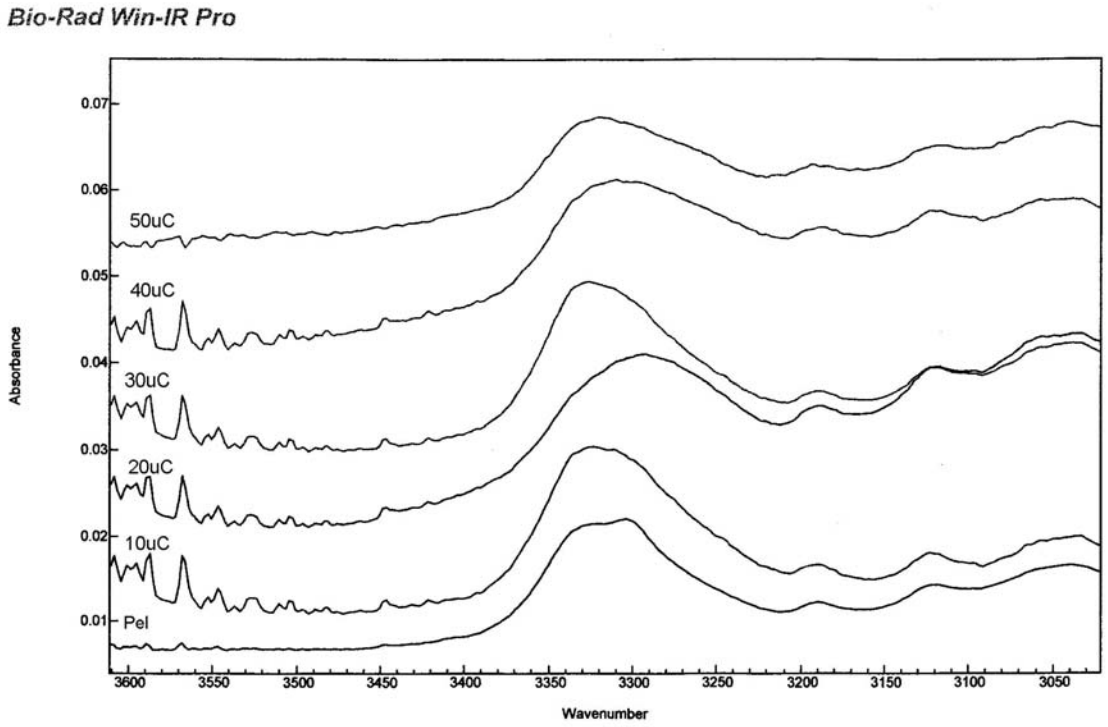

Figure 4.4.5. Composite spectra for untreated samples – (N-H s)

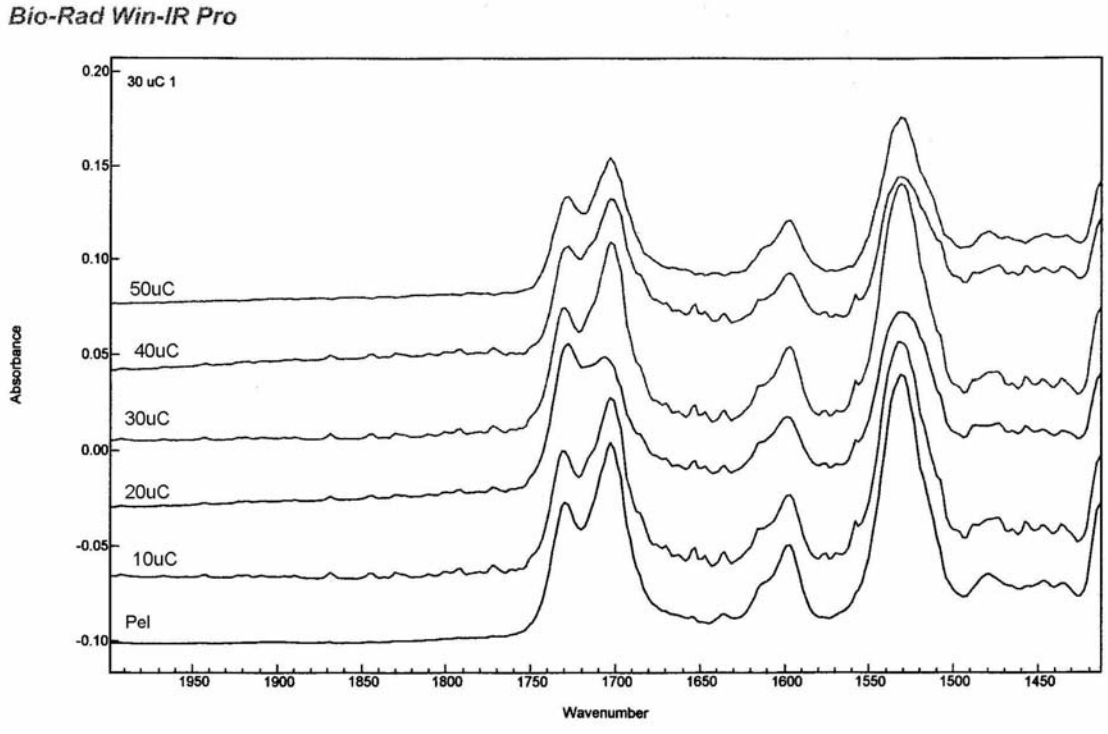

Figure 4.4.5. Composite spectra for untreated samples – (C=O)

4.5. Scanning Electron Microscopy

The fractured surfaces of the composites were analyzed by scanning electron microscopy. Figures 4.5.1 to 4.5.10 show the fracture surfaces of all composites. This technique was used to study the dispersion of the carbon fillers in the matrix. Due to the casting process, the filler apparently settled at the bottom of the samples (noticed in both types of composites but more intense in untreated carbon filled composites). In all micrographs the part of the samples that was touching the mold during the casting process are in the top of each micrograph i.e., all the micrographs apparently there is more carbon at the top. The arrows in the micrographs point to filler particles.

For low concentration it was clearly observed that the fillers concentrated more in one side of the sample, especially for the untreated samples. Increasing the carbon content for 20% and 30%, the layer of concentrated carbon filler increased. At higher carbon concentrations (40% and 50%), slightly better filler dispersion was observed, yet still with higher concentration of carbon in one side was present. No difference could be detected between the composites with treated carbon filler and the composites with untreated carbon fillers for higher carbon contents.

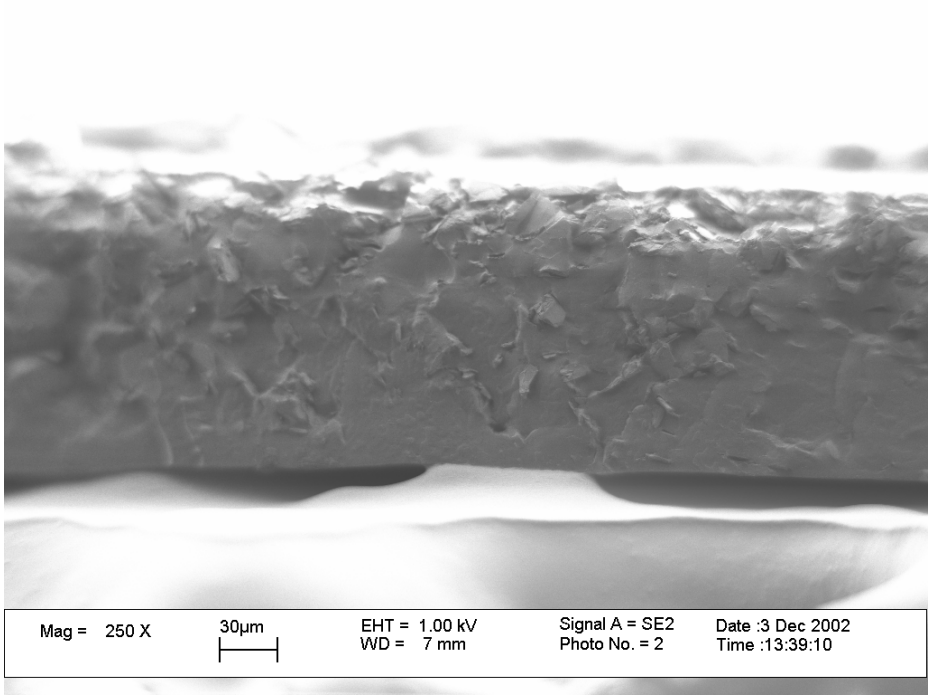

(a)

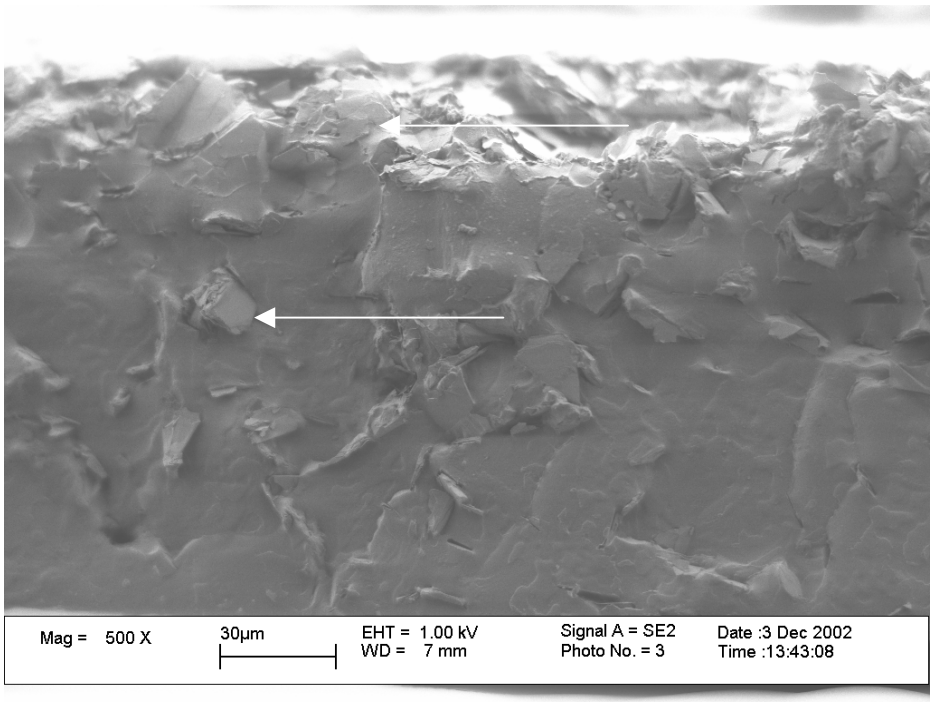

(b)

Figure 4.5.1. SEM for 10% treated carbon (a) 250 X (b) 500 X

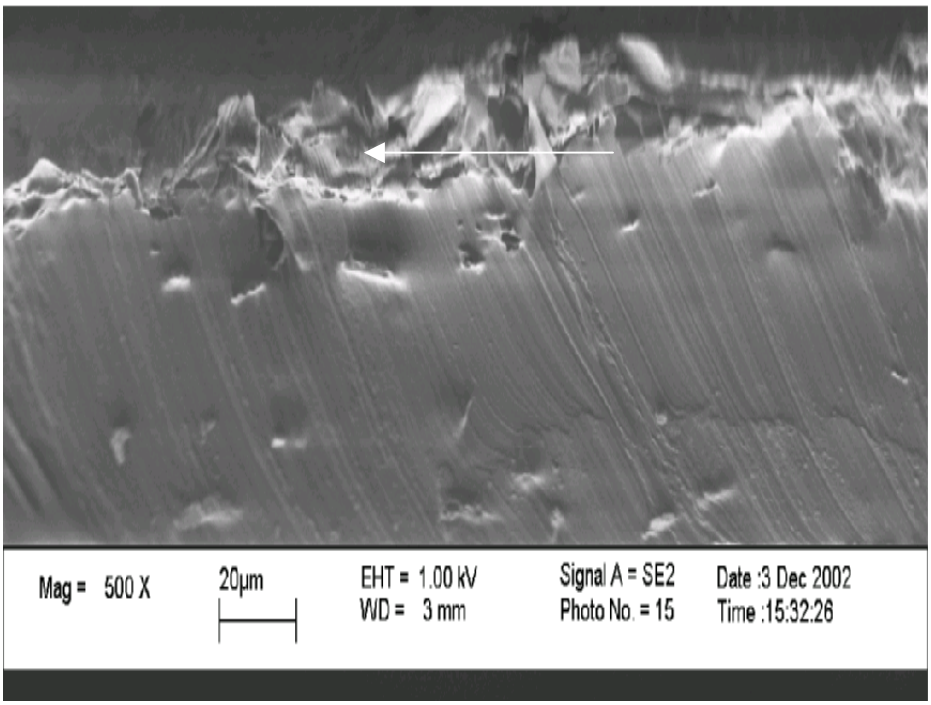

Figure 4.5.2. SEM for 10% untreated carbon

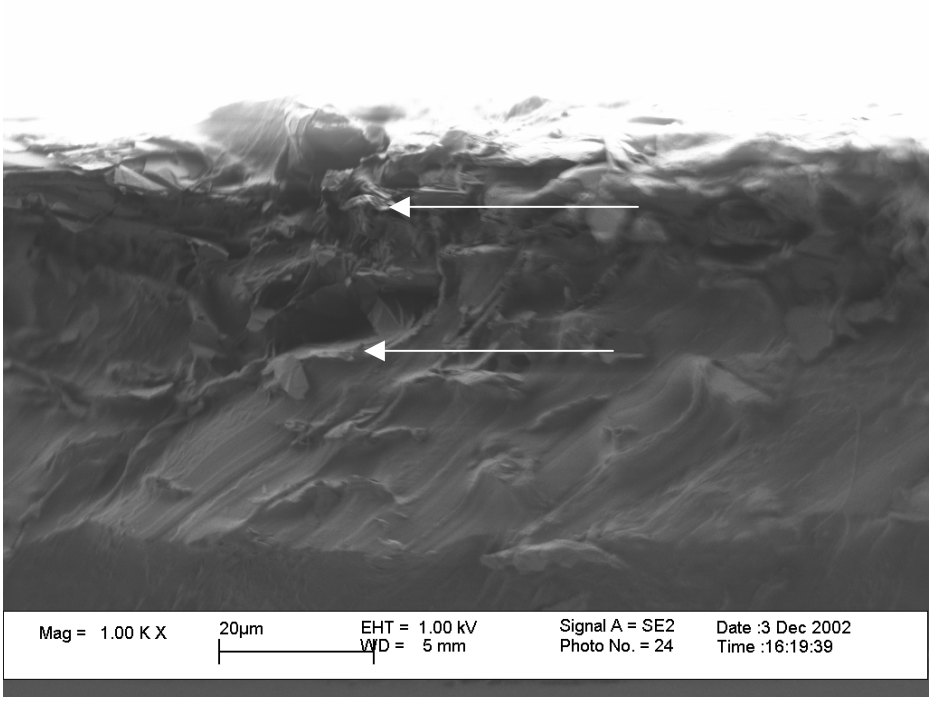

Figure 4.5.3. SEM for 20% treated carbon

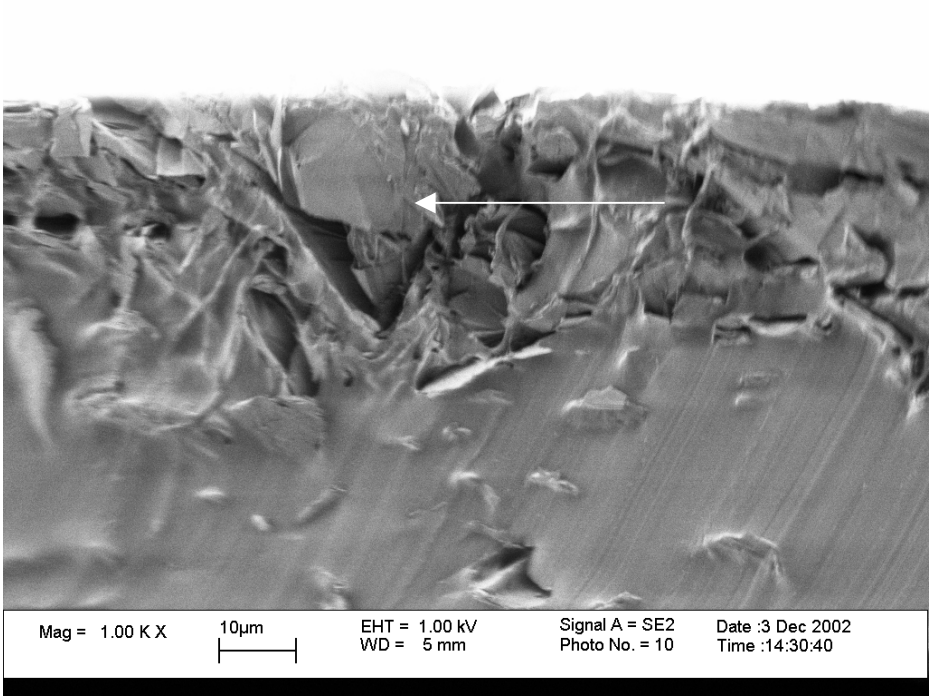

Figure 4.5.4. SEM for 20% untreated carbon

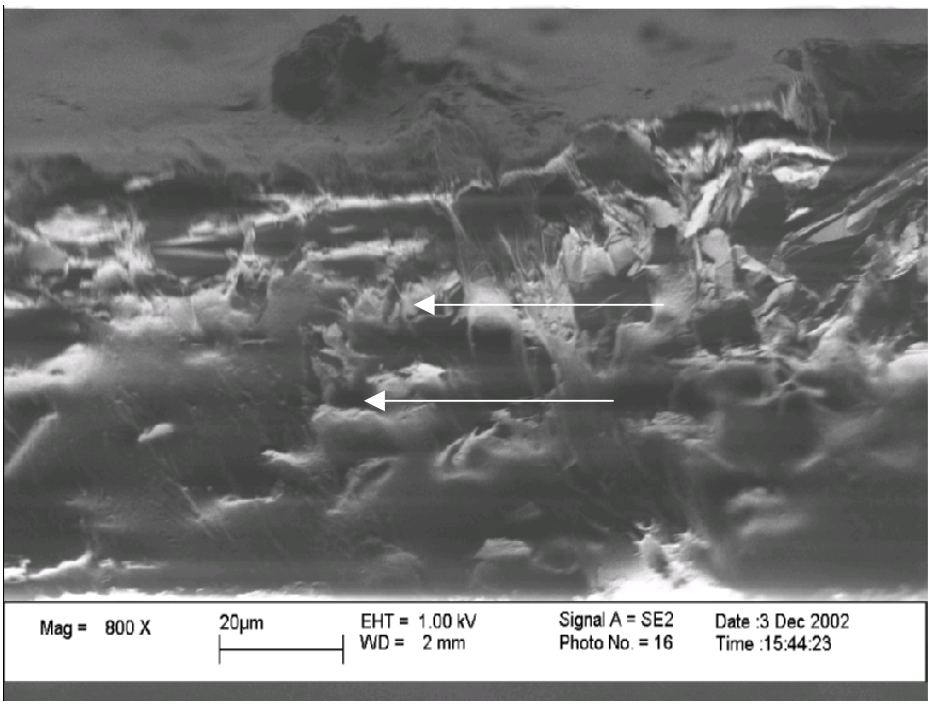

Figure 4.5.5. SEM for 30% treated carbon

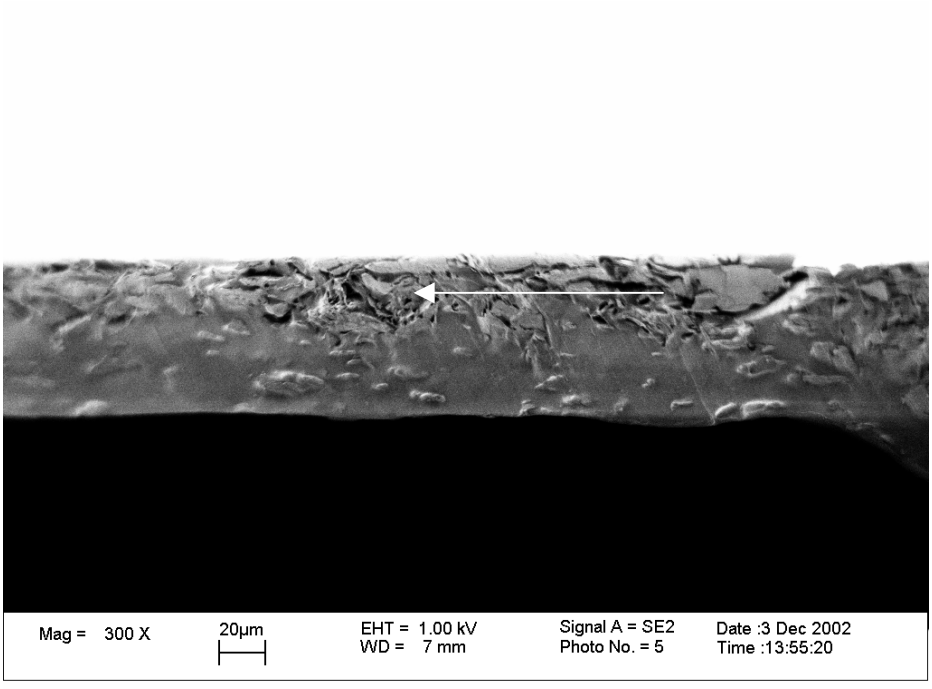

Figure 4.5.6. SEM for 30% untreated carbon

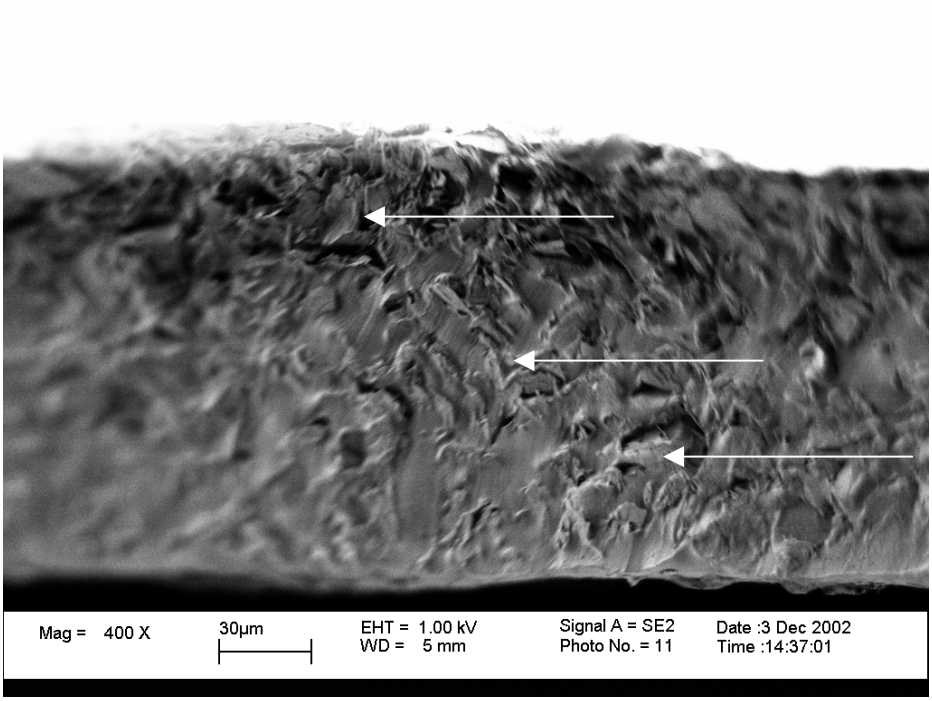

Figure 4.5.7. SEM for 40% treated carbon

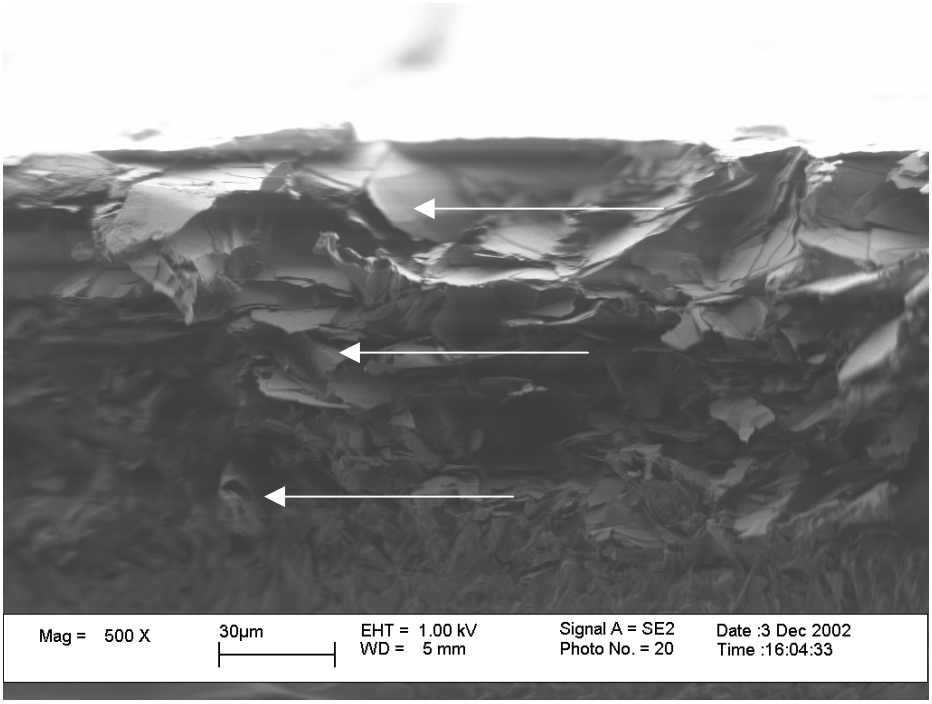

Figure 4.5.8. SEM for 40% untreated carbon

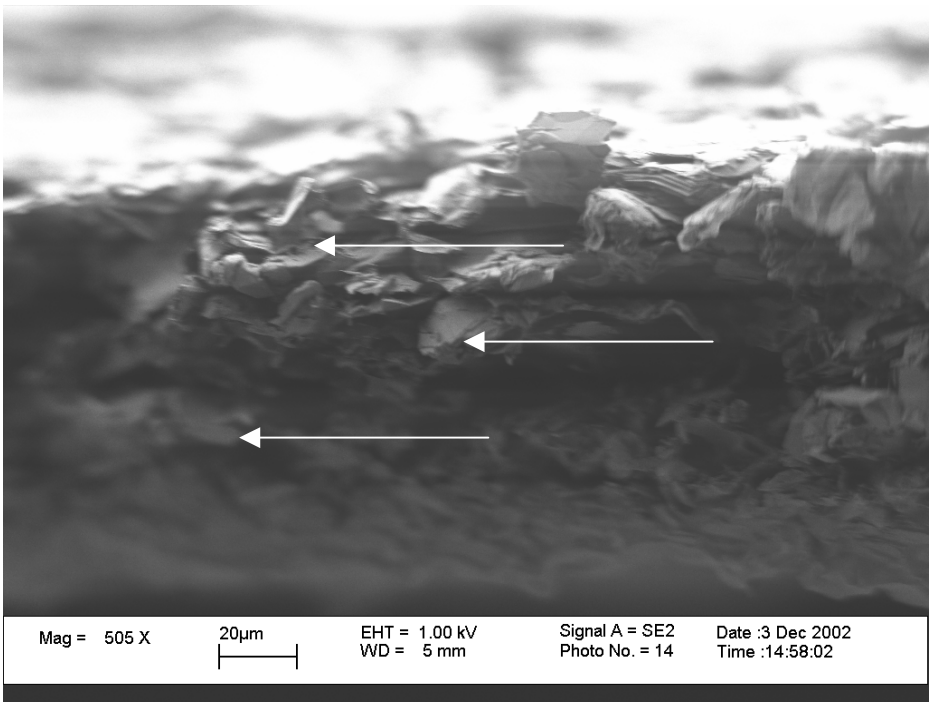

Figure 4.5.9. SEM for 50% treated carbon

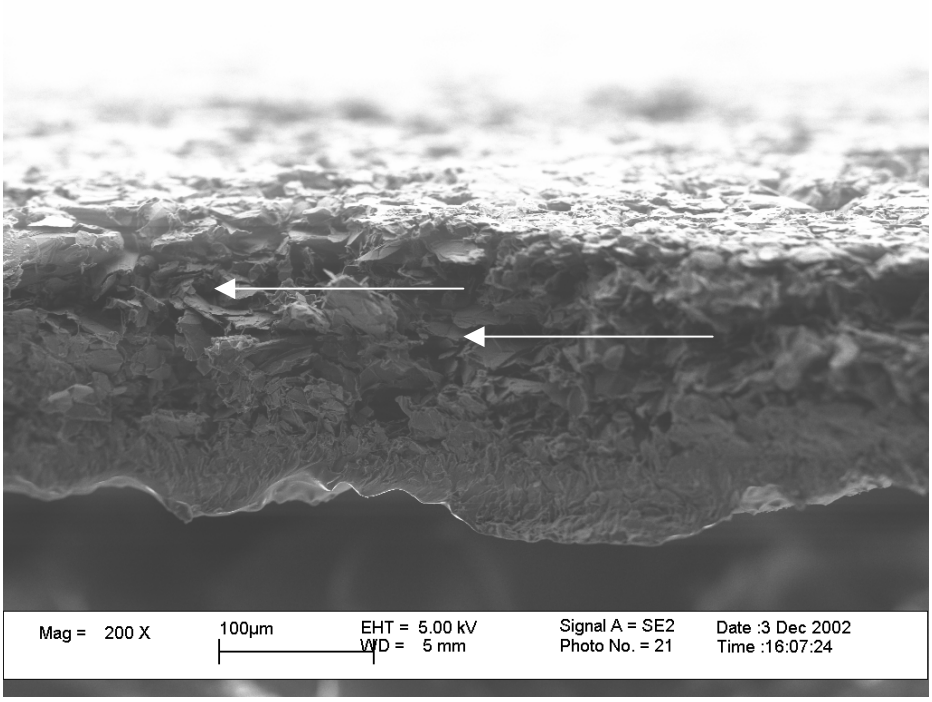

Figure 4.5.10. SEM for 50% untreated carbon

4.6. Fatigue

Fatigue test was performed in the samples to determine the effect of cyclic loads in the physical properties of treated and untreated carbon filled composites. Figures 4.6.1 and 4.6.2 show the elastic modulus behavior after 96,000 and 864,000 cycles. The modulus increased with the percentage of carbon filler and did not change as the number of cycles increased.

To understand the behavior of the conductive composites after fatigue test the samples were submitted to conductivity measurements and the relationship between electrical conductivity, carbon concentration and number of cycles was obtained for treated and untreated composites (Figures 4.6.3 and 4.6.4). The conductivity was measured only for 96,000 cycles and no difference in conductivity was noticed.

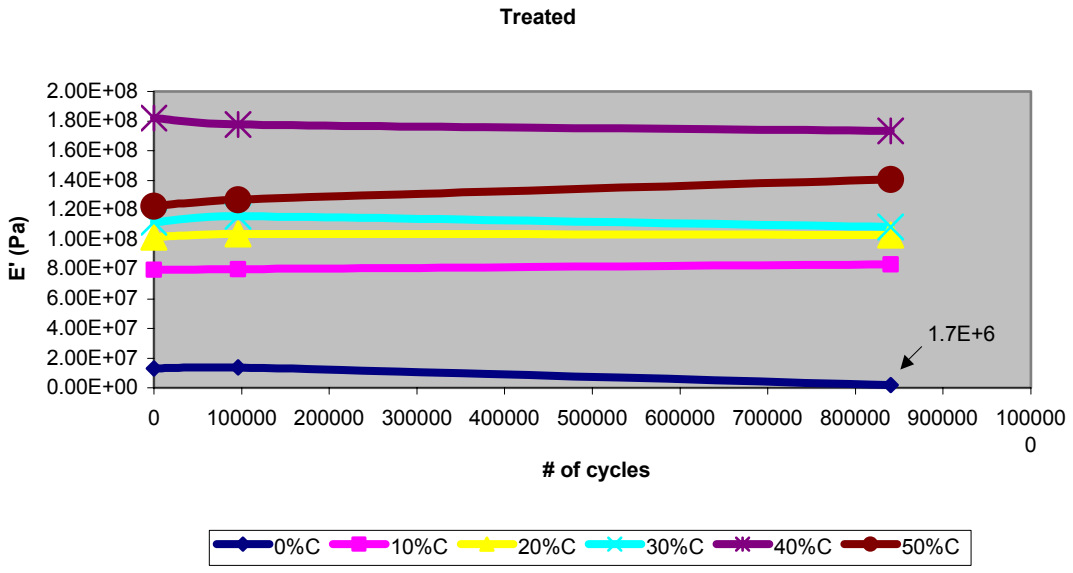

Figure 4.6.1. Relationship between elastic modulus and number of cycles for treated composites

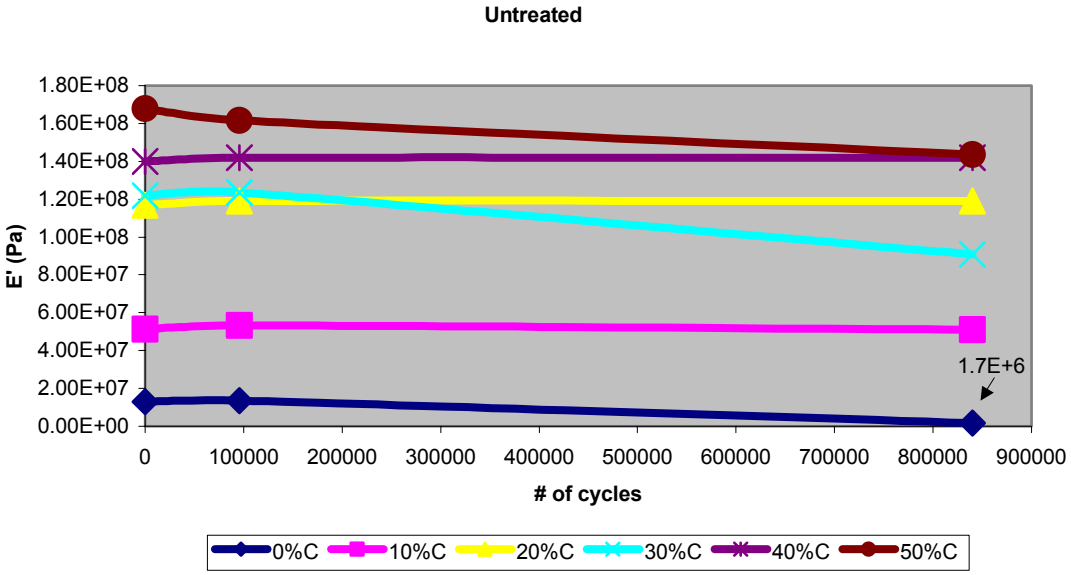

Figure 4.6.2. Relationship between elastic modulus and number of cycles for untreated composites

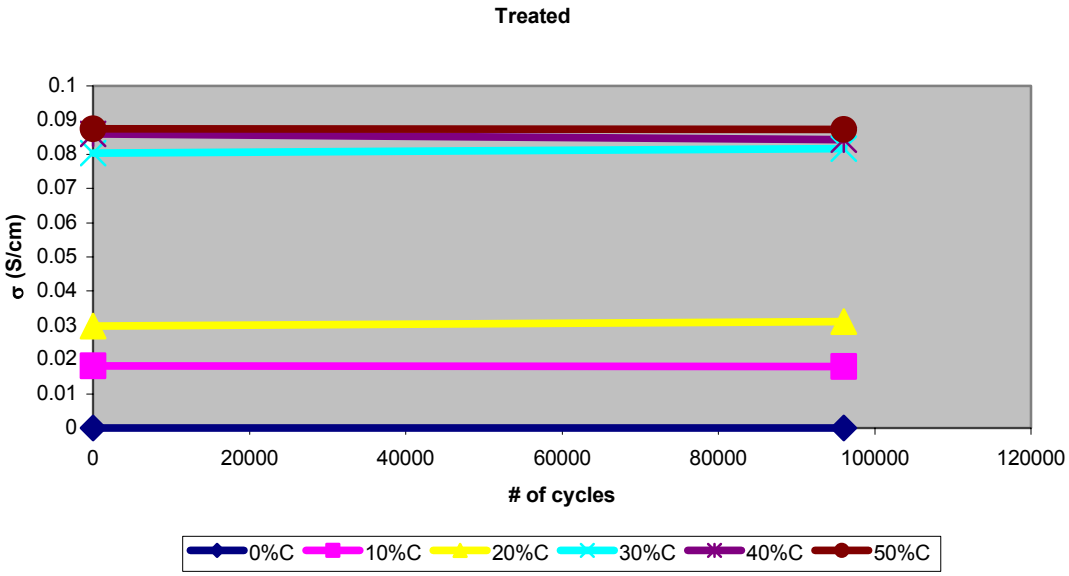

Figure 4.6.3. Relationship between conductivity and number of cycles for treated composites

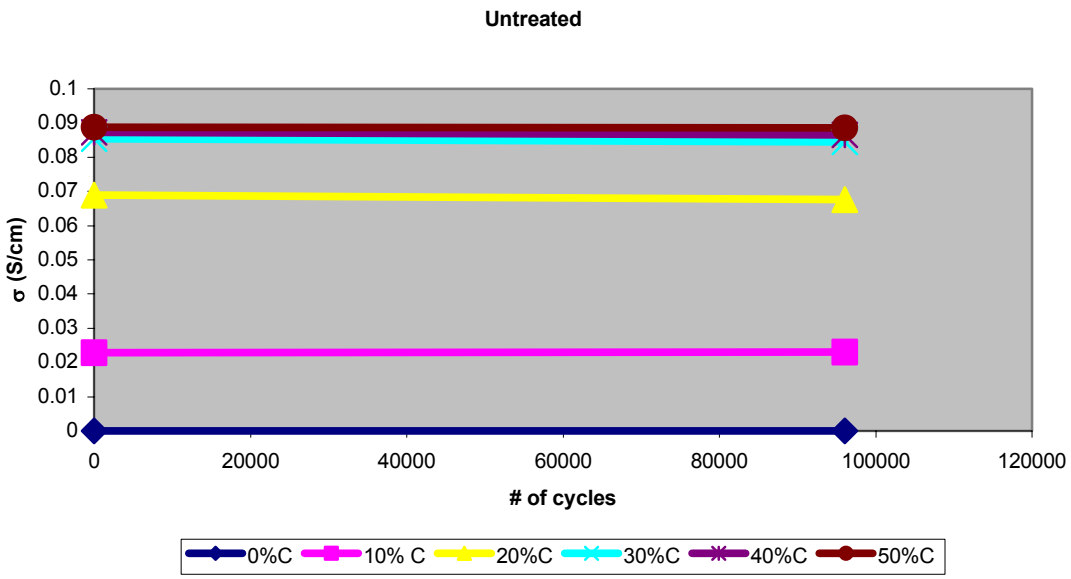

Figure 4.6.4. Relationship between conductivity and number of cycles for untreated composites

5. DISCUSSIONS

5.1. Conductivity

The electrical conductivity measurements are important to show the effect of filler content and its surface treatment. The conductivity was measured on one side of each sample, due to settling during the casting process did not allow the measurement in both sides. The final thin film of each composite presented different concentrations of filler in each side of the sample, probably due to the weight of the carbon filler and the poor compatibility between the filler and the polymer. Figure 5.1.1 illustrates the mold and the sample sides after casting. The low carbon filler concentration on the air-side of the films with low sensitivity of the instrument did not perform any conductivity measurement in the side opposite to the mold. Measurements were taken from the mold-side of the samples. The inhomogeneous dispersion of the carbon fillers is expected to affect the conductivity-concentration curve.

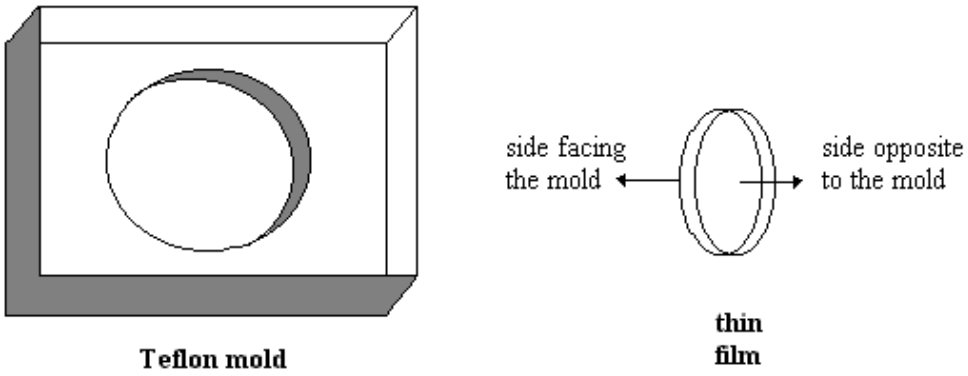

Figure 5.1.1. Sketch of the mold and sample sides

The electrical conductivity as a function of carbon filler content measured at 23°C and -185°C is shown in Figures 4.1.1 and 4.1.2. At both temperatures the composites exhibit similar behavior. The electrical conductivity of the composites increases as the percent of filler is increased. According to the theory (explained in more details in Section 2.2), at low concentration of carbon filler there is not enough filler to form a conductive network. As the concentration of carbon increases so does the conductivity of the material. When the conductivity is drastically increased, a percolation threshold is achieved. At high filler concentration, the conductivity reaches an asymptotic value. Figure 5.1.2 shows the comparison between the composites used on this research (data from Figure 4.1.1) and the results obtained by Li et al. [2] in their work with polyurethane/carbon black composites. According to the results, the percolation threshold of the composites is below 10% of carbon content. The reason for the shift in percolation threshold to higher values of conductivity as compared to Li et al., is due to the inhomogeneity of the films in this work. The conductivity values reported in this were obtained from the region of high filler loadings. The conductivity levels off due to the fact that filler settle down in the mold as previously indicated.

The treated carbon filler exhibited similar behavior as the untreated but at a different magnitude. It was expected that the performance of the treated composites would be better than that of the untreated filler samples. According to the results (Figures 4.1.1 and 4.1.2), the conductivity increased as a function of carbon content as was expected, but the untreated carbon filled composites showed higher conductivity values. The same trend was observed when comparing conductivity of treated carbon

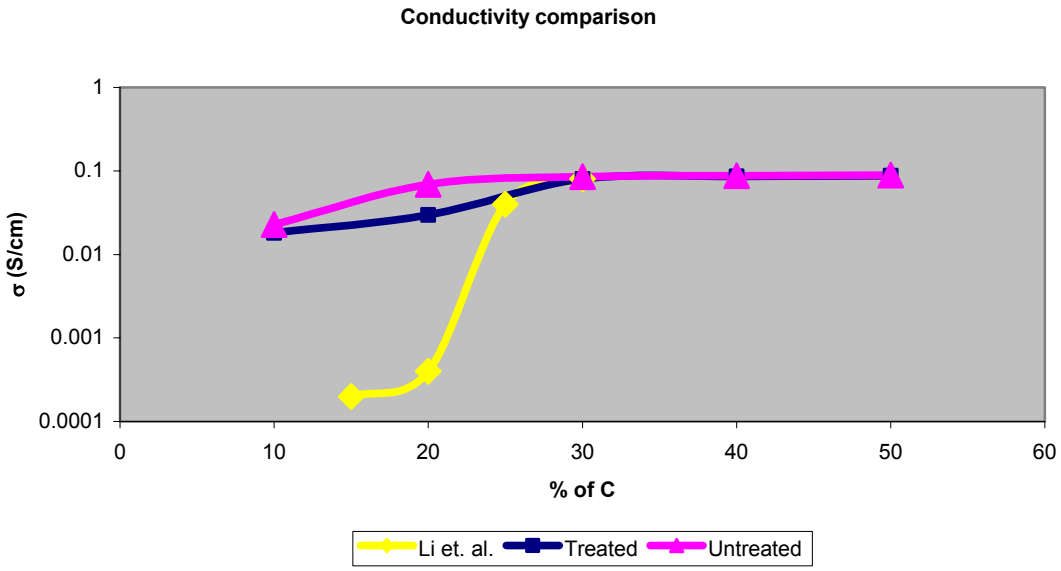

Figure 5.1.2. Conductivity comparison with the theory

filled composites with untreated carbon filled composites according to temperature (Figures 4.1.3 – 4.1.7), the untreated samples exhibits higher values. The difference in conductivity is attributed to plasma treatment which enhanced the filler-matrix interaction and reduced filler segregation. Minimum filler-matrix interaction is observed in the untreated samples (see micrographs in Figure 4.5.1 and 4.5.2). Increasing the percentage of carbon filler, the difference between the two types of composites decreases, once the amount of filler particles is so high that the surface treatment effect becomes insignificant as plenty of physical contacts between the particles occur.

In order to compare the results obtained in this research with the predicted values, the conductivity of Pellethane was estimated [36] and added in the plot of conductivity versus carbon content since the corresponding instrument was unable to make the measurement. Figure 5.1.3 illustrates the conductivity as a function of carbon filler content and the predicted curve obtained by the model proposed by Mamunya (Equations

11-15). According to the results, the percolation threshold of the composites is below 10% of carbon content. With the chosen filler loadings, it was not possible to find the exact percentage in which the composite change from an insulator to a conductive material due the lack of values between 0 % and 10% of carbon content. The predicted value was at around 15 wt %, and the reason for the shift in percolation threshold is likely due to the inhomogeneity of the films.

The segregation of the fillers as well the effect of treatment of the fillers can be observed in the scanning electron microscopy results (Section 4.5). The infrared analysis the effect of surface filler treatment will be discussed in detail (Section 5.4) and it is in agreements with the finds in conductivity.

After fatigue test (see Figures 4.6.3 and 4.6.4) the conductivity did not change for all composites, meaning that more than of 96,000 cycles (20 Hz) is necessary to be able to observe any change in conductivity.

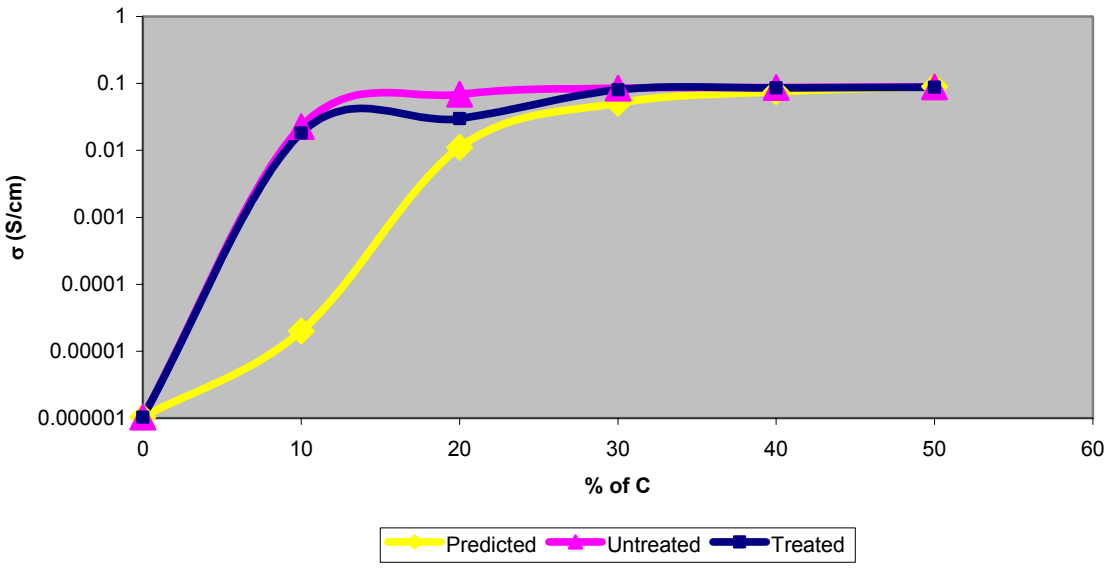

5.1.3. Comparison between experimental and predicted conductivity

5.2. Dynamic Mechanical Analysis

The dynamic mechanical properties of composites are in general dependent on the filler loading. To investigate the effect of the loading and the surface treatment of the fillers, elastic modulus, loss modulus and tanδ are discussed in this section.

According to the results illustrated in Figure 4.2.4 the elastic modulus (E') is readily increased with the presence of filler particles, approximating the composite modulus to that of the filler itself, more so at the rubbery plateau (T>Tg) than in the glassy region (T<Tg). To better understand this behavior, the ratio of the modulus of the pure polymer (E_1) and the filled polymer (E_2) was calculated and its influences the rubbery plateau and glassy region (Figures 5.2.1.). Note that the ratio of the modulus is approximately constant for the glassy region, an indication that in a brittle system the filler does not affect the composite's overall modulus, as opposed to a large effect observed for the rubbery plateau. At higher filler concentrations, there is a visible tendency for the storage modulus of the samples to decrease. This behavior is likely attributed to the agglomeration of filler (further discussed and visualized on 5.5) leading matrix regions unable to sustain higher applied forces, decreasing the performance of the overall composite.

On the plasma treated carbon filled composites the ratio of the modulus of the pure polymer and the filled polymer (E_2/E_1) based on the results of Figure 4.2.1 show the same trend as the untreated (Figure 5.2.2). The composites' overall modulus is affected by the filler content being more evident in the rubbery plateau. Evidence of some filler/matrix interaction was observed. In general, with increasing filler loading, the Tg of composites shift to higher temperatures, since fillers work as obstacles to the free movement of the

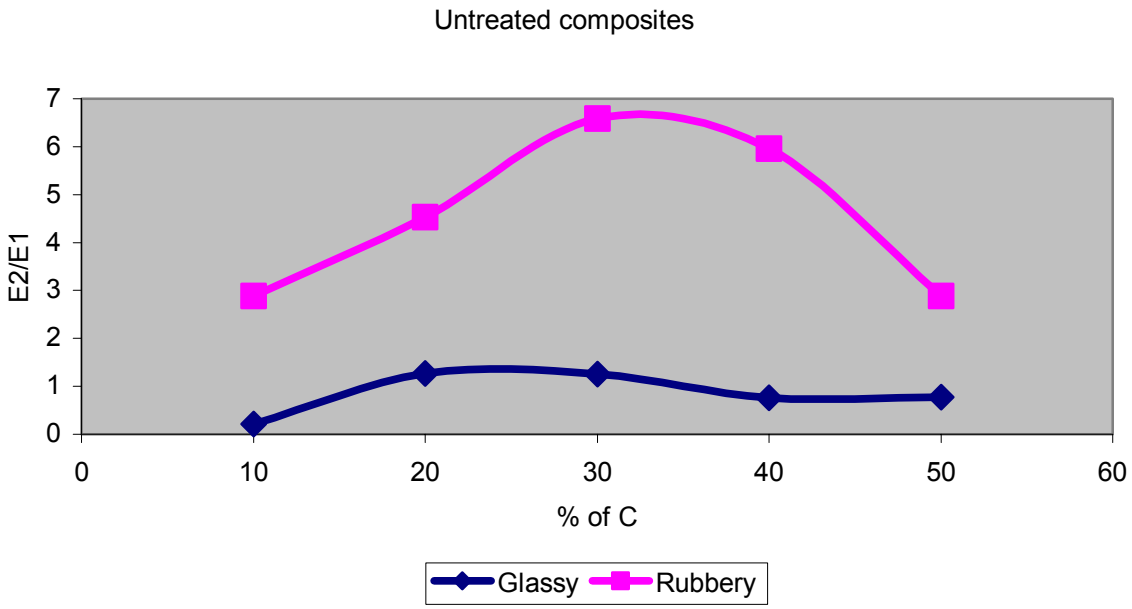

Figure 5.2.1. E_2/E_1 for untreated composites

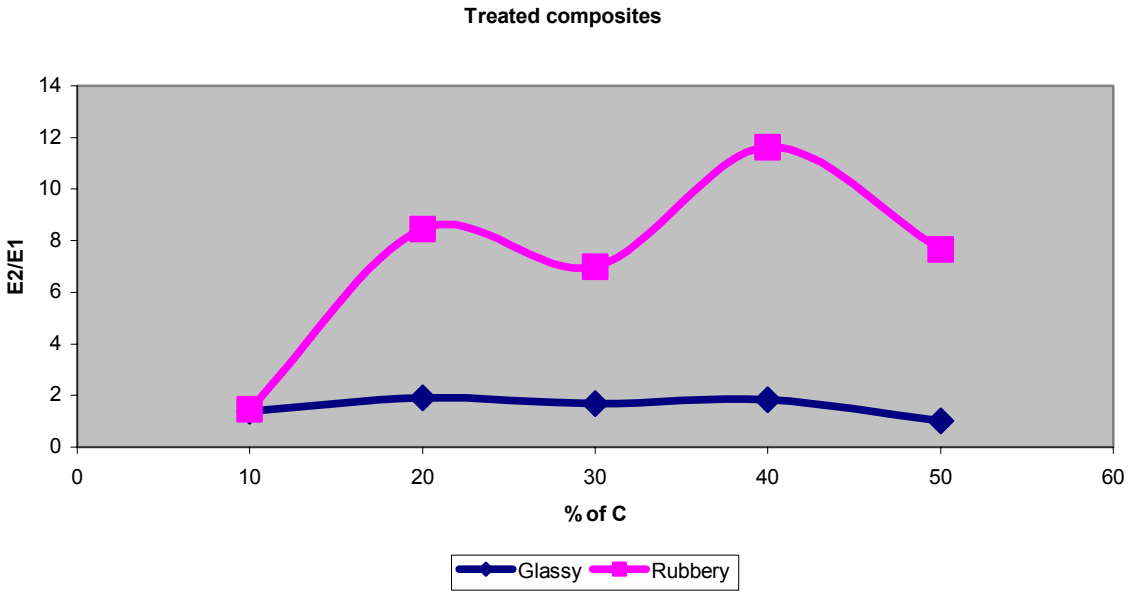

Figure 5.2.2. E_2/E_1 for treated composites

chains. Figures 4.2.3 and 4.2.6 show the results for the brittle to rubbery transition of the samples by plotting tanδ versus temperature. One of the effects of carbon fillers was the broadening of the transition region at high concentrations, observed in Figure 4.2.3 for 30%, 40% and 50% treated carbon filled composites, and Figure 4.2.6 for 20%, 30%, 40% and 50% untreated carbon filled composite. This behavior is associated with structural homogeneity, showing that at higher concentration the carbon in the composite tends to aggregate leading to phase separation and asymmetric loss tangent peak (Figure 5.2.3). Through deconvolution (Figure 5.2.4), the two separate relaxation processes were determined in the loss tangent curve of each composite. Table 5.2.1 shows the deconvoluted glass transition temperatures. Similarly, all filled samples show asymmetric loss tangent peaks, more asymmetric for the more filled samples. The asymmetric tanδ curves affect the overall breadth of the glass transition (obtained by the breath at half height), summarized on Table 5.2.2 being broader for the higher filler loads. The broadening of the glass transition is a strong indication that the molecular architecture of the composite is changing with the presence of filler i.e., some of the chains are relaxing at a higher temperature.

The glass transition (represented by T1 on Table 5.2.1 and on Figure 4.2.7) for the treated samples are in general higher than the untreated samples, in special for the 20, 30 and 40wt% filler. The increase in the glass transition temperature is an indication of chain movement restriction, attributed to the effect of the surface treatment of the fillers that generated improved interaction on the polymer/matrix interface. This effect is also verified with the readings of the breadth of half height and the results such as FT-IR, SEM and electrical conductivity.

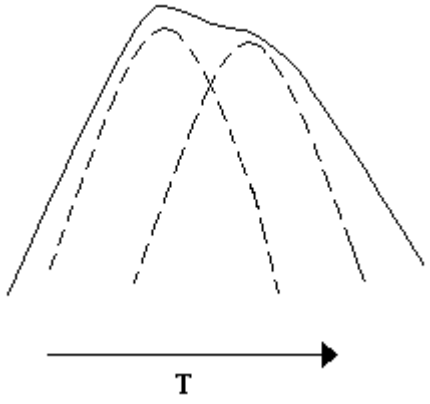

Figure 5.2.3. Sketch of the broad Tg

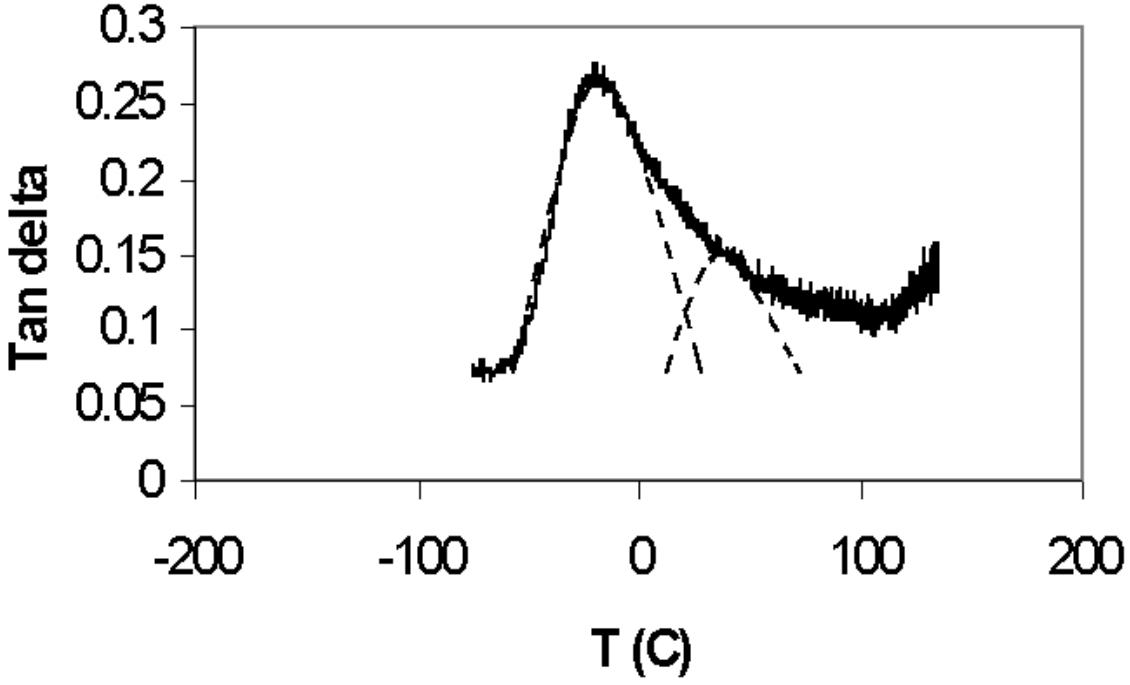

Figure 5.2.4. Tg peak for 50% treated carbon filled composite

Table 5.2.1. Transition temperatures (^{o}C) of deconvolved tanδ curves. U stands for untreated, T for treated, T1 is the main transition, T2 is the deconvolved peak temperature.

	0% Filler	10% Filler	20% Filler	30% Filler	40% Filler	50% Filler
UT1	-18	-16	-18	-17	-14	-12
UT2	-	41	29	27	35	38
TT1	-18	-17	-7	-7	-9	-13
TT2	-	26	41	33	32	38

Table 5.2.2. Breadth of half height of the tested materials (^{o}C).

	0% Filler	10% Filler	20% Filler	30% Filler	40% Filler	50% Filler
Untreated	43	43	54	62	64	65
Treated	43	42	47	46	52	58

5.3. Mechanical Properties

The theories for predicting mechanical properties of filled systems generally assume perfect adhesion between filler and polymer matrix, as well as perfect dispersion of the individual filler particles. These requirements are not entirely fulfilled by treated and untreated carbon filled Pellethane® composites. Studies of the morphology of the composite (Section 4.5) revealed that the carbon fillers aggregate in one side of the sample, widening this region of carbon as its content increases, as discussed before.

When carbon filler is added to a polymer matrix, the free movement of the chains is restricted as illustrated in Figure 5.3.1. As this filler concentration increases so does the restriction. This directly affects the properties of the composite, considering good adhesion between filler and polymer. Due to this restriction, the elastic modulus increases and tensile strength, elongation at break and toughness decreases. These filler effects on the mechanical properties of composites also depend on their dispersion on the polymer matrix and on their size. In the case of filler agglomeration for instance, the

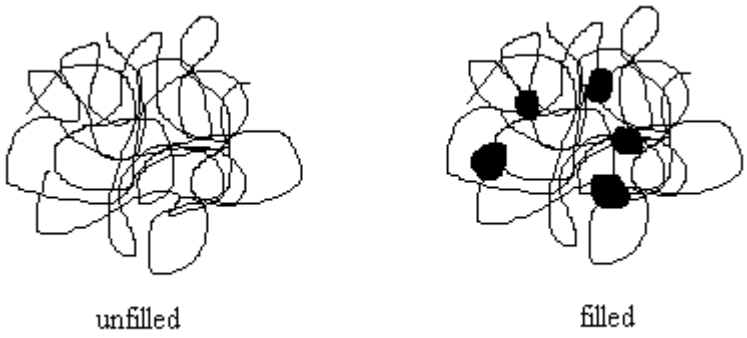

Figure 5.3.1. Sketch of the presence of filler in polymer matrix

small particles will act as a large imperfection or defect in the matrix and will concentrate stress, as weakening the overall material. Evidence of filler agglomeration was also deduced from the dynamic mechanical properties (Section 5.2) and observed in the scanning electron microscopy (SEM) micrographs in Section 4.5.

For treated carbon filled composites, the increase in carbon content increased the elastic modulus of the composite for up to 30wt% of carbon, decreasing at concentrations higher than 30wt%. In the dynamic mechanical analysis, phase separation was deduced for the high concentration of carbon samples, consequently the adhesion between the two phases is not strong enough, causing the drop in elastic modulus.

Normally, the addition of fillers makes the tensile strength and toughness of the composite decrease. In the treated carbon filled composites, the tensile strength decreased after 20 wt% of carbon content. For toughness, an increase was observed until 20wt% of carbon content, drastically dropping at higher concentration. This can be explained by the fact that at low carbon content (0 and 10%) the sample did not break, so the values obtained are from toughness at 300% of elongation. Theory has proposed that Pellethane® reaches 400% of elongation [29], which obviously would cause the increase in toughness for those samples.

For untreated carbon filled composite, increasing the carbon content, the elastic modulus increased, the tensile strength decrease after 20 wt% of carbon content, and toughness increased until 20 wt% of carbon content, drastically decreasing. In the comparison between treated and untreated carbon filled composites the difference in mechanical properties was not significant. In this case, the treatment did not show

effectiveness in mechanical properties, probably because the interaction was not sufficient to improve the reinforcement properties.

Although the trends observed for the mechanical properties of the studied materials do not seem perfectly linear for the increasing filler content, the observed trends approximate to that of the Kerner's prediction method (introduced on Section 2.1.1.1.), as illustrated in Figure 5.3.2.

While the storage modulus results for the untreated samples are very close to the predicted modulus for the studied materials, the treated composites deviate considerably for the 50wt% filler loading. This behavior may be attributed to either some source of experimental error (such as microvoids on the studied samples) or to some interaction between particles generating agglomeration and therefore concentrating stress. This is also reflected on the other mechanical properties as discussed earlier and could possibly be correlated to the plasma treatment used on the fillers once the same effect was not observed on the untreated filled composite with 50wt%. Similar behavior was observed in dynamic mechanical testing, where a lower modulus was measured on the 50wt% treated composite.

The fatigue results presented in Section 4.6 show that the elastic modulus did not change with the number of cycles used for this preliminary study. This is reflected by the mechanical analysis and by the electrical conductivity. For a more comprehensive study of the influence of fatigue on the properties of these composites, a greater number of cycles should be used.

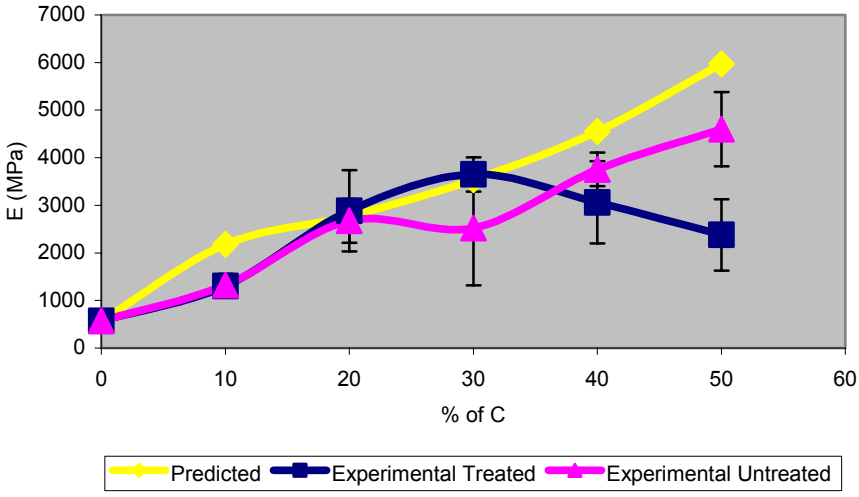

Figure 5.3.2. Predicted elastic modulus through Kerner's prediction method and experimental results for treated and untreated carbon black composites.

5.4. Infrared Spectroscopy

The use of infrared spectra allows the determination of the type of interaction that occurs between the surface treated fillers and the Pellethane® matrix. Some changes were observed between the treated and untreated carbon filled composites. Figures 4.4.1 and 4.4.4 show a spectra for both types of composites with varying the content of carbon.

The two major differences in IR absorptions comparing treated and untreated occur in the N-H stretching region around 3300 cm-1, and free and bonded carbonyl around 1730 cm-1 and 1703cm-1, respectively. For treated samples, the N-H stretching wavelength shifted to higher values, as the percentage of carbon fillers decreases (Table 5.4.1). The moving to a lower energy state, suggest that the overall amount of N-H hydrogen bonding was reduced. The two absorption bands relative to the N-H free and hydrogen bonded changed as the carbon content increased, changing to a single absorption band with a shoulder. After deconvoluting all absorptions in the N-H region (Figures 4.4.2 and 4.4.5), the ratio between the N-H free and hydrogen bonded suggest that N-H free are forming in greater number than hydrogen bonded. The ratio of the intensities of the free carbonyl to the H-bonded carbonyl suggest that H-bonded carbonyls are forming in greater number than free carbonyl. It is likely that the particle surface tratment is hydrogen rich, which is bonding to the carbonyl.

Figure 5.4.1 shows the behavior of the ratio of the intensity for free relative to the hydrogen bonded for N-H and C=O. The carbonyl behaves almost as opposite as N-H, i.e., as the hydrogen bonded carbonyl increases, the hydrogen bonded N-H decreases. Since the hydrogen bonding occurs between the N-H and carbonyl, this result suggest that probably the carbonyl is forming hydrogen bonds with the treated filler, proving that

Table 5.4.1. Table of absorption band for treated carbon filled composite

% of C	Wavelength (cm^{-1})	
	N-H (free)	N-H (H-bond)
0	3330	3304
10	3331	3303
20	3332	3302
30	3332	3302
40	3333	3302
50	3334	3303

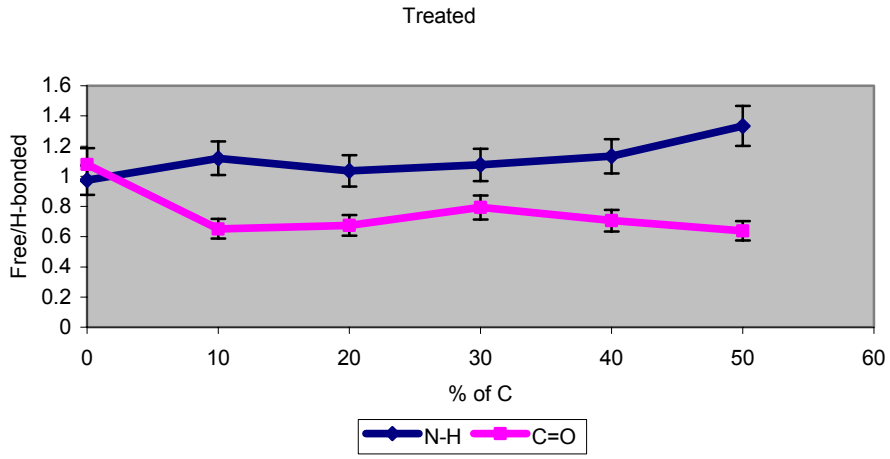

Figure 5.4.1. Free/bonded N-H and carbonyl ratio for treated carbon filled composites

some chemical interactions are occurring. Considering the morphology of Pellethane, the H-bonding of the carbonyl with N-H will occur on the hard domains. The presence of treated fillers will disturb the morphology of Pellethane, once the treated particles are H-bonding to the carbonyl of the polyurethane hard segments.

Considering that the carbonyl groups are electrophiles by nature, that they will have a tendency of attracting electron rich groups such as OH^- and regarding that the surface treatment used on the studied composites was a plasma type treatment, it is possible that the electron donor groups present in the fillers due to the surface treatment are hydrogen bonding with the carbonyl group on the Pellethane® and competing these groups with the N-H of urethane. In addition to this competing effect of the electron donors, the surface treated particles are better dispersed in the polymer matrix when compared to the untreated composites (see Section 5.5 for more details).

For the untreated carbon filled composites the wavelength for N-H stretching shifts to higher values (Table 5.4.2) but not as the treated ones, suggesting that the overall amount of hydrogen bonded N-H is decreasing. Ratio of the intensities of free and hydrogen bonded carbonyl are plotted against the ratio of free and hydrogen bonded N-H (Figure 5.4.2) and the results suggests that at low concentration there are no expressive changes, but after 30% of carbon content, free N-H occur more frequently than hydrogen bonded (ratio>1) at the same time that there are no significant changes with the carbonyl ratios, suggesting that the filler decreases the hydrogen bonding between the N-H and carbonyl.

Table 5.4.2. Table of absorption band for untreated carbon filled composite

% of C	Wavelength (cm^{-1})	
	N-H (free)	N-H (H-bond)
0	3330	3304
10	3331	3302
20	3329	3266
30	3333	3277
40	3332	3265
50	3332	3266

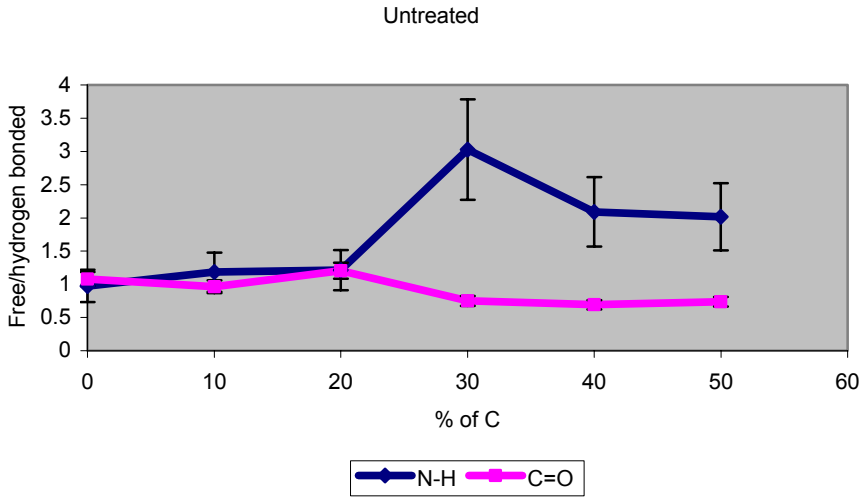

Figure 5.4.2. Free/bonded N-H and carbonyl ratio for untreated carbon filled composites

The comparison of the treated and untreated carbonyl ratios (Figure 5.4.3) further validate the theory that the treated particles are in fact hydrogen bonding with the carbonyl groups of the pellethane. Note that while the ratio increases significantly for the untreated samples for percentages of up to 20wt%, meaning that the amount of free carbonyl increases in relation to the amount of bonded (particles are acting as physical barrier for the interaction), the ratio is maintained for the treated, a strong evidence that the treatment is acting toward the maintenance of the interactions population.

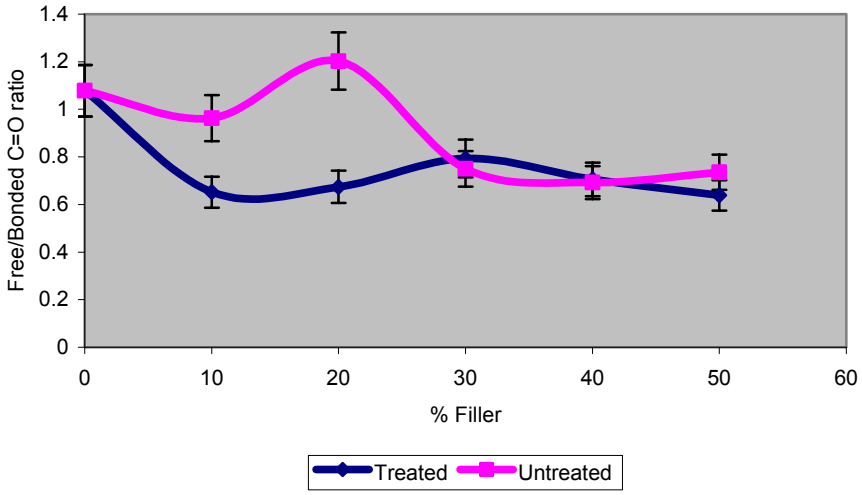

Figure 5.4.3. Free/bonded C=O ratio for the treated and untreated composites

5.5. Scanning Electron Microscopy

SEM was used to visualize the particle dispersion on the studied materials and ultimately to allow the understanding of the effect of particle agglomeration/dispersion and plasma treatment on their properties. At 10 wt% of carbon content the effect of treatment was more observable comparing to the untreated sample, meaning that a improve in dispersion was obtained. This effect can be observed in Figures 4.5.1 and 4.5.2; and it is an indication that there is some interaction between the interface region of the filler and polymer matrix, avoiding the extensive agglomeration on the bottom of the cast film as in the untreated sample. This can explain the dynamic mechanical behavior and conductivity results. At 20 wt% of carbon content, the layer in the bottom of the film increased in thickness and the difference between treated and untreated was not as expressive as observed in the 10 wt%. The same trend was observed for the 30 wt% filled composite. As reaching 40 wt% and 50 wt% of carbon content, the amount of filler was too high to detect treatment efficacy. As far as carbon content, it is noticeable that dispersion occurs throughout the sample for those composites.

The fact that fillers were relatively better dispersed in the treated composites will impact most of the experimental procedures discussed earlier. In fact, the conductivity readings will be directly affected by this effect. As the conductivity measurements were done at the bottom surface of the samples, their values will be much closer to that of the carbon alone when compared to the treated composites. Similarly, the mechanical properties such as the elastic modulus, the untreated material will in most cases have a behavior intermediate of that observed for the treated composites and pure Pellethane®. In addition, the dynamic mechanical properties will also be impacted in the same way as

the transient tensile testing, for the same reason. In the case of FT-IR, the treated samples allow interaction between filler and matrix, and agglomeration will impact the chain separation affecting the results for IR.

The fact that particles agglomerate during the casting of the films could be used towards a specific engineering application. For example, a film with one highly conductive side could be cast and yet its overall mechanical properties would not be as poor in terms of fatigue and tensile strength as a perfectly homogeneous film would, and yet the conductivity of the films that precipitates its particles could be much higher on its "particles rich" side at a much lower filler loading when compared to a highly dispersed composite material.

6.CONCLUSIONS

The main conclusions of this research are as follows:

- There is a significant difference between the air and mold sides of the samples with respect to the casting process, due to the precipitation of the fillers at the time of casting. This effect was more emphatic for the untreated sample than the treated ones, suggesting an interaction between the treated particles and the polymer matrix is present. SEM results clearly illustrate the poor particle distribution and conductivity measurements of the mold-side is always higher than air-side.
- Interactions between the surface treated fillers and the Pellethane® polyurethane matrix was observed and noted according to the chemical analysis (FT-IR) and in terms of mechanical properties (phase separation in DMA, tensile strength and elastic modulus in transient tensile). It is likely that the surface treatment is enriching the surface of the filler particles with electron rich atoms that will compete the hydrogen bonding of the carbonyl groups with the N-H of urethane (FT-IR).
- The fact that the carbon particles precipitate during the casting of the composite samples could be used as an engineering tool for the design of a polymer matrix-like properties conductor with one side that will conduct an electric current with the conductivity near that of carbon.

7. RECOMENDATIONS

The following suggestions for future work would enrich the results of this study:

- Further consider the use of a filler that precipitates during its casting in practical everyday applications through an economic and practicality study.
- Use different particle sizes and particles with varying compatibility with the polymer matrix through different surface treatments to better control the degree of precipitation and therefore use this effect as an engineering tool that is applicable in the industry.
- Use intermediate filler loadings than the ones chosen in this initial study for obtaining better resolved curves in the conductivity and for reducing the effect of experimental error on the test results.
- Consider study of the life time estimate through fatigue.
- Chemical and physical characterization of the fillers prior to the composite.

REFERENCES

1. Grunlan, G.C., Gerberich, W.W., Francis, L.F., *Lowering the Percolation Threshold of Conductive Composites Using Particulate Polymer Microstructure.* Journal of Applied Polymer Science, 2001. **80**: p. 692-705.

2. Li, F., Qi, L., Yang, J., Xu, M., Luo, X., Ma, D., *Polyurethane/Conducting Carbon Black Composites: Structure, Electric Conductivity, Strain Recovery behavior, and Their Relationships.* Journal of Applied Polymer Science, 2000. **75**: p. 68-77.

3. Zois, H., Apekis, L., Omastova, M., *Electrical Properties of Carbon Black-filled Polymer Composites.* Macromol. Symp., 2001. **170**: p. 249-256.

4. Chodak, I., Omastova, M., Pionteck, J., *Relation Between Electrical and Mechanical Properties of Conducting Polymer Composites.* Journal of Applied Polymer Science, 2001. **2001**: p. 1903-1906.

5. Yurekli, K., Krishnamoorti, R., Tse, M.F., Mcelrath, O., Tsou, A.H., Wang, H.-C., *Structure and Dynamics of Carbon Black-Filled Elastomers.* Journal of Applied Polymer Science, 2001. **39**: p. 256-275.

6. Akovali, G., Torun, T.T., *Properties of Blends Prepared from Surface-modified Low-density Polyethylene and Poly(vinyl chloride).* Polymer International, 1997. **42**: p. 307-314.

7. Pell, R.M., Warren, C.D., Carpenter, J.A., Skalad, P.S., *Economical Carbon Fiber and Tape Development from Anthracite Coal Powder and Development of Polymer Composites Filled with Exfoliated Graphitic Nanostructures*. 2001, Automotive Lightweighting Materials.

8. Inagaki, N., Tasaka, S., Kawai, H., Yamada, Y., *Surface Modification of Aromatic Polyamide Film by Remote Oxygen Plasma.* Journal of Applied Polymer Science, 1997. **64**: p. 831-840.

9. Inagaki, N., Tasaka, S., Umehara, T., *Effects of Surface Modification by Remote Hydrogen Plasma on Adhesion in Poly(fluoroethylene)/Copper Composites.* Journal of Applied Polymer Science, 1999. **71**: p. 2191-2200.

10. Jones, R.M., *Mechanics of Composite Material*. 1975: Taylor & Francis.

11. M., W.I., W., H.D., *An Introduction to the Mechanical Properties of Solid Polymers*. 1993, New York: Wiley.

12. Manson, J.A., Sperling, L.H., *Polymer Blends and Composites*. First Edition ed. 1976, New York: Plenum.

13. Holliday, L., *Composite Materials*. 1966, New York: Elsevier.

14. Nielson, L.K., *Mechanical Properties of Polymers and Composites*. Vol. 2. 1974, New York: Dekker.

15. Lee, M.-W., *The Preparation of Nano-structured Polymeric Systems of Polyurethane/Polyimide Blends*, in *MSE*. 1996, University of Tennessee: Knoxville.

16. Peters, S.T., *Handbook of Composites*. Second Edition ed. 1998, New York: Chapman & Hall.

17. Grummitt, D.W., *Mechanical and Morphological Characterization of Polyamide Bone Analogues*, in *MSE*. 1995, University of Tennessee: Knoxville.

18. Nielson, L.E., *Mechanical Properties of Polymers and Composites*. Vol. 1. 1974, New York: Dekker.

19. Schueler, R., Petermann, J., Schulte, K., Wentzel, H.-P., *Agglomeration and Electrical Percolation Behavior of Carbon Black Dispersed in Epoxy Resin.* Journal of Applied Polymer Science, 1997. **63**: p. 1741-1746.

20. Delmonte, J., *Metal/Polymer Composites*. 1990, New York: VNR.

21. Kortschot, M.T., Woodhams, R.T., Polymer Composites, 1985. **6**(4): p. 296.

22. Yu, G., Zhang, M.Q., Zeng, H.M., Hou, Y.H., Zhang, H.B., *Effect of Filler Treatment on Temperature Dependence of Resistivity of Carbon-Black-Filled Polymer Blends.* Journal of Applied Polymer Science, 1999. **73**: p. 489-494.

23. Pinto, G., Maidana, M.B., *Conducting Polymer Composites of Zinc-Filled Nylon 6.* Journal of Applied Polymer Science, 2001. **82**: p. 1449-1454.

24. Clingerman, M.L., *Development and Modelling of Electrically Conductive Composite Materials*, in *Chemical Engineering*. 2001, Michigan Technlogical University: Michigan.

25. Clingerman, M.L., King, J.A., Schulz, K.H., Meyers, J.D., *Evaluation of Electrical Conductivity Models for Conductive Polymer Composites.* Journal of Applied Polymer Science, 2002. **83**: p. 1341-1356.

26. Szycher, M., *Szycher's Handbook of Polyurethanes*. 1999, New York: CRC Press.

27. Edwards, K.N., *Urethane Chemistry and Applications*. ACS Symposium Series 172, ed. Comstock, M.J. 1981, Washington: ACS.

28. Benli, S., Yilmazer, U., Pekel, F., Ozkar, S., *Effect of Fillers on Thermall and Mechanical Properties of Polyurethane Elastomes.* Journal of Applied Polymer Science, 1998. **68**: p. 1057-1065.

29. Wong, R.P., *The Effects of Calcification on the Structure and Properties of Biomedical Polyurethanes*, in *MSE*. 1991, University of Tennessee: Knoxville.

30. Kim, H.-J., *Effects os Structure and Blending Calcium Salts on Fatigu Crack Propagation Behavior of Model Polyurethanes*, in *Materials Science and Engineering*. 1993, University of Tennessee: Knoxville.

31. Wang, C.B., Cooper, S.L., *Morphology and Properties of Segmenteed Polyether Polyurethaneureas*. Macromolecules, 1983. **16**: p. 775-786.

32. Kraus, G., *Reinforcement of Elatomers*. 1965, New York: Wiley & Sons.

33. Chan, C.-M., *Polymer Surface Modification and Characterization*. 1993, New York: Hanser.

34. Garbassi, F., Morra, M., Occhiello, E., *Polymer Surfaces*. 1994, New York: Wiley.

35. d'Algostino, R., *Plasma Deposition, Treatment, and Etching of Polymers*. 1990, San Diego: Academic Press.

36. Krevelen, D.W.V., *Properties of Polymers - Their Estimation and Correlation with Chemical Structure*. 1976, Amsterdam: Elseevier.

VITA

Leina Barros Tocchetto was born in Cajazeiras, northeast Brazil on May 12, 1977. She started her B.S right after High School in 1994, graduating in 1999 from the Federal University of Paraiba, focusing her work in Polymer Science. After a short period of internship in a PE synthesis factory, she came to U.S. to begun her Master Degree in Polymer Engineering at The University of Tennessee Knoxville in the Fall 2000. Under Dr. Benson supervision, she finished her Master in the end of Fall 2002.